ASSESSING THE APPLICABILITY OF THE GREULICH AND PYLE (1959) SKELETAL AGE ESTIMATION METHOD TO SOUTH AFRICAN CHILDREN BETWEEN 0 AND 13 YEARS

Belinda Speed
RFFBEL001

Submitted to the University of Cape Town in fulfilment of the requirements for the degree:

M.Sc (Med) - Anatomy

January 2012

Supervisor: Professor Alan. G. Morris
Department of Human Biology
Faculty of Health Sciences
University of Cape Town

DECLARATION

I declare that this thesis is my own, unaided work. It is being submitted in fulfilment for the degree of Masters of Science in Medicine at the University of Cape Town.

It has not been previously submitted for any degree or examination at any other university.

Each significant contribution to and quotation within this thesis, from the work or works of others, has been attributed, cited and referenced.

Signed: _____

Date: _____ day of _____ 20___

I dedicate this thesis to my husband, Kenneth.

Thank you for helping me keep on 'keeping on.'

TABLE OF CONTENTS

CHAPTER PAGE

CHAPTER PAGE

Chapter 3: Materials and Methods

CHAPTER PAGE

Chapter 4: Results

CHAPTER PAGE

CHAPTER PAGE

ABSTRACT

The assessment of skeletal age (SA) in both clinical and forensic settings serves to estimate the degree of development and biological maturation of a child. This is a suitable and frequently used technique, as skeletal age is a valuable indicator which can be analysed from birth until the attainment of the fully-developed adult body form.

Radiographs of the hand-wrist region are most often used to estimate skeletal age, by comparing a sample radiograph against an established standard. The most internationally accepted method for skeletal age estimation is the Atlas method of Greulich and Pyle (GP) (1959). Extensive research has been conducted regarding the flexibility and applicability of this method to other race and socio-economic groups, with most research indicating that the GP Atlas is not a suitable method for skeletal age estimation for other world populations. As little research in this regard has been done using South African samples, this project aims to determine whether the GP Atlas is still an applicable method of skeletal age estimation for South African children between the ages of 0 and 13 years.

Skeletal age estimates using the GP Atlas were performed on 1356 (821 males, 535 females) pre-existing digital radiographs from Red Cross War Memorial Children's Hospital, Salt River Mortuary and Tygerberg Mortuary. The target age range for this sample was birth (0) to 13 years, in order to incorporate the appearance of the ossification centres of the hand and wrist, but exclude epiphyseal fusion in this region.

Although there was a strong positive correlation between skeletal age (SA) and chronological age (CA) [Males: $R = 0.96$; Females: $R = 0.97$], there was a high degree of variation in the sample, with overestimation and underestimation of skeletal age across both sexes and all age groups. This variation increased with an increase in age.

Regression analysis, using a best-fit fixed-effect model, random-intercept mixed-effect model and a random intercept-random slope mixed-effect model, attempted to account for the variation in the sample by using skeletal age as a predictor for chronological age. The random intercept-random slope mixed effect model was shown to be the most appropriate model for this sample.

Variables for sex, race and socio-economic status were included in the regression analysis to determine their effect on predicted chronological age. The regression model indicated that sex (and the interaction between sex and skeletal age) influenced predicted chronological age by slightly reducing the sample variation, but the sample was too variable for the effects of race and socio-economic status to be determined. The model also indicated that the majority of the variation within the sample was due to random variation.

Possible reasons for this include the differences in biological origin between the South African and GP samples, the GP methodology, and the timing of growth and development of South African children on the whole.

Due to the high degree of random variation in this sample, which cannot be accounted for completely by sex, race or socio-economic status, the GP Atlas is not reliable for skeletal age estimation of South African children. Other methods, such as the Phillips (2008) method for dental maturation, should be sought as an alternative when the chronological age of a child comes into question.

LIST OF TABLES

TABLE PAGE

TABLE PAGE

LIST OF FIGURES

FIGURE PAGE

FIGURE PAGE

FIGURE PAGE

FIGURE PAGE

FIGURE PAGE

FIGURE PAGE

ACKNOWLEDGMENTS

When I started my Masters, I had no idea that so many people would be involved in helping me create the final, finished product. I would like to acknowledge, in no particular order, each person who was part of this process. Your role, however large or small, has not gone unnoticed.

My thanks to God for getting me this far in my academic career. It has been a long journey with many trials, and I often didn't know if I'd finish. Here it is, the final product.

A very big thank you to the various funders who made it possible for me to complete this degree: the National Research Foundation, the Deutscher Akademischer Austausch Dienst (DAAD), and the Harry Crossley Foundation, as well as all the staff at the Post-Graduate Funding Office – your extremely generous financial contributions are greatly appreciated.

Without the assistance of the staff at Tygerberg and Salt River Mortuaries, and Red Cross Children's Hospital, this project would still be just a good research idea. Professor Lorna Martin and her very capable group of Forensic Pathologists from Salt River mortuary, thank you all for your help for allowing me into your facility. Shirees Benjamin, the Chief Forensic Officer at Salt River – you are, indeed, a blessing. Your hard work did not go unnoticed, and I am so grateful for every minute you availed yourself to my constant requests for information. To the staff at Tygerberg Mortuary, Prudence Flaendorp, Kim, and especially Dr Lene Burger, who painstakingly X-rayed each child, thank you for your time and help in adding to my database. Ann Vlok, the Assistant Director of Radiology at Red Cross Children's Hospital – the images from your facility are top-class, and your attention to body position when radiographing children is astounding, especially under the pressures that a Trauma unit brings.

A medal should definitely go to Stef Steiner of Lodox Systems. You made my task of data-collection so much easier, and I appreciate your tenacity when dealing with my laptop that wouldn't load the viewer and my external hard-drive that died on us in the night - all of this whilst you had your own work to do. You seem to take it all in your stride. Your help, your jokes and efficiency made a large part of my project hassle-free, and for that I owe you a great debt of thanks.

Statistics has never been my strong point. I am very aware of this, and will seek help whenever possible. Katya Mauff is the extremely competent statistical consultant at UCT's Department of Statistical Sciences. Thank you, thank you, thank you for explaining and re-explaining mixed effects models, p-values, t-values and all the gobbledygook that is statistics. My project was riding on your abilities, and you did a fantastic job of getting results from a method that is unreliable at best.

To my supervisor, Professor Alan Morris – Firstly, thank you for being a willing and able supervisor in the midst of your sabbatical and book-writing endeavours. Not only have you managed to graduate yet another student, but you have also managed to create a literary masterpiece, the first book I have read from cover to cover in about 3 years. Thank you for the endless hours of help via email, and for allowing me to become a semi-permanent resident of your office, with all the questions I had. I'm quite certain there is an imprint on your office carpet which will fit my shoe size.

It warms me when colleagues become friends. In my case, my colleagues have become not only friends, but like sisters to me. Nhlanhla, Kundi, Laché and Emma – you ladies hold a very special and important place in my life. Your wise words, help and guidance have helped me more than you will ever know. I appreciate you all, and hope we can laugh together for many years to come.

To my parents, your strength is what has kept me going through this degree. You continue to face one adversity after the next, but you never give up. Whenever I felt like throwing in the towel, I thought of what you'd do in my situation, and it made me face the next challenge with even more gusto and determination. Thank you for supporting your 'professional-student' daughter and for believing me every step of the way. I promise it will all be worth it in the end. I love you both.

My late-grandfather, Gogs, and my one-of-a-kind grandmother, Virg – thank you for driving me to do better, to strive for perfection in all that I do, and for your wisdom when I need it. I couldn't have asked for better grandparents. I hope I will always make you proud.

To my family, friends and colleagues who I have not mentioned by name – you have all played an integral role in this process. Thank you for being there when I needed you, and for the interest and support you've shown, even when I explained my project in a way that made no sense to anyone but me.

Last, but by no means least, to my husband, Kenneth – I met you right at the beginning of this journey, and the support and love you have shown me during this time has been overwhelming. Thank you for waiting patiently for me whilst I pursued my dreams in the USA, thank you for listening when I needed a sounding-board, thank you for loving me, supporting me, and lighting that fire-cracker when it was needed most. Knowing you has enriched my life in more ways than I could ever explain. Thank you for walking beside me throughout this journey. I am grateful for you every single day.

CHAPTER 1:

INTRODUCTION

1.1 Importance and Applications of Skeletal Age Estimation

1.1.1. Skeletal Age and Skeletal Maturity

Skeletal age and skeletal maturity are described by Bogin (1999) as "a measure of biological maturation (as distinguished from chronological age) based on stages of formation of the bones". Bone growth and maturation is an ordered process, with various developmental stages. It commences with the appearance of ossification centres and ends on attainment of the adult bone structure (Scheuer and Black, 2000). An explanation of terms and definitions relating to skeletal age estimation, which are used in this section, can be found in *Appendix A*.

Skeletal maturation progresses throughout an individual's growing years and the various hard tissue changes which occur are unique and defining to each stage of development (Bogin, 1999). This is a key advantage of skeletal age estimation and is one of the main reasons for its common use as an assessor of biological or chronological age (Büken *et al.*, 2009; Santos *et al.*, 2011). It is considered by some authors to be one of the most accurate (Loder *et al.*, 1993; Koc *et al.*, 2001). Various influences (environmental or genetic) may affect growth during the developmental stages. The ossification of the bones of an infant provides information about the development status of the child, which, aside from changes in the genetic ordering of events, may become delayed for a number of reasons.

During early childhood, the development of a child is a reflection of its ability to adapt to the surrounding environment. Any occurrences where the child was not able to sufficiently adapt will be evident in the developmental process. The release of steroid hormones during adolescence overrides the environmental influence on development to a certain extent. This is seen by the extensive growth and development which occurs during adolescence and puberty (Anderson, 1971). Skeletal age therefore serves as a suitable estimation and reflection of not only skeletal maturity, but also physiological maturity, as it is the only developmental indicator which is able to be assessed from birth to the attainment of the mature adult body form (Tanner, 1978; Wheeler, 1991; Cox, 1997; Bogin, 1999, Uysal *et al.*, 2004).

Previously, height-weight-age tables were used to assess development (Greulich and Pyle, 1959), but the discovery of X-rays has allowed skeletal age to be estimated through the use of radiographic techniques (Bogin, 1999). The developmental processes involved in skeletal growth can be captured on radiograph. At lower levels of X-ray exposure, ossified bone is radio-opaque, whilst cartilaginous regions remain radio-lucent and are therefore not visible (Bogin, 1999). This is one of the oldest applications of radiology and has been known and used for over a century (van Rijn *et al.,* 2001; Khan *et al.,* 2009). Nowadays, using radiographic imaging for this purpose (and thus ascertaining the developmental status of an individual) fulfills an important function within paediatric radiology (Schmeling *et al.,* 2004; Schulz *et al.,* 2005; Zhang *et al.,* 2009). Other methods of assessing development include mental age (Haiter-Neto *et al.,* 2006), sexual maturation/voice change (Soegiharto *et al.,* 2008) and the relationship between weight, height and age (Greulich and Pyle, 1959). Individuals are highly diverse, and these non-skeletal methods often prove to be unsatisfactory for age estimation (Greulich and Pyle, 1959).

1.1.2 Analysis of the Hand and Wrist

Radiographic analyses can be performed on various regions within the body, but it is the hand-wrist region which is most commonly used for assessment of skeletal age in growing children and adolescents (Cameriere *et al.,* 2006; Cameriere and Ferrante, 2008; Soegiharto *et al.,* 2008; Tisè *et al.,* 2011). It is used for many reasons including the absence of other hard tissues and the presence of a large number of ossification centres in one small area (Mora *et al.,* 2001; Haiter-Neto *et al.,* 2006; Cameriere *et al.,* 2008). Bone mineralization in this region begins at birth and over various developmental stages the change in size, morphology and the degree of epiphyseal union of the bones can be used to evaluate skeletal age (Cameriere *et al.,* 2006). The hand-wrist area has the added benefit of being relatively easy to position during radiography, whilst only low doses of radiation are required to attain a high quality image (Cameriere and Ferrante, 2008; Cameriere *et al.,* 2008; Giordano *et al.,* 2010).

1.1.2.1 Ossification of the Hand and Wrist

The hand has 30 ossification centres, all of which have cartilaginous precursors which develop endochondrally (Phillips and Thompson, 2000). Bones in this area include the carpals, metacarpals, phalanges and the epiphyses of the ulna and radius (Greulich and Pyle, 1959), the ossification centres of which appear in an ordered sequence (Phillips and Thompson, 2000).

Although the timing of appearance of these centres differs between males and females (females are in advance of males), the features used to assess skeletal age remain common. Ossification of the carpal bones and epiphyseal union of the metacarpals, phalanges, ulna and radius can therefore be considered 'maturity indicators', in that they are features which are used as indicators of advancement towards maturity (Dembetembe, 2010). These specific features of the individual bones are easily visible on a radiograph and they occur in a definite and irreversible pattern (Greulich and Pyle, 1950, cited in Cameron 1984).

When comparing the hand-wrist region of two individuals of the same sex, there may be disparities in the rates of maturity up to as much as three years (Anderson, 1971). In addition, there may be difference in the sequence of appearance of the maturity indicators, occurring most frequently in the carpal region. The carpals usually appear in the following order: Capitate, Hamate, Triquetral, Lunate, Trapezium, Scaphoid, Trapezoid and Pisiform.

In males, however, the Scaphoid may appear in advance of the Trapezium, whereas in females, it may appear only after formation of the Trapezoid (Greulich and Pyle, 1959). This variation in order of appearance between the Scaphoid, Trapezium and Trapezoid is of little significance, considering these bones all appear within the same 1 to 3 month period. One must, however, take into account the overall variation when assessing skeletal maturity. The variation may exist between two children who share the same chronological age; between the right and left hand of one individual; or between the bones of one hand (Anderson, 1971).

Despite the variation which exists in this region, the hand-wrist remains a useful tool for skeletal age estimation.

1.1.3 Applications of Skeletal Age Estimation

The broad application of skeletal age estimation is of particular importance in answering clinical questions as well as in forensic age diagnostics (van Rijn *et al.*, 2001; Schmidt *et al.* , 2007).

1.1.3.1 Clinical Application

In a clinical context, important decisions can be made based on useful data provided by skeletal maturation (Haiter-Neto *et al.,* 2006). Skeletal age and skeletal maturity are of interest to the endocrinologist, pediatrician, orthopedic surgeon and pediatric radiologist (Anderson, 1971; Gilli, 1996).

Assessment of skeletal age, along with an evaluation of primary and secondary sexual characteristics and height-weight measures (Dembetembe, 2010), allows the clinician to determine whether a child is growing and developing in accordance with other individuals of the same sex and age (Ontell *et al.*, 1996; Tisè *et al.*, 2011).

Development which is too rapid or too slow may indicate the presence of a growth disorder (Bogin, 1999). These disorders could be due to an endocrinological abnormality (Tanner *et al*., 2001; Zhang *et al.*, 2009) and in such cases, an awareness off the individual's level of skeletal maturity may aid the diagnosis, evaluation, follow up and timing of medical therapy (Mora *et al.*, 2001; Uysal *et al.*, 2004; Cameriere *et al.*, 2006). Heyerdahl *et al*. (1994) and Satoh *et al.* (1997) provide examples of such growth disorders which include "constitutional growth retardation and growth hormone deficiency" and "endocrinological diseases, such as hypothyroidism, congenital adrenal hyperplasia and precocious puberty" (Uysal *et al.*, 2004).

According to Khan *et al.*, (2009), as much as 5% of children will be affected by growth concerns. Bone age estimates may be performed when corrective surgery of the long bones or vertebral column is required in individuals with skeletal deformities (Gertych *et al.*, 2007).

Skeletal age estimates are also used in dentistry. Knowledge of the maturity level of a child, in conjunction with an evaluation of craniofacial growth, is of utmost importance as it can influence treatment planning and clinical management, especially when orthodontic treatment and dental modification is required (Haiter-Neto *et al.*, 2006; Soegiharto *et al.*, 2008). The timing of craniofacial growth during the pubertal growth period is closely related to stages of ossification in the hand-wrist region. It is for this reason that the hand-wrist proves invaluable in orthodontic diagnostics (Soegiharto *et al.*, 2008; Cameriere *et al.*, 2008).

It is important to note that skeletal age assessment (using radiographic analysis) allows objective comparison of one individual to another of the same sex and chronological age (Greulich and Pyle, 1959). Under 'normal' growth conditions skeletal age provides an indication of the growth potential of children (Mora *et al.*, 2001; Khan *et al.*, 2009) and it is also a fair predictor of final adult stature (Koc *et al.*, 2001; Uysal *et al.*, 2004).

1.1.3.2 Forensic Application

Ascertaining the correct age of an individual for forensic investigations of both living and deceased individuals is paramount (Varkkola *et al.,* 2011). When skeletal age estimation is applied in a legal context, it is referred to as forensic age estimation. (Krogman and Işcan, 1986).

Forensic age estimation, together with additional postmortem findings, can aid the process of personal identification of deceased individuals, if in concordance with antemortem data (Cameriere *et al.,* 2006; Varkkola *et al.,* 2011). It can be used in the sorting of interred and commingled remains, as individualizing features on each bone can be viewed using radiographic analysis (Greulich, 1960; Shaefer and Black, 2007).

In recent years, the need for forensic age assessments of living individuals has increased (Büken *et al.,* 2009; Varkkola *et al.,* 2011). In Europe, due to the 'open border' policy within the European Union countries, forensic age estimates are required for illegal immigrants, refugees and asylum seekers who do not have the correct documentation regarding their age and identity (Cameriere *et al.,*2006; Büken *et al.,* 2007). Such individuals often claim to be minors in order to increase their chances of obtaining a residency permit (Giordano *et al.,* 2007).

The focus of forensic age estimation lies mainly, however, in the assessment of criminal capacity and criminal liability in order for the correct and appropriate legal procedures to be observed when processing a court case (Büken *et al.,* 2007; Cameriere and Ferrante, 2008; Büken *et al.,* 2009; Tisè *et al.,* 2011). This is especially true in developing countries where birth records are not well maintained (Büken *et al.,* 2007).

South African law stipulates an irrebuttable presumption that a child under the age of 7 years lacks criminal capacity. A child older than 7 years but younger than 14 years is rebuttably presumed to lack criminal capacity unless it can be proven by the State that the alleged offending child is able to make the distinction between right and wrong, and that he or she was aware of the wrongfulness of their actions at the time the offense was committed. This rule dates back to Roman law. It is also not uncommon for South African children to be unaware of their age or date of birth, and in some cases the parents of such children are unable to provide particulars in this regard (South African Law Commission, 1997).

In terms of Section 337 of the Criminal Procedure Act 51 of 1977, "the presiding judicial officer may estimate the age of a person if in any criminal proceedings the age of that person is a relevant fact, or which no or insufficient evidence is available. The Court has correctly indicated, however, that the finding of the presiding officer may not be simply based on observation. There should be a proper attempt at finding evidence and in the absence of such evidence, the accused should, for example be examined by a district surgeon" (Criminal Procedure Act, Section 337). Under these circumstances, a skeletal age assessment in conjunction with other physiological examinations would assist in most accurately estimating the age of the individual in order to proceed with the correct prosecution (Schmeling *et al.,* 2000).

1.2 Available Methods for Skeletal Age Estimation

Many methods exist for skeletal age assessments using the hand-wrist region (Büken *et al.,* 2009). They can be divided into two groups, based on the methodological approach of each. Using the *single-bone method,* specific skeletal elements of individual bones are used to evaluate the degree of skeletal maturity. The *atlas method,* however, allows estimation of skeletal age by comparing a hand radiograph from a test subject with standard, sex-matched control radiographs in an atlas (Schmidt *et al.,* 2007; Schmidt *et al.,* 2008).

In both the clinical and forensic contexts, the most important methods used to date are the atlas method of Greulich and Pyle (GP) and single bone method of Tanner and Whitehouse (TW2) (Bilgilli *et al.,* 2003; Haiter-Neto *et al.,* 2006; Cameriere and Ferrante, 2008). The GP method was developed using radiographs of white children from mid- to upper-class families in Ohio, USA. The radiographs were taken during the 1940s (Greulich and Pyle, 1959; Zhang *et al.,* 2009). The TW2 method was derived from Scottish children, from low socio-economic backgrounds (Tanner *et al.,* 1975; Bull *et al.,* 1999).

The atlas method (GP) is considered to be less time-consuming and less difficult to perform than the single-bone method (TW2) (Andersen, 1971; Schmidt *et al.,* 2007; Khan *et al.,* 2009). Based on these reasons, the GP atlas method is the most commonly used of the two (Ontell *et al.,* 1996; Mora *et al.,* 2001; Khan *et al.,* 2009; Zhang *et al.,* 2009) and it is also the most internationally accepted (Schmidt *et al.,* 2007).

It is for these reasons that this research project focuses mainly on the GP method and it's applicability to South African children.

The methods of GP and TW2 will be discussed in greater detail in *Chapter 2*.

1.2.1 Skeletal Age Estimation in a South African Context

Despite the difficulties of bone age assessment, and the assumptions on which the various methods are based, determination of skeletal development is still clinically and forensically relevant, providing essential information regarding the nutritional status of an individual and identifying potential imbalances in skeletal development, all the while prevailing as the only means of assessing changes in the skeleton throughout the entire growing period (Cox, 1997).

The GP Atlas method is primarily used to assess skeletal age for South African children; yet the applicability of this method to South African children has not been fully and conclusively researched as yet. In terms of development, it is not known how South African children fair compared to children of other countries; and if variation in development does exist, the potential causes thereof have yet to be investigated.

1.3 Research Aim and Objectives

This current research project aims to determine whether the GP Atlas method is still applicable to South African children between the ages of 0 and 13 years.

This research seeks to realise this aim, based on the following objectives:

- Assess the skeletal age of South African children between the age of 0 and 13 years, using the GP Atlas method.
- Test for significant differences between skeletal age and actual chronological age.
- Determine the degree of variation across the sample as a whole and then address possible causes for this variation based on sex, racial classification, and socio-economic status.
- Use regression analysis to account for the variation observed.
- Outline the difference in development patterns in the hand-wrist region of South African children, compared to the GP sample.
- Assess whether the results of this research are in agreement with other South African research by Philips and Thompson (2000), Roff (2008) and Dembetembe (2010).
- Provide final clarity on issues surrounding the applicability of the GP Atlas, when used to assess skeletal age for South African children.

CHAPTER 2

REVIEW OF THE CURRENT SKELETAL AGE ESTIMATION METHODS and FACTORS AFFECTING SKELETAL DEVELOPMENT

2.1 Manual Skeletal Age Estimation Methods

2.1.1 Greulich and Pyle Standards

2.1.1.1 History and Background

The discovery of radiographs in 1895 was followed shortly by its application for the assessment of dental and skeletal development throughout an individual's lifespan, hence its effective use in age estimation (Bogin, 1999; Dembetembe, 2010). Starting in the early 20th century, several works which depicted normal human skeletal growth and development were published. Pryor (1928) used radiographic techniques to further investigate ossification in the hand-wrist region based on a sample of males and females. In the study by Pryor (1928) several conclusions were formulated and these remain valid to date. It was noted that (a) females develop in advance of males, with ossification centres in the hand-wrist appear sooner in females than in males; (b) the timing of termination of skeletal growth, characterized by epiphyseal union, differs between the sexes; (c) there is a degree of variation in the timing of appearance of the hand-wrist bones which appears to be a heritable trait, and thus, skeletal growth and the termination thereof is under genetic control. Supporting evidence by Dunham *et al.* (1939) indicated not only sex, but ancestry related differences in skeletal development of infants, with 'negro' infants developing in advance of 'white' infants (Dembetembe, 2010). Dunham *et al.* (1939) agreed with Pryor's (1928) findings that genetics are involved in controlling developmental sequences (Greulich and Pyle, 1959).

In 1937, the first *Atlas of Skeletal Maturation* was published by Todd. It was later revised by W.W . Greulich and S.I. Pyle, who, in 1950, published their first edition of the *Radiographic Atlas of Skeletal Development of the Hand and Wrist,* hereafter referred to as the GP Atlas (Bogin, 1999; van Rijn *et al.,* 2009). This atlas took into account the differences in timing of development between the sexes, as outlined by Pryor (1928) and Dunham *et al.* (1939), as well as research that showed a degree of variation in the appearance of ossification centres and the sequence of epiphyseal union in the hand-wrist region (Beresowski and Lundi, 1952).

2.1.1.2 Brush Foundation Longitudinal Study

The Greulich and Pyle skeletal age estimation standards were derived from the Brush Foundation longitudinal study which took place between 1931 and 1942. The 1000 subjects in this study were White children of Northern European ancestry, who were born in the United States of America. They ranged in age from newborn (0 years) to 18 years of age and came from mid- to high-socioeconomic backgrounds (Greulich and Pyle, 1959; Lee, 1971; Zhang *et al.,* 2009). At a later stage children of lower socioeconomic status were also included in the study, upon which, differences in skeletal development were noted (Greulich and Pyle, 1959).

In order to assess whether each study subject was developing in accordance with the normal sequence of ossification and epiphyseal union of the major joints, the left elbow, hip, foot, knee, hand-wrist and shoulder of each study subject was radiographed. This allowed for an establishment of normality, specific to the study population (Greulich and Pyle, 1959). Under normal growth circumstances, skeletal development follows a specific and uniform patter, a phenomenon which had already been documented by Stevenson (1924) for the major joints in the body at the time of the study by Greulich and Pyle (1959). Epiphyseal union begins at the elbow, followed by the hip, ankle, knee, wrist and finally, the shoulder. It is a sequence still used by physical anthropologists for age estimation (Buikstra and Ubelaker, 1994).

In the Atlas, standard radiographs represent various age categories for each sex. To formulate these standards, Greulich and Pyle gathered 100 radiographs from each sex and age category and selected the radiograph which was most representative as the standard for that age group (van Rijn *et al.,* 2001). Thus, the standards represented in the GP Atlas are the radiographs which contained the most commonly observed maturity indicators (Dembetembe, 2010). Each standard is accompanied by line drawings and a description of those characteristics which indicate maturity level (Greulich and Pyle, 1959). A selection of the drawings and descriptions which are relevant to this study can be found in *Chapter 3.* The first edition of the GP Atlas was published in 1950, the second edition in 1959 and the third, most recent edition was published in 1988 (Groell *et al.,* 1999; Schmeling *et al., 2000;* Büken *et al.,* 2007). The second edition was used for the purposes of this research project.

The method of Greulich and Pyle (1959) involves a comparison of the overall appearance of a radiograph from an individual of unknown age to the same-sex standard to which it most

closely resembles. This is a modified and more rapid version than was initially outlined in the GP Atlas, the use of which is further explained in Chapter 3 (Bull *et al.,* 1999). The use of the GP Atlas as a method of skeletal age estimation in children results in the assigned skeletal age representing a degree of maturity that is relative to the particular group of White American children used in the Brush Foundation study (Lee, 1971). For the GP Atlas standards relevant to this research, see *Appendix B*.

2.1.2 Tanner and Whitehouse (TW2) Standards

The Tanner, Whitehouse, Marshall, Healy and Goldstein or TW2 method was developed after the first publication of the GP Atlas in 1950. In 1962, Tanner, Whitehouse and Healy devised the first TW method. The TW2 method is a revised version and is discussed below (Tanner *et al.,* 1975).

When the GP standards were applied to the sample of Tanner *et al.* (1975), a delay in skeletal development was noted. Tanner *et al.* (1975) postulated that this may be due to the high socioeconomic status and relatively small size of the GP sample. In an effort to create a more applicable standard for skeletal age estimation using the hand-wrist region, Tanner *et al.* (1975) selected a wider and more representative sample comprising of 3000 British children of 'normal' development, from lower socioeconomic backgrounds. (Büken *et al.*, 2007)

Tanner *et al.* (1975) identified 17 developmental stages to which a subject could be assigned, based on individual maturity ratings for the carpals, metacarpals, phalanges and the radius and ulna (Dembetembe, 2010). Each stage differs based on the specific features observed on each bone and how these features change with an increase in chronological age; and are such that the amount of change between one developmental stage and the next is significant and easily distinguished (Tanner *et al.,* 1975). The TW2 method is mathematical in nature. It involves systematically evaluating and individually scoring the development of 20 bones in the hand and wrist (Castriota-Scanderberg *et al.,* 1998; Bull *et al.*, 1999; Hsieh *et al.,* 2007). This results in their classification into one of several stages (Haiter-Neto *et al.,* 2006; Büken *et al.,* 2009). A specific score for each bone is associated with the assigned stage (Niemeijer *et al.,* 2003; Giordano *et al.,* 2007; Giordano *et al.,* 2010). The sum of the scores gives a net maturity rating, which, when compared directly to sex-specific tables, may be converted into a skeletal age estimate (Castriota-Scanderberg *et al.,* 1998; Haiter-Neto *et al.,* 2006; Büken *et al.,* 2009). This score may also be used to estimate adult height (Lin *et al.,* 2004).

2.2 Digital Skeletal Age Estimation Methods

2.2.1 Shortcomings of the GP Atlas and TW2 Methods

Although the GP Atlas method is an easy and rapid method of skeletal age estimation, it is not without its shortcomings. Any method which is used to estimate skeletal age is only as good as the reference sample on which it is based (Mellits *et al.,* 1971) and it is advised that the most recent and established standards be used for assessment of growth and development (Dembetembe, 2010).

A common criticism is that Greulich and Pyle (1959) used radiographs from children of specific ethnic background and socioeconomic standing, resulting in an Atlas which is not fully representative of populations the world-over, and can therefore not necessarily be used to correctly assess skeletal age in all children (van Rijn *et al.,* 2009).

Over the past few decades some populations have displayed an increase in maximum weights and heights, in particular during the period from 1965 to 2005, where an increase in long bone lengths, heights and weights was documented by authors (Meadows and Jantz, 1995; Kim *et al.,* 2008). This was also noted when long bone lengths from an 18th century sample were compared to those of a 20th century sample (Meadows and Jantz, 1995). Due to the association between the rate of skeletal development and maximum limb length (Tanner *et al.,* 1975), the rate of development and termination of growth in the hand-wrist region could also differ over time (Dembetembe, 2010). Considering the data for the GP Atlas was collected in the 1940s, it may no longer be entirely applicable to modern-day society (Zhang *et al.,* 2007).

Another disadvantage of the GP Atlas method is its subjective nature and that it is, in part, dependent on the expertise and experience of the observer (Pietka¸1995; Gertych *et al.,* 2007; Zhang *et al.,* 2007). The method is not always reliable and in some cases the sample radiograph may not match any standards within the GP Atlas (Giordano *et al.,* 2007). Under these circumstances, a subjective interpretation is needed for the skeletal age assessment (Hsieh, Jong and Tiu, 2007), which may result in considerable discrepancies between the age estimates of qualified versus inexperienced observers (Hsieh *et al.,* 2007).

The TW2 method is considered to be more accurate than the GP Atlas method as it is derived from a solid mathematical basis. It is also more objective and adaptable than the GP Atlas method; however it is not popular clinically as it is complex, time-consuming and difficult to perform (Castriota-Scanderberg *et al.,* 1998). It is also not completely without observer subjectivity and some variability may exist in the results, depending on the expertise of the observer; thus, TW2 method for skeletal age estimation is only used in approximately 20% of cases (Pietka, 1995; Gertych *et al.,* 2007).

2.2.2 Progression into a Digital Era

2.2.2.1 The Need for Digital Methods

Regardless of whether the GP Atlas or TW2 method is used to assess skeletal age, one of the main problems with using manual methods is the observer variability. There exists a certain degree of difficulty in quantifying the inherently continuous change that is skeletal maturation. The manual methods available aim to provide a scale on which to measure skeletal development; this leaves room for ambiguity in the assessments by observers, especially due to the high degree of biological variation amongst individuals (Thodberg, 2009).

As there has been little improvement in the field of manual age estimation techniques in the last 30 years (Thodberg *et al.,* 2009), it would be worthwhile establishing a reliable computer-based skeletal age estimation system (Hsieh, Jong and Tiu, 2007; Thodberg *et al.,* 2009). This has the potential of reducing the amount of time expended on viewing a radiograph and would aim to reduce the burden on radiologists and pediatricians, allowing them to assess skeletal age more efficiently (Niemeijer *et al.,* 2003; Pietka, 2003; Pietka 2004; Giordano *et al.,* 2007)

A program such as this would also seek to decrease or eliminate intra- and inter-observer variations (Hsieh *et al.,* 2007; van Rijn *et al.,* 2009), whilst providing a more objective and accurate skeletal age assessment which generates reproducible and reliable measurements (Pietka, 1995, Pietka, 2003; Lin *et al.,* 2004; Pietka 2004, Schmidt *et al.,* 2009).

2.2.2.2 Early History of Computer Automation

The realisation of this of this digital concept has been remarkably slow. Michael and Nelson (1989) developed the first semi-automated system, based on measurement techniques. Their model-based computer system, HANDX, was able to identify specific phalanges from a radiograph in order to measure the perimeter, area, and length of the minor and major axes of each bone (Pietka, 1995).

In 1992, Tanner *et al.* presented the Computer-Assisted Skeletal Age Scores (CASAS) system. It is based on nine exemplar images for each bone which represent nine stages of maturity. In order to conduct a skeletal age estimate on a new radiograph, the CASAS operator must first manually zoom in on each bone using a video camera and match each bone with two or three of the most similar templates. Thereafter, a measure of correlation between each bone and template is calculated automatically by the system, based on the similarity of the two as a whole. At the time, the CASAS system was viewed a positive step towards fully automated bone age estimation, especially since the method was able to reduce observer variability (Thodberg, 2009).

Unfortunately, as with the manual methods, CASAS has limitations. Firstly, it is not as efficient as manual methods because the user has to locate each bone manually, which is time consuming. In addition, the rigid and unyielding nature of the templates allows manipulation of size but not shape or density of the image. This results in some bones being matched to the incorrect template, generating incorrect results which need to be overruled by the user (Thodberg, 2009). Since then, methods by Hill and Pynsent (1994), and Pietka (1995) aimed to modify the system of Tanner *et al.* (1992), but neither of these was applied to common clinical practice (Thodberg, *et al.*, 2009).

Subsequent research by Pietka *et al.* (2001); Lin *et al.*(2004); Gertych *et al.* (2007); Hsieh, Jong and Tiu (2007); Hsieh *et al.* (2007); Zhang *et al.* (2007); Giordano *et al.* (2007); Thodberg *et al.* (2009) and Giordano *et al.* (2010) have created various algorithms in an attempt to fully automate skeletal age estimation. These algorithms use specific, designated Regions of Interest (ROIs) upon which the automated analysis is based.

The majority of these algorithms use Epiphysis-Metaphysis Regions of Interest (EMROIs), also cited in the literature as Phalangeal ROIs (PROIs), and do not consider the Carpal ROI (CROI), radius or ulna for analysis (Giordano *et al.*, 2007). The analysis of EMROIs is a relatively easy task in terms of image-processing, but it does not provide complete bone age assessment based on bone growth from birth to adulthood. This would require CROI processing for a more complete skeletal age analysis (Giordano *et al.*, 2010). These ROIs are shown radiographically in *Figure 2.01*.

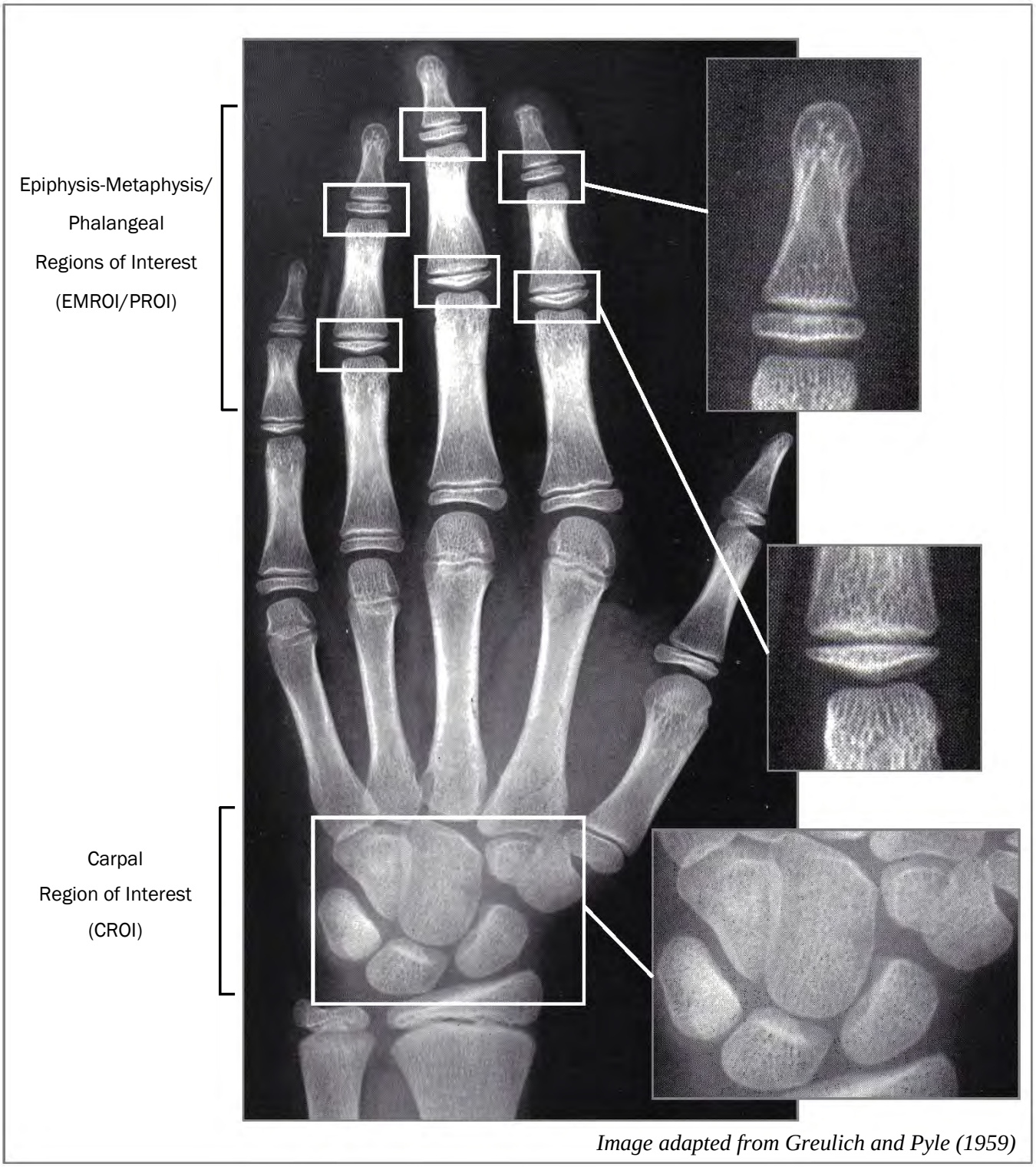

Figure 2.01 *Epiphysis-Metaphysis/Phalangeal Regions of Interest (EMROIs/PRIOs) , and Carpal Region of Interest(CROI) which are used in various digital methods of skeletal age estimation*

During the early stages of development, the carpal ossification centres are small and appear individually on the radiograph. This allows for fairly simple separation and description of the features on each bone (Pietka, 1995). With an increase in age comes an increase in carpal size, resulting in several overlapping CROIs. There exists now the challenging task of identifying the border of each bone on radiograph and determining the degree of calcification, which is exacerbated by the presence of soft tissue (Pietka, 1995; Lin *et al.,* 2004; Zhang *et al.,* 2007; Giordano *et al.,* 2010). Thus, CROI analysis is generally only used for children under the age of 9 year (Pietka, 1995), after which the use of EMROIs enables a more reliable and effective analysis (Zhang *et al.,* 2007).

In the aforementioned EMROI methods, the algorithms are divided into several common steps including image pre-processing, background removal, orientation correction, image segmentation and features analysis (Giordano *et al.,* 2007).

Image pre-processing is required to standardise all radiographic images due to the irregularities and variation present in each (Giordano *et al.,* 2010). This enables reliable and accurate feature information to be gathered from the radiograph. (Lin *et al.,*2004). The first two steps of the proposed pre-processing technique include background suppression and removal of radiological markers (such as the "L" or "R" metallic disc which is used to indicate side when the radiograph is taken). These first two steps are completed by removing all pixels from the image which do not belong to the hand. The third step is to correctly orientate the hand (Giordano *et al.,* 2010). Once this is completed, the EMROIs can be easily extracted from the image. Selection, positioning and feature analysis of the EMROIs depends on the method used, and various options have been detailed in Pietka *et al.* (2001); Lin *et al.*(2004); Gertych *et al.* (2007); Hsieh, Jong and Tiu (2007); Hsieh *et al.* (2007); Zhang *et al.* (2007); Giordano *et al.* (2007); Thodberg *et al.* (2009) and Giordano *et al.* (2010). Feature analysis yields a bone age which is more objective when compared to manual methods, and has a much reduced of observer variability.

2.2.2.3 Limitations

In accordance with manual methods, digital skeletal age estimation has its own unique limitations. Many of these methods have a strong dependence on their user settings, for example, hand orientation, to such a degree that many authors provide a very specifically defined standard hand position within the image (Giordano *et al.,* 2007). No single method

provides an age estimation technique which encompasses all age groups, from newborn to fully mature, but instead are only valid for certain age ranges. This is also reflected in the ROI selection as EMROIs and CROIs are only analysed together in two of the studies (Gertych *et al.*, 2007; Giordano *et al.*, 2010).

2.2.3 BoneXpert ™ - Computerised Age Estimation Software

Only a few of the digital methods to date are available in user-friendly computer software packages. The majority of these are based on the TW2 method, due to its modular nature and few provide a digital alternative for the GP Atlas. There is, however, a recently developed skeletal age estimation software package which aims to overcome some of the limitations of digital age estimation methods and is presented in a user-friendly form. This program is BoneXpert™ and it was devised by Hans Henrik Thodberg in 2008.

2.2.3.1 Overview

BoneXpert™ is intended for the automatic assessment and estimation of bone age. It is also able to compute the Bone Health Index (BHI) and provide a prediction of final adult height, based on the bone age. Skeletal age estimations are computed using either the GP Atlas or TW2 methods as a reference, depending on the preference of the user. The GP Atlas reference has, however, been more carefully calibrated and validated compared to the TW2 reference. BoneXpert™ analyses 13 bones including the radius, ulna and the bones in digits I, III and V. As with other methods, the carpals are not included in the analysis as they can be difficult to reconstruct due to overlapping CROIs. They are also less important in the prediction of adult height. Possible assigned bone ages range from 2.5 to 17 years for males, and 2 to 15 years for females. Skeletal age assessments can also be performed according the four 'ethnic' groups included in the software. These are as stated: Caucasian, African-American, Hispanic and Asian (drawn from USA and Japanese samples) (Thodberg, 2009).

2.2.3.2 How BoneXpert™ Works

BoneXpert™ is able to analyse each digital radiograph completely automatically and independent of the rotation of the hand. Both left and right hands are accepted, as results from a recent study by Martin *et al.* (2010) show that, on average, the left and right hands give the same skeletal age.

Image analysis is divided into three steps or 'layers'.

In Layer A, active appearance models are used to determine the borders of each bone. These models have been 'trained' on the allowed density distribution and shape of the bones, which facilitates not only the location of the bones on radiograph but also the rejection of a bone, should it be in conflict with parameters of the method (Thodberg, 2009).

An intrinsic skeletal age is established for each of the 13 bones, in Layer B, based on the bones appearance and the sex of the subject. Excluding the bones rejected in Layer A, the skeletal ages for all bones is averaged to give an overall intrinsic skeletal age. Thereafter, a second, validation step takes place. Bones with a skeletal age deviating from average by more than 2.4 years are rejected from analysis. The entire radiograph is rejected should less than eight of the 13 bones be accepted for analysis (Thodberg, 2009; Thodberg *et al.*, 2009)

Although the intrinsic skeletal ages could be used as a new standard for skeletal age assessment, this would require clinicians to familiarise themselves with yet another skeletal age scale in addition to the standards already in use. The purpose of Layer C, therefore, is to convert the intrinsic skeletal ages from Layer B into a scale already familiar to clinicians. Thus, automated versions of the TW2 and GP Atlas methods were created. The automated skeletal ages agree strongly, on average with the manually assigned ages for each method (Thodberg, 2009). It is important to note that BoneXpert™ is a unique and new bone age estimation method which is based on principles different to those of the GP and TW2 methods.

2.2.3.3 Validation Studies

Clinical validation studies have been published on the accuracy of this newly developed automated method (Martin *et al.*, 2009; van Rijn *et al.*, 2009). This accuracy measure is defined as the root mean square (rms) deviation from the manual rating.

In the study by Martin *et al.* (2009), 531 radiographs of 'normal' children, ranging from four to 20 years of age were analysed using BoneXpert™. The rms for this sample was 0.71 years for boys up to the age of 17 years, and up to 15 years of age for girls.

van Rijn *et al.*(2009) tested the accuracy of BoneXpert™ against 188 patients who presented with various diagnoses of short stature, including individuals who were Growth Hormone deficient (44%), short for gestational age (7%), individuals diagnosed with Turner Syndrome (29%), Silver Russell Syndrome (4%) and others (16%). Of the 188 radiographs, 98.7% were

accepted for analysis and analysed correctly by the system. Results indicate a rms deviation of 0.72 years, with no difference between the diagnoses of short stature.

Validation studies using children diagnosed with precocious puberty (Martin *et al.,* 2008) and children of different 'ethnicities' (Thodberg and Sävendahl, 2008) have indicated rms deviations of 0.69 years and 0.59 years respectively.

The reliability of BoneXpert™ has also been tested, based on a sample of radiographs from a longitudinal growth study by Tanaka (2006). This study yielded a precision of 0.17 years, indicating that BoneXpert™ has the ability to reliably provide the same age estimate for a repeated analysis of a radiograph.

BoneXpert™ has been tested against the GP Atlas itself, yielding a rms deviation of 0.47years for both males and females (Martin *et al.,* 2009).

2.2.3.4 Achievements

An automated method such as BoneXpert™ has the potential of replacing manual methods such as the GP Atlas or TW2. This would be advantageous as observer variability and bias are eliminated; there is a low frequency of errors when compared to manual methods; the age estimates provided have been transformed into a scale used by the manual methods, allowing for "backwards compatibility" between the automated and manual age assessments; the method is efficient and saves time for the user; and it claims to be highly reliable, with good precision. The method has also been validated on both normally developing children and those diagnosed with paediatric endocrinological disorders (Thodberg, 2009; Thodberg *et al.,* 2009).

BoneXpert™ is designed to be equal to the GP Atlas method, on average (Martin *et al.,* 2009); however improvements have been made to overcome the issue of secular trends and racial differences. Reference curves for the four ethnicities (Caucasian, African-American, Hispanic and Asian) have been created for this purpose (Thodberg, 2009).

BoneXpert™ already has clinical use status in Europe, whilst in the USA it is only used as an investigation tool (ie not for clinical use) at present (Thodberg, 2009). It has been used on South African children in the Birth to Twenty study (Richter *et al.,* 2007). The progress of this research is slow, and the study is large, but it may result in the creation of reference curves for South African White and Black children, and potentially even adult height

prediction models (from personal communication with the creator of BoneXpert™, Hans Henrik Thodberg, October 2011).

2.2.3.5 Limitations

BoneXpert™ lacks any image pre-processing capabilities. The program will reject an image of poor quality or where the bone structure is considered too abnormal for analysis (Giordano *et al.*, 2010). The method does not cover the entire age range, from birth to attainment of maturity in the hand-wrist region, and therefore should be extended to cover the ranges newborn to 2 years, and 17 to 19 years in males and females. Larger validation studies may be needed which include a more diverse array of populations groups, ethnicities and observers (Thodberg *et al.*, 2009).

Although more objective than manual methods, BoneXpert™ was not used for skeletal age estimates in this research project, as it is only designed to be equal to the GP Atlas, on average, and not an improvement on the GP method (Martin *et al.*, 2009). The age range which is covered by the program is not consistent with the age ranges of the subjects of this research.

2.3 Comparative Studies of World Populations

The most important factor when performing a skeletal age assessment is the reliability and applicability of the method being used (Cameriere and Ferrante, 2008), and over the past few decades, many researchers have questioned the application of the GP Atlas for skeletal age assessment of modern children (Zhang *et al.*, 2009; Varkkola *et al.*, 2011). As mentioned previously, a common criticism is that, due to the sample on which the method is originally based, the GP Atlas may no longer be representative of the modern child, and therefore should be updated to be more applicable (van Rijn *et al.*, 2009).

Two issues are in debate: whether biological origin or ethnicity (that is, genetics) plays a role in development, or whether it is the environment in which an individual develops which has an effect on the bone growth pattern. Many authors have conducted comparative studies to determine the genetic effect on skeletal maturation by comparing world populations to the GP sample, the details of which are below. In contrast, certain non-genetic factors are believed to have an effect on the rate of skeletal maturation, including poor nutrition, bad sanitation, access to healthcare, hormone imbalances and socioeconomic status, resulting in delays or

advancement of skeletal maturation (Chan *et al.*, 1961; Mellits *et al.*, 1971; Garn *et al.*, 1972; Krogman and Işcan, 1986; Schmeling *et al.*, 2000, 2006; Schaefer and Black, 2005; Olze *et al.*, 2007).

Since the first edition of the GP Atlas was published in 1950, many authors have sought to test its applicability to other populations. A summary of the results from these studies can be found in *Table 2.01*. One issue of concern is the inconsistency of the category names for the populations under investigation in these studies, which creates difficulty when comparing the results of these studies. The issue of political categories, versus biological categories, also comes into play. Racial categories include: Caucasoid, Mongaloid and Negroid; whereas ethnic/nationality categories may include European, Indonesian, or Japanese. Racial and ethnic/nationality categories differ from each other, as they do from categories of ethnicity, such as White, Black or Mixed. Ethnicity is a reflection of one's ancestry, and refers to the biological and cultural background from which an individual comes (from personal communication with Professor Alan Morris). Some studies may compare samples from not only different ethnic categories, but also geographical categories. One such study is that of Soegiharto *et al.*(2009). Growth of White children from the USA was compared to Deutero-Malay[1] children from Jakarta, Indonesia. It can become complicated when attempting to determine whether differences in growth are due to the ethnic differences or geographical differences and effects thereof. It is important to keep these categories in mind when comparing results of these various studies. This research project uses recognised South African categories: White, Black and Coloured (explained further in *Chapter 3).* Although not present in the current sample, 'Indian' is an additional racial category recognised in South Africa, which includes people whose genetic origins stem from the Indian sub-continent.

1 Deutero-Malays are the modern Indonesian population whose biological roots include Arabs, Chinese, Indians, Siamese and aboriginal Malays
http://www.asianinfo.org/asianinfo/malaysia/pro-history.htm

Table 2.01 Summary of Comparative Studies Testing Applicability of the GP Atlas

Author	Population Studied	Age Group (years)	Sample Size	Results
Sutow (1953)	Japanese	6 to 19	2370	Delayed by 6.24 mo, depending on age
Greulich (1957)	Japanese (USA)	5 to 18	898	High similarity
Chan *et al.* (1961)	Chinese (Hong Kong)	0.25 to 19	262	♀: delayed by 0.83 years ♂: delayed by 1.06 years
Johnston (1963)	White - USA (Philadelphia)	7 to 17	120	Advanced by up to 0.65 years depending on age group
Thiemann & Nitz (1991)	East German	0 to 18	5200	Up to 1.5 year delay in appearance of ossification centres
Loder *et al*. (1993)	Black & White (Lake Erie Region)	13 to 18	841	♀: advanced by 0.4 - 0.7 years except during middle childhood. White ♂: delayed by 0.9 years (middle childhood), 0.4 years (late childhood), advanced by 0.5 years (adolescence)
Haiter-Neto *et al.* (1996)	Brazilian	7 to 15	360	GP method applicable, but a correction factor was created for clinical use
Ontell *et al* (1996)	White, Black, Hispanic, Asian	< 19	599	GP Atlas should be used with caution especially for Black and Hispanic ♀ and Asian and Hispanic ♂ (late childhood & adolescence). Age is overestimated by 9 - 11 months
Shaikh *et al*. (1998)	Pakistan	8 to 18	402	♀: Age 8-13 delayed by 0.5 years, advanced from 13 years ♂: Age 8 - 15 delayed by 1 year, advanced from 15 years
Koc *et al*. (2001)	Turkish Males	7 to 17	225	Ages 7 to 13 years: delayed by between 0.25 and 0.72 years. Ages 14 to 17: advance by 0.13 to 0.89 years
Mora et al. (2001)	African (AA)/ Euro (EA) American	0 to 19	534	Pre-pubertal EA children are delayed compared to AA. Post-pubertal EU ♂ are in advance of post-pubertal AA
Büken *et al*. (2007)	Turkish	11 to 18	492	♀: advanced by 0.17 - 1.1 years, ♂: advanced in 15 - 17 years by 0.88 – 0.98 years
Zhang *et al.* (2009)	White, Black, Hispanic, Asians	0 to 18	1390	Significant difference between skeletal and chronological ages of Hispanics and Asians. Cross-racial differences show Hispanics and Asians develop earlier than White and African-American children
Tisè et al.	Italian Caucasian	11 to 19	484	Large error in age estimation especially between the ages of 14 and 18 years

2.3.1 Genetic Effect on Skeletal Development

In 1975, Roche *et al.* demonstrated that the average child living in the USA was less physically mature than predicted by the GP Atlas. This study also revealed differences in development between Black and White populations.

Results from Sutow (1953); Chan *et al.* (1961); Thiemann and Nitz (1991); Loder *et al.* (1993); Haiter-Neto *et al.* (1996); Ontell *et al.* (1996); Shaikh *et al.* (1998); Mora *et al.* (2001); Koc *et al.* (2001); Büken *et al.* (2007); Zhang *et al.* (2009) and Tisè *et al.* (2011) indicate that genetics plays a role in skeletal development, as all samples which differed genetically from the GP Atlas sample were delayed or advanced in their development (see *Table 1.01*). Interestingly, the children from the Loder *et al.* (2003) study were from the same geographic location as the GP Atlas sample, yet they still displayed delayed and advanced skeletal development.

In another study of skeletal development, which did not make use of the GP Atlas for skeletal age estimation, Soegiharto *et al.* (2008) noted marked variations between skeletal and chronological ages of Deutero-Malay children from Jakarta, Indonesia, compared to White children from New York, USA. It was also noted that the timing of skeletal maturity differed between the sexes and ethnicities (Soegiharto *et al.,* 2008).

Serinelli *et al.* (2011) performed a meta-analysis of studies testing the applicability of the GP Atlas. Results of the meta-analysis indicated that 6 of 11 studies resulted in significant under-estimations in Caucasian[2] males; 1 of 10 showed overestimation of Caucasian* females, whilst underestimation was observed in 4 of 10 studies. For the Mongoloid males, 3 of 4 studies showed significant differences between chronological and skeletal ages; whilst all studies of Mongoloid females indicated an overestimation of age (Serinelli *et al.*, 2011).

These studies favour the notion that skeletal development is under genetic control.

2.3.2 Environmental Effect on Skeletal Development

It has been noted that individuals from similar populations living in different regions develop at different rates. An example of this is the study by Sutow (1953). Results show that Japanese children living in Japan are delayed in development by 6 months when compared to the GP Atlas sample. Japanese children living in the United States (Greulich, 1957) faired

2 For consistency, Serinelli *et al.* should have labelled this group 'Caucasoid'

considerably better against the GP Atlas sample, with a high correspondence between chronological age and skeletal age.

Garn *et al.* (1972) recognised the effect of socioeconomic status on skeletal development whilst conducting research on children of African ancestry, from low-income families. Results from this research show that skeletal development in the African-low-income sample was in advance of children of European ancestry, from birth to 7 years of age (Garn *et al.,* 1972). A later study on epiphyseal union in the lower limb supported this claim (Cardoso, 2008a). The influence on development could not be isolated to socioeconomic status, however, as the samples being compared were also of different biological origins.

It has been the suggestion of researchers that the GP Atlas be used with caution, due to potential population and socioeconomic differences which may affect skeletal development (Chan *et al.,* 1961; Büken *et al.,* 2007; Schmidt *et al.,* 2007). These issues need to be addressed when performing a skeletal age estimate (Schmidt *et al.,* 2008). This is especially for South African children as there are many population groups with a disproportion of low- to high-income families. Some authors have even recommended population-specific standards be created, using parameters which are best able to measure growth and development in that specific group, in order to decrease the effect of genetics on skeletal development (van Rijn *et al.,* 2009). The effect of genetics and environment has the potential of affecting the development of South African children considerably, but little has been researched in this regard.

2.4 Skeletal Development Studies on South African Samples

Limited research on skeletal maturation, in particular, the hand-wrist region, is available for South African children. Using radiographic techniques, carpal ossification and carpal fusion were researched by Beresowski and Lundie (1952) and Levine (1972), respectively. Both studies revealed a difference in incidence of these skeletal phenomena in the four South African populations studied. These results suggest that skeletal development may be under genetic control.

In contrast, two studies by Cameron (1984) and Cameron *et al.* (1992) compared and documented growth and nutrition patterns between South African children in rural and urban communities, using measures of height and weight as parameters. These studies indicated

that children living in urbanised communities, with elevated socioeconomic environments tended to develop in advance of their rural counterparts (Cameron, 1984; Cameron *et al.*, 1992). These results are further supported by research in other African countries which suggest that growth and development are strongly influenced by environmental factors (Corlett, 1986; Corlett and Woollard, 1988).

A recent pilot study by Phillips and Thompson (2000) correlated bone age and dental age in South African children, to ascertain whether age determined by dental and hand-wrist development was in agreement with chronological age. The two methods assessed in this study were the GP Atlas method for skeletal age estimation, and the dental age estimation method of Moorees, Fanning and Hunt (1963).

The applicability of these methods was tested on children of similar genetic make-up and socioeconomic status, comprising of "Caucasian, Negroid and Mixed"[3] population groups, living in the Western Cape region of South Africa (Phillips and Thompson, 2000). Results of the study indicate that the GP Atlas method consistently under-estimated skeletal age for children from all three population groups, with some cases exhibiting a difference between chronological age and estimated skeletal age of up to 1 year. Whilst dental age estimation remained fairly accurate for children of mixed ancestry, the method was only fairly accurate for Caucasian children. The same method was deemed inaccurate for Negroid children (Phillips and Thompson, 2000). In light of the results from this pilot study, Phillips and Thompson (2000) suggested further research be conducted in this regard, the results of which may be used to create an age estimation database for African, and more specifically, South African population groups.

In 2008, the author of this research project conducted a pilot study to assess the applicability of the GP Atlas for South African children (Roff, 2008). Skeletal age estimates using 169 radiographs from the four main population groups in South Africa (White, Black, Coloured and Indian) was performed using the GP Atlas method. It was found that skeletal age was underestimated in 66% of males and 59% of females, and overestimated in 34% of males and 40% of females.

It was suggested that new standards for age estimation be created for South African populations; although the GP Atlas was still a useful age estimation tool, it was no longer

3 These categories most probably refer to White, Black and Coloured children from the Western Cape region as used in this current study

applicable to South African children. Due to the small sample size, further research was to be conducted.

Dembetembe (2010) advanced this concept by researching age estimation at the wrist joint for individuals between the ages of 14 and 22, focussing specifically on those of African origin. Results of this study concurred with the results of Phillips and Thompson (2000) and Roff (2008). Dembetembe (2010) found that the GP Atlas method was not directly applicable to South African children of African biological decent (that is, Black children), citing differences in biological origin of their sample compared to the GP Atlas sample as a possible reason for the discrepancies. More specifically between the ages of 15.5 years in females and 16.5 years in males, the GP Atlas method under-estimated skeletal age by 1 year on average, for this sample. It was suggested by Dembetembe (2010) that further research be conducted to create new population specific skeletal age estimation standards for South African children. Due to the small sample sizes in the studies by Roff (2008) and Dembetembe (2010) little advancement has been made to create new age estimation standards from these areas of research.

This study aims to put to rest the questions surrounding the applicability of the GP Atlas method for skeletal age estimation on a South African sample.

CHAPTER 3

MATERIALS AND METHODS

3.1 Materials

3.1.1 Source of Materials

Pre-existing full-body, digital radiographs were obtained from the Trauma Unit at Red Cross War Memorial Children's Hospital (hereafter termed 'Red Cross') and from the Tygerberg and Salt River Mortuaries in Cape Town, South Africa. Permission to use these images was granted by the Head of Forensic Medicine at the Universities of Cape Town and Stellenbosch, and the Head of the Division of Paediatric Radiology at Red Cross. The use of pre-existing radiographs is preferred to prevent the unnecessary exposure of any healthy, living individual to radiation, no matter how small the dose.

The radiographs were taken using a StatScan™ system (LODOX™ Systems, (Pty) Ltd., Sandton, South Africa). This is a fan-beam, linear-slot scanning radiography unit, which uses a low-radiation dose, whilst still producing bodygrams with an image-quality comparable to that of conventional radiographs (Pitcher *et al.,* 2008; Douglas *et al.,* 2010). The fully-body radiograph of an adult is generated in approximately 13 seconds, depending on the height of the patient, and is even faster in children. It is for this reason that the StatScan™ system in the Trauma Unit of Red Cross is very valuable in triage evaluation (Douglas *et al*., 2010). All individuals from the Red Cross sample were alive at the time of radiography.

All individuals radiographed at the mortuaries were already deceased. The radiograph generated from each deceased individual forms part of the post-mortem report. It is considered standard practice at Salt River Mortuary to radiograph every individual. The protocol at Tygerberg Mortuary differs somewhat. A child will only be radiographed in cases where child abuse is suspected or the location of ballistics is required. On request by the researcher, a Forensic Pathologist at Tygerberg Mortuary radiographed all children under the age of 14 years, from June 2009, regardless of their cause of death.

Regular back-ups of the digital images generated at each of the three StatScan™ locations was done by a technician from LODOX™ Systems, based at the University of Cape Town. These images were duplicated onto an external hard-disc drive and updated bi-annually for the purposes of this research project.

3.1.1.2 Areas Covered by Hospital and Mortuaries

The areas covered by Tygerberg and Salt River mortuaries are based on South African Police Force stations in the Cape Town Metro area.

In the event of an unnatural death (regardless of the race, culture, sex or age of the individual), the deceased's body will be transported to either Salt River or Tygerberg mortuary for a post-mortem. The choice of mortuary depends solely on the Police station at which the death was reported, that is, the Police station whose jurisdiction encompasses the area in which the person died. In some cases, this may not be the station in closest proximity to the residence of the deceased.

Red Cross Children's Hospital has a much wider coverage area, with approximately 40 % of patients referred from hospitals or clinics outside of the Western Cape Province. Patients may hail from any of the nine provinces within South Africa or from countries outside of South Africa, such as Kenya, Botswana, Zimbabwe, Mauritius and Namibia. Red Cross is the only institution in the country which is dedicated solely to child healthcare, and more specifically, for the care and treatment of children under the age of 13 years. The majority of patients are 'hospital' or government-funded patients, with only 5% of patients funded by a private medical aid or healthcare scheme (Children's Hospital Trust, 2008). Trauma patients (used in this research project) may be flown in from areas surrounding Cape Town, as there is an emergency medical helicopter facility available.

Table 3.01 outlines the areas covered by each of the mortuaries, whilst the accompanying map provides a geographical representation of these areas. The separation of jurisdiction of these facilities can be seen by the black dotted line in the map of *Table 3.01*.

Salt River mortuary covers more suburbs than Tygerberg mortuary; however, the geographical area is approximately the same for each.

Table 3.01 Suburbs covered by Salt River and Tygerberg Mortuaries

Salt River Mortuary			Tygerberg Mortuary	
Athlone	Langa	Philippi East	Belhar	Khayelitsha
Atlantis	Lansdowne	Pinelands	Bellville	Kleinvlei
Camps Bay	Maitland	Rondebosch	Bellville South	Kraaifontein
Cape Town	Manenberg	Sea Point	Bishop Lavis	Kuilsriver
Claremont	Melkbosstrand	Simons Town	Bonteheuwel	Lingelethu West
Diep River	Milnerton	Steenberg	Bothasig	Macassar
Fish Hoek	Mitchell's Plain	Strandfontein	Brackenfell	Mfuleni
Grassy Park	Mowbray	Table Bay Harbour	Delft	Parow
Gugulethu	Muizenberg	Table View	Durbanville	Ravensmead
Hout Bay	Nyanga	Woodstock	Elsiesriver	
Kensington	Ocean View	Wynberg	Goodwood	
Kirstenhof	Philippi		Harare	

Adapted from City Map Viewer © City of Cape Town, SDI & GIS Departments

▪▪▪▪▪▪ Separation of jurisdictions of Salt River and Tygerberg Mortuaries.

3.1.2 Research Sample

From a potential sample of over 10 000 images, 1356 radiographs met the following selection criteria and were used for age estimation analysis:

(a) *Age:* Only individuals between the age of 0 – 13 years (inclusive) were selected; that is, any individual 14 years and older was excluded. This age range was chosen in order to incorporate all ages where formation of the carpal bones and epiphyses of the bones of the hand and wrist takes place, but epiphyseal union has not yet occurred.

(b) *Correct positioning of the hand:* Radiographs were included if at least one hand was in Anterior-Posterior (AP) or Posterior-Anterior (PA) position. LODOX™ Systems has a specific protocol relating to body position, which is to be followed when using the StatScan™. It is easier to apply this protocol to living individuals as the patient can be instructed to remain as still as possible and to position themselves in a specific way whilst the radiograph is being captured. This is especially true at Red Cross because the StatScan™ is used in triage evaluation and it is in the best interest of the medical staff and the patient for the correct position to be employed. At the mortuaries, however, the main purpose of the StatScan™ is to locate ballistics and identify any major injuries (such as broken bones) which may not be visible in the soft tissue of the deceased. Correct body positioning according to the LODOX™ protocol is not paramount, especially as the mortuaries process a large number of bodies each day. Added to this is the effect of rigor mortis on the corpse, making it more difficult to position the body correctly. This often results in an image which does not represent a clear AP or PA position and is one of the contributing factors to the large sample size from Red Cross as opposed to the mortuaries (see *Table 3.02*).

(c) *Visible regions of the hand:* the carpal, metacarpal and proximal phalangeal regions had to be fully visible in all individuals, regardless of age. In older individuals (older than 7 years) it was required that the epiphyses of the intermediate and distal phalanges were also visible in the radiograph.

(d) Clarity of the image: Clarity of the radiograph in at least one hand-wrist region was required in order for it to be incorporated into the sample. The radiograph was excluded if there was evidence of trauma, movement of the individual whilst the radiograph was being captured (which is seen as an "undulating distortion of the relevant limb" – Pitcher *et al*., 2008), or if hospital or mortuary identification tags or hospital equipment (tubes, etc.) covered any region of the hand.

(e) Sex of the individual: In some cases from Red Cross, the sex of the individual was not provided. Soft tissue, however, is visible on StatScan™ images so the sex of the patient could be determined in the majority of individuals. Radiographs were excluded if sex could not be determined by soft tissue.

(f) Use of the Left hand: Wherever possible, the left hand was used to estimate skeletal age; however, for various reasons (see point *(d)*, above), not all left hands were viable for analysis. In these cases, the right hand was used instead. Use of the left hand is stipulated in the International Agreement for the Unification of Anthropometric Measurements to be made on Living Subjects, which was drawn up at the Monaco (1906) and Geneva (1912) Conferences for Physical Anthropologists (Greulich and Pyle, 1959), and is the same method used in the GP Atlas. It allows standardisation and comparison between studies.

Examples of (b), (c) and (d) can be found in *Appendix C*.

Table 3.02 summarizes the number of samples obtained from each StatScan™ location.

Table 3.02 Summary of Sample Number Based on StatScan™ Location

Location	Male	Female	Total
Red Cross	639	379	1018
Salt River	141	126	267
Tygerberg	41	30	71
Total	821	535	1356

3.2 Methods

Every radiograph captured by the StatScan™ has a unique number which is generated by the StatScan™ computer software. It is, essentially, the number of the image on the StatScan™ database. This was used as a means of reference for each radiograph that was analysed (See "Data #" in *Appendix D*). This should not be confused with the reference number (See "Ref #" in *Appendix D*) which was generated by the researcher.

3.2.1 Information Collected from Radiographs

Once a radiograph met the selection criteria (as outlined in *Section 3.1.2*) the following data were collected:

(a) Red Cross radiographs: Data number (generated by the StatScan™ software); medical record number; sex; date of birth; date of radiograph; and the hand which was analysed (left or right). Red Cross' Trauma Unit does not record the race of the patient, so no data for race was available from these radiographs.

(b) Salt River and Tygerberg mortuaries: Data number and mortuary docket number (WC##/Body Count Number/Year) were captured from the radiographs. Additional mortuary records provided the age to the nearest day, week or month (for individuals younger than 1 year); date of birth (for individuals older than 1 year); date of death; sex; race (Black, White or Coloured); and police station (area) at which the death was reported. Also noted was the hand selected for analysis (left or right).

Racial categories were based on those outlined in the Population Registration Act, No 30 of 1950. Although this act was abolished in 1991, the concept of racial classification is still used in many arenas in South Africa, including identification of deceased individuals. In such instances, it is either the family of the deceased, the mortuary technician who collects the body or the Police official on the scene of the death who assigns racial classification. Under these circumstances, racial classification is highly subjective.

3.2.1.1 Assessment of Socio-Economic Status (SES)

The police station (area) and average monthly house-hold income were used as indirect indicators of socio-economic status (SES) of the mortuary sample. This was done using an internet-based program called Lightstone © which provides extensive information on most suburbs within South Africa.

The program is predominantly used by financial, retail, insurance, automotive and property institutions (Lightstone, 2011).

Since, 1993, the data for average valuation of free-hold or sectional-title homes, number of adults per suburb, and average monthly house-hold income, amongst others, has been collected from the Deeds offices and local municipalities throughout the country. It is updated weekly and is suburb specific.

Assessment of SES involved two steps. Firstly, a total of 41 Police stations were contacted to determine their geographic jurisdiction, which most often included more than one suburb. Each suburb was entered into the Lightstone© database, where the average monthly house-hold income (which is given as a range) and total number of adults was noted for that suburb. This was completed for each suburb within a given Police station 'area'. In some cases, the suburb search within Lightstone© yielded no result, and these suburbs were excluded from the final analysis.

Secondly, the median monthly house-hold income was calculated according to the number of people in the Police station 'area' who earned within that income range. An average monthly household income was then calculated based on the median house-hold income, and used as an indirect indicator of SES. For example, a given Police station area may have a median house-hold income of R 1 500 – R 3 000 per month. The average house-hold income would therefore be R 2 250 per month.

Once these data had been collected, a skeletal age estimate using the GP Atlas was performed (see *Section 3.2.3* for a detailed explanation of this method).

3.2.2 Age Groups and Organisation of Data

Following the completion of skeletal age analysis, the chronological age of each individual was calculated. This was done in this sequence to reduce observer bias. The data were then organised according to chronological age, in ascending order; thereafter the researcher assigned a unique alphanumeric reference number to each individual (see "Ref #" in Appendix B). The first 3 letters of this reference refers to the database from which the radiograph was obtained (RXH - Red Cross; SRM – Salt River Mortuary; and TYM – Tygerberg Mortuary). The fourth letter of the reference number indicated the sex of the individual, either male (M) or female (F).

Finally, the number at the end of the reference indicates the number of that individual within the sample (e.g. RXHM10 would be the tenth radiograph found in the database of males from the Red Cross). These numbers proved to be a useful reference once the data from each database was merged into one data-sheet.

Individuals were then grouped into age categories that corresponded to the standards in the GP Atlas. These skeletal age standards are divided according to sex, and the age categories differ between the sexes. According to Bogin (1999), the neonatal or 'newborn' period includes the "first 28 days postpartum". The GP Atlas does not have a standard or age group for children who are older than 28 days, but have not yet reached 3 months of age (which is the next sequential age standard in the GP Atlas). It is for this reason that an additional age group, namely '1-3 months' was created for both sexes, by the researcher. The age categories can be found in *Table 4.02* in *Chapter 4, Section 4.1.1*.

3.2.3 Analysis of Hand-Wrist Radiographs using the GP Atlas Method

Although non-experienced users of the GP Atlas method fair almost as well as trained users when conducting skeletal age estimates (Lynnerup *et al.,* 2008), the researcher was trained by a Paediatric Radiologist from Red Cross, prior to the commencement of this research, on the features of importance when examining a radiograph for skeletal age estimation. It is assumed that the researcher's skill will increase the more radiographs are analysed (Roff, 2008), and the consultation with the Radiologist served merely to ensure the analysis was performed correctly at the outset.

Selection and analysis of the radiographs involved the following process:

(a) Following points (a) to (e) in *Section 3.1.2*, radiographs were selected based on the age of the individual; at least one hand (preferably the left) being in the correct orientation and position; sex identification based on radiograph information or soft tissue; and sufficient image clarity. Radiographs were grouped by sex into the age groups outlined in the GP Atlas.

(b) Once a radiograph had been selected it was compared to the same sex standard in the GP Atlas to which it most closely resembled (A complete explanation from pages 35-37 of the GP Atlas can be found in *Appendix E*). This method follows that used by clinicians to estimate skeletal age using the hand-wrist region. It stipulates in the GP Atlas that one should compare a sample radiograph to the same-sex standard which is

closest in chronological age; however, the clinicians compare a radiograph with the same-sex standard to which it most closely resembles. Excluding chronological age from the assessment reduces observer bias and is a more realistic method of skeletal age analysis.

(c) Images were viewed on a Desktop Computer using the Digital X-ray Diagnostic Viewer *D.V.S Version 2.8.8.0* (Copyright LODOX™ 2005).

3.2.3.1 Features used during Skeletal Age Assessment

According to Greulich and Pyle (1959), features used for a preliminary selection of a specific standard vary depending on the stage of development of the individual.

Developmental features of infancy and early childhood include the appearance, size and state of ossification of the carpal bones and the epiphyses of the ulna, radius, metacarpals and phalanges. In later childhood, it is the change in size, shape and structure of these regions of the hand-wrist that are of interest. No features of termination of bone growth were included in the analyses, as these occur later than the targeted age range for this research. The features and regions used for preliminary radiograph selection can be seen in *Figure 3.01*.

Ossification sequences of the bones of the hand-wrist region can be seen in *Figure 3.02* and a detailed explanation of the changes which occur in each sequence is outlined in *Figures 3.03.1 – 3.18.3* (Adapted from Greulich and Pyle, 1959). These provide a stage-by-stage explanation of the features analysed for each bone in the hand-wrist region, when performing a skeletal age estimate on individuals younger than 14 years.

Once a standard was selected from the GP Atlas, the radiograph was compared to the adjacent standards (younger and older) for accuracy and reference purposes. If a radiograph did not correspond entirely to one specific standard, but instead was a representation of the intermediate developmental stage between two standards, the average age of the two adjacent standards was taken as the skeletal age of the individual.

Observed features on sample radiographs differed slightly from the features represented in the corresponding standard, in 398 individuals. One example of this is the appearance of an ossification centre either earlier or later than specified in the GP Atlas (e.g. the frequent early appearance of the Triquetral). Due to the high degree of corresponding features present in both the radiograph and the standard in the GP Atlas, skeletal age was hence assigned, and the additional or lacking feature was duly noted. The frequency of these features can be seen in *Table 4.12, Chapter 4*.

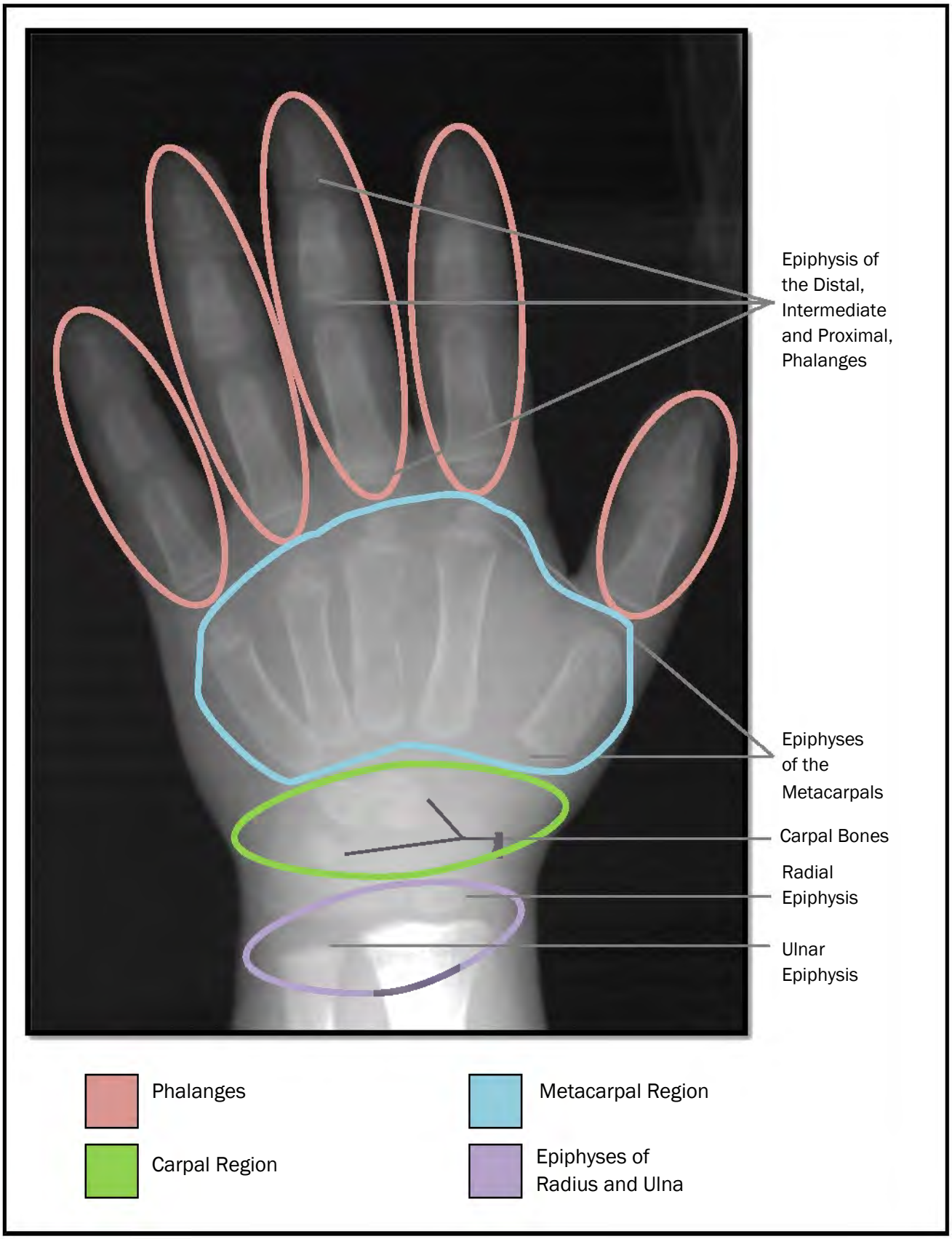

Figure 3.01 *Features and regions used for the preliminary selection of a radiograph. Developmental features of infancy and early childhood include the appearance, size and state of ossification of the Carpal bones and the epiphyses of the Ulna, Radius, Metacarpals and Phalanges. In later childhood, it is the change in size, shape and structure of these regions of the hand-wrist that are of interest.*

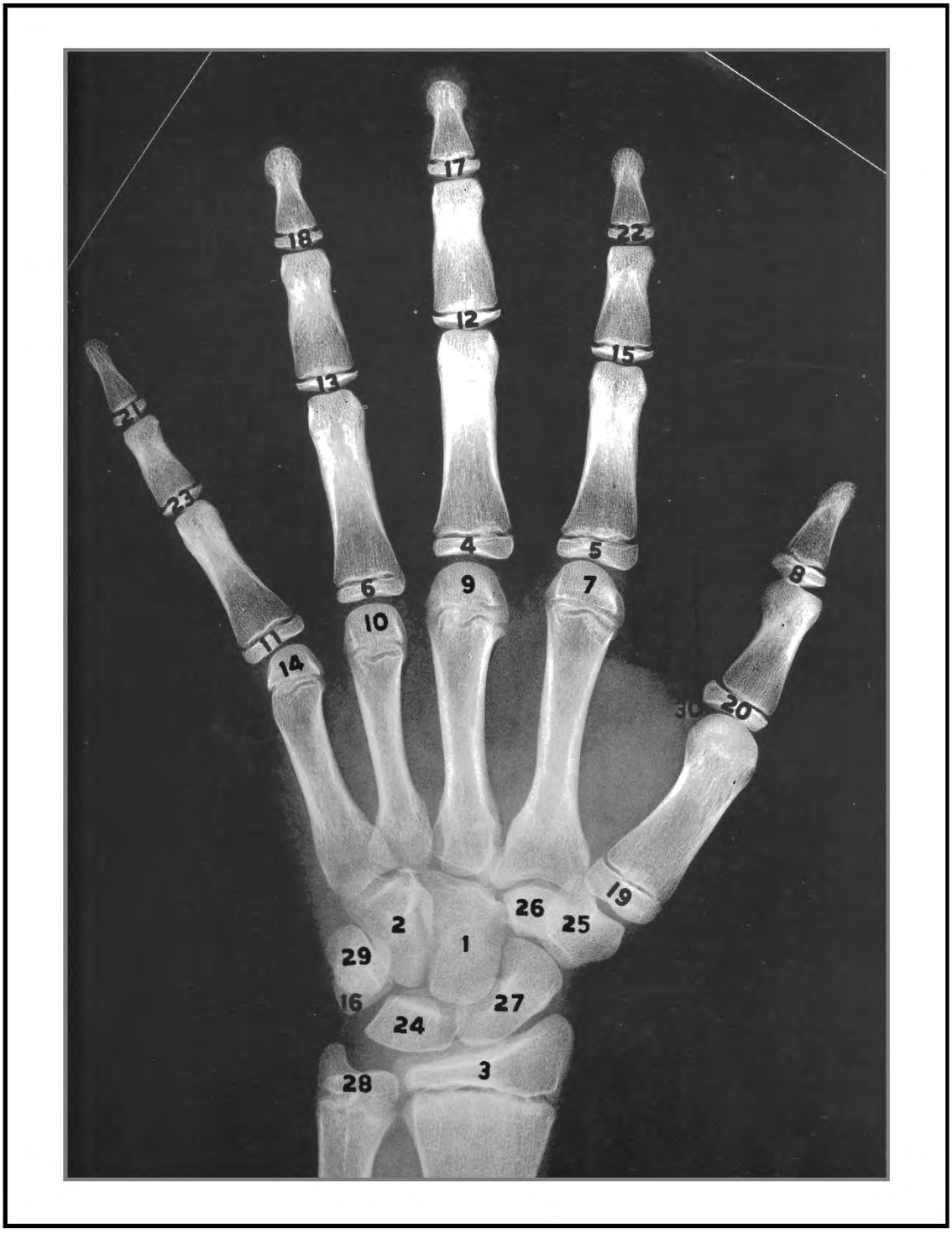

Figure 3.02 *Maturity indicators of the hand and wrist – taken from pages 186 and 187 in* Radiographic Atlas of Skeletal Development of the Hand and Wrist *(Greulich and Pyle (1959). The numbers indicated the approximate order in which ossification begins. 1, Capitate; 2, Hamate; 3, Distal Epiphysis of the Radius; 4*, epiphysis of proximal phalanx of Digit III; 5*,epiphysis of proximal phalanx of Digit II; 6*, epiphysis of proximal phalanx of Digit IV; 7, epiphysis of Metacarpal II; 8, epiphysis of distal phalanx of Digit I; 9, epiphysis of Metacarpal III; 10, epiphysis of Metacarpal IV; 11, epiphysis of proximal phalanx of Digit V; 12, epiphysis of middle phalanx of Digit III; 13, epiphysis of middle phalanx of Digit IV; 14, epiphysis of Metacarpal V; 15, epiphysis of middle phalanx of Digit II; 16, Triquetral; 17, epiphysis of distal phalanx of Digit III; 18, epiphysis of distal phalanx of Digit IV; 19, epiphysis of Metacarpal I; 20*, epiphysis of proximal phalanx of Digit I; 21, epiphysis of distal phalanx of Digit V; 22, epiphysis of distal phalanx of Digit II; 23*, epiphysis of middle phalanx of Digit V; 24* Lunate; 25* Trapezium; 26* Trapezoid; 27*, Scaphoid; 28 distal epiphysis of Ulna; 29, Pisiform; 30 Sesamoid of adductor pollicus.*

I

In the full-term newborn, the distal end of the diaphysis is flared and its margin is somewhat flattened. The epiphysis is entirely cartilaginous.

Male Standard *1*

Female Standard *1*

II

The initial small ossification centre for the epiphysis forms slightly nearer the lateral than the medial border of the distal margin of the shaft.

Male Standards *5 and 6*

Female Standards *4 and 5*

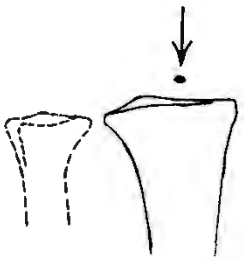

III

The proximal margin of the epiphysis has begun to flatten. As a rule, the ulnar side of the epiphysis is now pointed; its radial side is relatively thicker and rounded. The longest axis of the epiphysis is transverse.

Male Standards *6 and 7*

Female Standards *5 and 6*

IV

The growth cartilage plate has attained its characteristic thickness centrally. The outline of the volar margin of the epiphysis begins to be visible within the epiphyseal shadow close to its distal dorsal margin and extending around its ulnar tip.

Male Standards *9 and 10*

Female Standards *8 and 9*

V

The epiphysis has elongated transversely. The white outline of the volar margin of the epiphysis is now distinct as it extends laterally from the ulnar tip along the inner bone margin of the epiphysis beyond the centre of the shaft.

Male Standards *11 and 12*

Female Standards *9 and 10*

(Image adapted from Greulich and Pyle, 1959)

Figure 3.03.1 *Age related changes in the distal epiphysis of the radius, for males (newborn to 4 years) and females (newborn to 3 years).*

VI

Along the ulnar tip, the distal margin of the epiphysis is slightly flattened as its lunate and ulnar articular facets begin to differentiate.

Male Standards *12 and 13*

Female Standards *11 and 12*

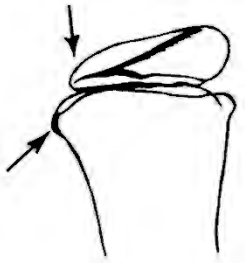

VII

That portion of the epiphysis from which the styloid process develops begins to enlarge. The central arrow points to the approximate centre of the distal articular surface of the radius. Comparison of Male Standard 6 and Female Standard 5 with the standards listed below shows that the original ossification centre, according to its alignment with the lateral side of the capitate, formed beneath the approximate centre of this epiphyseal articular surface.

Male Standards *14 and 15*

Female Standards *13 and 14*

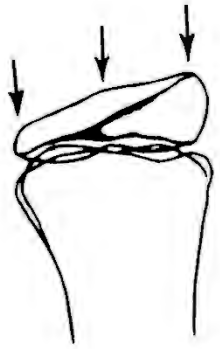

VIII

The epiphysis is now as wide as the adjacent margin of the diaphysis. The styloid process, which requires a period of years for its full development, is now well formed.

Male Standards *21 and 22*

Female Standards *18 and 19*

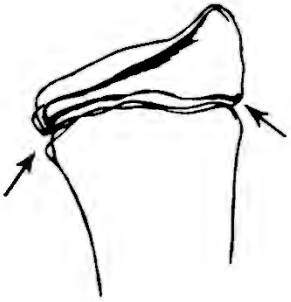

IX

The proximal margin of the epiphysis has shaped further to the contour of its diaphysis. The ulnar articular facet is flattened, and the epiphysis cape the shaft on the lateral side as well. The extent of each articular surface is now defined.

Male Standards *24 and 25*

Female Standards *19 and 20*

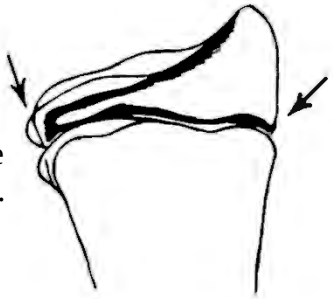

(Image adapted from Greulich and Pyle, 1959)

Figure 3.03.2 *Age related changes in the distal epiphysis of the radius, for males (4 to 14 years) and females (3.5 to 12 years).*

I

In the full-term newborn, no centre of ossification is visible in the epiphysis. The distal end of the shaft is flared, and it has a small beak-shaped projection on the radial side. The distal margin is usually proximal to the corresponding margin of the radius.

Male Standard *1*

Female Standard *1*

II

A small ossification centre is now visible in the epiphysis; occasionally multiple centres are seen. The space between the nodule and the shaft is wide.

Male Standards *14 and 15*

Female Standards *14 and 15*

III

The epiphyseal nodule has a smooth, rounded margin. The space between the nodule and the distal margin of the shaft remains about as wide as it was in stage II.

Male Standards *15 and 16*

Female Standards *15 and 16*

IV

The epiphysis usually differentiates according to one of two patterns. In that shown in "A" the future styloid portion develops first. At this stage the epiphysis is oval and its long axis is oblique. In that shown in "B" the epiphysis is flatter and grows principally radialward and there is no early enlargement of its styloid portion.

Male Standards *15 and 16*

Female Standards *15 and 16*

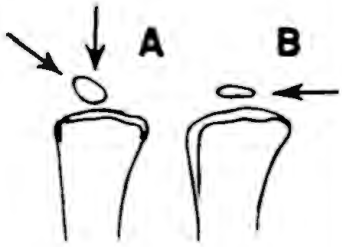

V

In type "A" the epiphysis begins to grow radialward and its proximal margin flattens. In type "B" it widens more symmetrically, and there is as yet no thickening of its future styloid region. In both types the central portion of the growth cartilage plate is now as thin as it will become until the epiphysis begins to fuse with its shaft. Beginning with stage V, type "A", the larger bone, was traced from a boy's film, and type "B", the smaller bone, was traced from a girl's film.

Male Standards *16 and 17*

Female Standards *16 and 17*

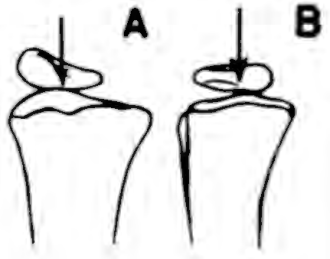

(Image adapted from Greulich and Pyle, 1959)

Figure 3.04.1 *Age related changes in the distal epiphysis of the ulna, for males (newborn to 8 years) and females (newborn to 8.8 years).*

VI

The outline of the volar margin of each type of epiphysis can be distinguished from that of the dorsal margin by the white (volar) marking which begin to appear within the shadow of the epiphysis.

Male Standards *17 and 18*

Female Standards *16 and 17*

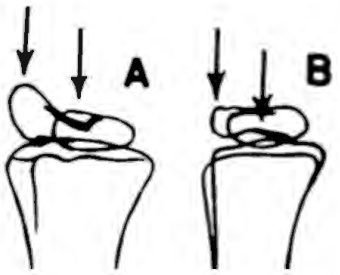

VII

The epiphysis enlarges in the region of the future styloid process, and its lateral (radial) margin is bevelled. In type "B" the development of the smaller styloid tip is not so far advanced.

Male Standards *21 and 22*

Female Standards *18 and 19*

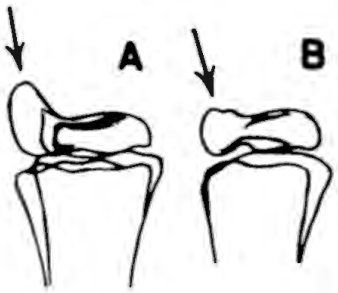

VIII

The shape of the ulnar half of the radial-ulnar joint is beginning to be defined. The epiphysis shapes to the contours of the adjacent articular surface of the radius and to that of the radial side of its own shaft. The non-articular styloid region can now be identified as the part of the epiphysis lateral to its thinnest mid-portion.

Male Standards *22 and 23*

Female Standards *18 and 19*

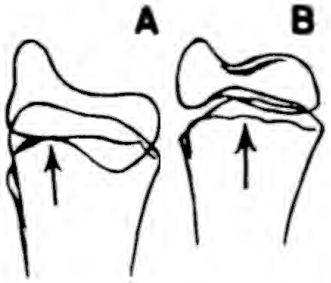

IX

The epiphysis is now as wide as the shaft and its articular surface have now attained their adult form. The growth cartilage plate is very thin centrally, where the epiphyseal-diaphyseal fusion is about to begin.

Male Standards *24 and 25*

Female Standards *19 and 20*

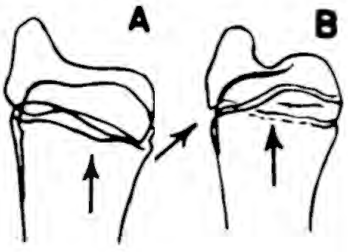

(Image adapted from Greulich and Pyle, 1959)

Figure 3.04.2 *Age related changes in the distal epiphysis of the ulna, for males (8 to 14 years) and females (8.8 to 12 years).*

I

Capitate: Ossification usually begins from a single centre which is visible below (proximal to) the base of the third metacarpal.

Hamate: Ossification usually begins from a single centre which is visible below the base of the fourth metacarpal and very slightly distal to the capitate nodule.

	CAPITATE	HAMATE
Male Standards	*1 and 2*	*1 and 2*
Female Standards	*1 and 2*	*1 and 2*

II

Capitate: The bony nodule is rounded and its margin is smooth

Hamate: The bony nodule, slightly smaller than the capitate nodule, is rounded and its margin smooth.

	CAPITATE	HAMATE
Male Standards	*2 and 3*	*2 and 3*
Female Standards	*2 and 3*	*2 and 3*

III

Capitate: Its hamate surface begins to flatten. Its long axis is now approximately vertical.

Hamate: The margin of the hamate remains undifferentiated.

	CAPITATE	HAMATE
Male Standards	*3 and 4*	*3 and 4*
Female Standards	*3 and 4*	*3 and 4*

IV

Capitate: Flattening of its hamate margin is spreading vertically and is now distinct in the centre of this margin.

Hamate: Its future triquetral surface has begun to flatten.

	CAPITATE	HAMATE
Male Standards	*5 and 6*	*6 and 7*
Female Standards	*4 and 5*	*4 and 5*

V

Capitate: The arrow on the right points to the centre of the capitate-hamate joint. The articular centre can be identified in the film before the margin begins to be concave centrally by noting the site of closest apposition of the two bones.

Hamate: Its longest axis is now oblique and is directed distally toward the base of the fifth metacarpal.

	CAPITATE	HAMATE
Male Standards	*7 and 8*	*8 and 9*
Female Standards	*7 and 8*	*7 and 8*

(Image adapted from Greulich and Pyle, 1959)

Figure 3.05.1 *Age related changes in the capitate and hamate, for males (newborn to 2.8 years) and females (newborn to 2 years).*

VI

Capitate: Its hamate surface is beginning to appear concave. The upper right-hand arrow points to the small, convex portion of the margin where its metacarpal II and trapezoid articular facets will subsequently develop. The curvature of the radial side of the capitate is beginning to be reduced. In some capitates a notch has now begun to form at the junction of its trapezoid and scaphoid facets.

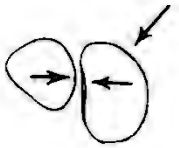

Hamate: Its capitate margin has begun to shape vertically to the contour of the adjacent margin of the capitate. Its metacarpal IV facet has begun to flatten.

	CAPITATE	HAMATE
Male Standards	*16 and 17*	*13 and 14*
Female Standards	*10 and 11*	*9 and 10*

VII

Capitate: A small facet which will articulate with the base of the second metacarpal is now visible. The concavity on the hamate surface has enlarged vertically and has deepened, in the process of conforming further to the adjacent surface of the hamate.

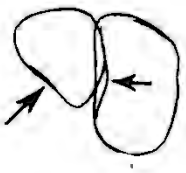

Hamate: A concavity has begun to form on its ulnar margin opposite the distal end of the triquetral. That portion of the bone which articulates with the base of the fifth metacarpal begins to project.

	CAPITATE	HAMATE
Male Standards	*17 and 18*	*15 and 16*
Female Standards	*16 and 17*	*14 and 15*

VIII

Capitate: Parts of the volar margin of its hamate and metacarpal articular surfaces are distinguishable as white outlines within the bone shadow. Approximately midway on its lateral (radial) margin, the junction of its trapezoid and scaphoid facets can be seen.

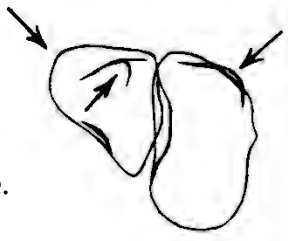

Hamate: The volar and dorsal margins of its surface which articulates with the fourth metacarpal are becoming distinguishable. The angular white outline of the tip of the hamulus is often superimposed upon the volar outline. The proximal end of the bone has become relatively constricted as it shaped further to the adjacent surface of the capitate and triquetral.

	CAPITATE	HAMATE
Male Standards	*19 and 20*	*21 and 22*
Female Standards	*18 and 19*	*18 and 19*

(Image adapted from Greulich and Pyle, 1959)

Figure 3.05.2 *Age related changes in the capitate and hamate, for males (4.5 to 12.5 years) and females (2.5 to11 years).*

I

Ossification of the triquetral usually begins from a single centre. The initial nodule forms between the hamate and the distal end of the ulna.

Male Standards *8 and 9*

Female Standards *7 and 8*

II

The nodule is rounded and its margins are smooth and undifferentiated. Its characteristic longest axis is as yet not visible.

Male Standards *10 and 11*

Female Standards *8 and 9*

III

Its hamate surface has begun to flatten. Its longest axis extends obliquely from its distal tip to its proximal end.

Male Standards *13 and 14*

Female Standards *12 and 13*

IV

The developing triquetral is distinctly elongated. Its distal half is now narrower than its proximal half, and its free ulnar margin appears less convex than it was in the preceding standards. Some triquetrals have a narrow, pointed distal end at this stage of development.

Male Standards *14 and 15*

Female Standards *13 and 14*

V

The blunted, angular osseous corner now forms at the junction of its hamate and lunate facets; these facets have begun to flatten. The proximal end of the bone is squarish, and the distal end remains rounded or pointed.

Male Standards *17 and 18*

Female Standards *15 and 16*

(Image adapted from Greulich and Pyle, 1959)

Figure 3.06.1 *Age related changes in the triquetral and pisiform, for males (2 to9 years) and females (1.5 to 7.8 years).*

VI

As part of the volar margin of the triquetral can now be seen as a white outline within the bone shadow close to its hamate margin.

At this stage, the pisiform usually begins to ossify, but the first small nodule is likely to be obscured completely by the triquetral unless the position of the hand is as favourable as it is in Male Standard 20.

Male Standards *19 and 20*

Female Standards *16 and 17*

VII

The distal half of the triquetral expands and becomes either blunted or squarish. The hamate articular surface is beginning to acquire its characteristic concavo-convex shape. The outline of its volar margin, within the bone shadow, has thickened and now extends around the osseous corner at the junction of its hamate and lunate facets. The free ulnar margin of the triquetral seldom shows a volar outline of comparable density.

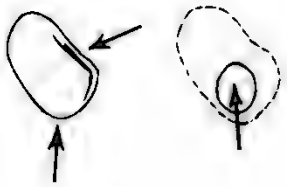

The ossification centre of the pisiform is now large and dense enough to be visible through the shadow of the triquetral. Its margin remains somewhat thing and roughened.

Male Standards *22 and 23*

Female Standards *17 and 18*

(Image adapted from Greulich and Pyle, 1959)

Figure 3.06.2 *Age related changes in the triquetral and pisiform, for males (10 to 13 years) and females (7.8 to 10 years).*

I

Ossification begins from a single centre, or occasionally, from two centres. The initial nodule appears distal to the ulnar tip of the shaft of the radius and the developing capitate-hamate joint.

Male Standards *9 and 10*

Female Standards *9 and 10*

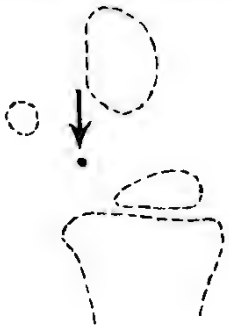

II

Its capitate margin begins to flatten.

Male Standards *11 and 12*

Female Standards *10 and 11*

III

The bone has elongated transversely, and its longest axis has thus become visible. Its triquetral half is now its thickest portion.

Male Standards *13 and 14*

Female Standards *12 and 13*

IV

The dorsal and the volar aspects of the bone are beginning to be distinguishable. A short white marking is visible within the bone shadow, just inside the distal border. This outline forms across the mid-portion of its volar surface.

Male Standards *15 and 16*

Female Standards *14 and 15*

V

Its triquetral facet is well flattened, and a blunted osseous corner is forming between this facet and the proximal margin of the bone. The thick white marking within the bone shadow is developing quite transversely; the thin dorsal portion of the capitate articular surface is enlarging to for a somewhat triangular process distal to the marking

Male Standards *18 and 19*

Female Standards *17 and 18*

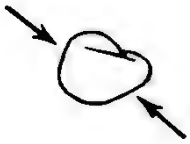

(Image adapted from Greulich and Pyle, 1959)

Figure 3.07.1 *Age related changes in the lunate, for males (2.7 to 10 years) and females (2.5 to 10 years).*

VI

Its scaphoid facet has become as well flattened as its triquetral facet, and their flatness gives the bone a somewhat squarish appearance. The thick white marking within the bone shadow distally now forms the middle third of a tripartite, crescent marking which extends across the proximal row of carpals.

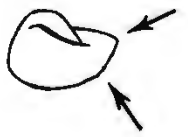

Male Standards *20 and 21*

Female Standards *18 and 19*

VII

The articular facets are each individualised in shape. Blunted osseous corners mark off the extent of each facet. The spacing between the thin dorsal outline of the capitate surface of the bone and the transverse marking across the bone shadow denotes the depth of its capitate articular surface. The outline of the transverse marking is now completed.

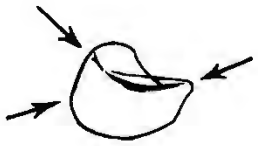

Male Standards *23 and 24*

Female Standards *19 and 20*

VIII

The osseous corners are distinct and smooth. The young adult contours of the lunate have now been attained.

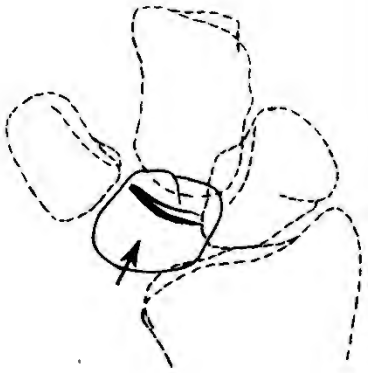

Female Standards *22 and 23*

(Image adapted from Greulich and Pyle, 1959)

Figure 3.07.2 *Age related changes in the lunate, for males (11 to 14 years) and females (10 to 14 years).*

I

Ossification usually begins from a single centre. The initial nodule is usually distal to the lateral (thickest) portion of the radial epiphysis.

Male Standards *14 and 15*

Female Standards *11 and 12*

II

The bone nodule is oval, its margin is smooth and undifferentiated.

Male Standards *14 and 15*

Female Standards *12 and 13*

III

The nodule has elongated. The direction of its longest axis has become apparent.

Male Standards *15 and 16*

Female Standards *12 and 13*

IV

The distal end of the nodule begins to be wider than its proximal end. Differentiation of its margin begins; its capitate surface is becoming less convex.

Male Standards *16 and 17*

Female Standards *13 and 14*

V

Its capitate surface begins to be concave and the outline of the volar margin of this surface is becoming discernible. The radial and trapezoid-trapezium articular facets begin to be flattened.

Male Standards *18 and 19*

Female Standards *15 and 16*

(Image adapted from Greulich and Pyle, 1959)

Figure 3.08.1 *Age related changes in the scaphoid, for males (5 to 10 years) and females (3.5 to 7.8 years).*

VI

The thin dorsal margin of its capitate surface begins to project toward that bone, overlapping it when the palm of the hand is flat upon the film. The mid-portion of the white volar edge of the capitate surface forms a crescentic outline which curves distally toward the trapezoid and proximally toward the lunate. The surface which articulates with the trapezium and trapezoid is now flattened.

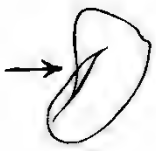

Male Standards *22 and 23*

Female Standards *18 and 19*

VII

The distal arrow points to the site of the scaphoid tubercle, a short white marking in the film, near the osseous corner at the junction of the radial and the trapezoid-trapezium surfaces. A thickened outline begins to form within the shadow of this surface. This outline represents the slightly roughened crest of the bone between the articular facet and free portion of this side of the bone.

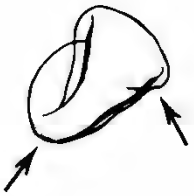

Male Standards *23 and 24*

Female Standards *20 and 21*

(Image adapted from Greulich and Pyle, 1959)

Figure 3.08.2 *Age related changes in the scaphoid, for males (12.5 to 14 years) and females (10 to 13 years).*

I

In the full-term newborn, the proximal end of the first metacarpal is slightly flared and its margin is flattened. The trapezium is still cartilaginous.

Male Standard *1*

Female Standard *1*

II

Ossification of the epiphysis of the first metacarpal begins from a single centre or, occasionally, from several small centres which subsequently coalesce to form a single nodule.

Male Standards *8 and 9*

Female Standards *7 and 8*

III

The nodule has become elongated transversely. Its margin is smooth and undifferentiated. Hereafter, its long axis will be transverse.

Male Standards *9 and 10*

Female Standards *8 and 9*

IV

Ossification begins in the trapezium. The nodule usually appears proximal to the volar (ulnar) third of the shaft of the first metacarpal. The distal margin of the epiphysis flattens as it begins to conform to the shape of the base of its shaft. The central portion of the growth cartilage plate has attained its definitive thickness.

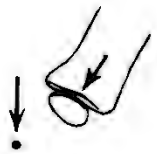

	EPIPHYSIS OF METACARPAL 1	TRAPEZIUM
Male Standards	*13 and 14*	*11 and 12*
Female Standards	*10 and 11*	*10 and 11*

V

The nodule in the trapezium is round or oval and its margin is smooth. The space between the nodule and epiphysis remains wide. The proximal margin of the epiphysis remains convex. At this stage, some epiphyses develop a pointed volar (ulnar) side, while others remain symmetrical. The epiphysis is now about two-thirds as wide as the diaphysis.

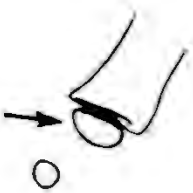

	EPIPHYSIS OF METACARPAL 1	TRAPEZIUM
Male Standards	*14 and 15*	*13 and 14*
Female Standards	*12 and 13*	*12 and 13*

(Image adapted from Greulich and Pyle, 1959)

Figure 3.09.1 *Age related changes in the trapezium and the proximal epiphysis of the first metacarpal, for males (newborn to 5 years) and females (newborn to 5 years).*

VI

The centre for the trapezium has elongate obliquely and its metacarpal and scaphoid surface are beginning to flatten. The middle part of the proximal margin of the epiphysis is now slightly flattened.

	EPIPHYSIS OF METACARPAL 1	TRAPEZIUM
Male Standards	*15 and 16*	*15 and 16*
Female Standards	*15 and 16*	*14 and 15*

VII

The metacarpal surface of the trapezium is indented. Its distal, ulnar corner is beginning to project toward the base of the second metacarpal. Its scaphoid margin is rather flat. A slight indentation is now visible on the future articular surface of the epiphysis. Its lateral (dorsal) border has not yet reached the level of the corresponding border of its shaft.

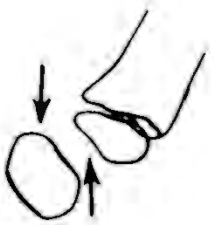

	EPIPHYSIS OF METACARPAL 1	TRAPEZIUM
Male Standards	*18 and 19*	*18 and 19*
Female Standards	*17and 18*	*16 and 17*

VIII

The scaphoid facet of the trapezium is now distinctly outlined, and, as is best seen in Female Standard 20, it is becoming concave. Parts of the white outline of its volar margin are now clearly visible along its scaphoid and metacarpal border. The distal margin of the epiphysis is now as wide as the adjacent margin of its shaft. A distinct concavity is developing across its articular surface. According to the positioning of the thumb, the volar end of the epiphysis can either overlap the base of the second metacarpal or be separated from it by some inter-osseous space

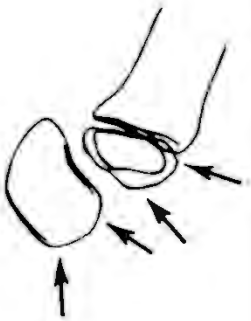

	EPIPHYSIS OF METACARPAL 1	TRAPEZIUM
Male Standards	*20 and 21*	*20 and 21*
Female Standards	*18 and 19*	*19 and 20*

(Image adapted from Greulich and Pyle, 1959)

Figure 3.09.2 *Age related changes in the trapezium and the proximal epiphysis of the first metacarpal, for males (6 to 11.5 years) and females (5.8 to 12 years).*

IX

The volar margin of the trapezoid side of the trapezium is now visible as a curved white line within the overlapping bone shadows. The volar (ulnar) side of the epiphysis has thickened and its margin has flattened.

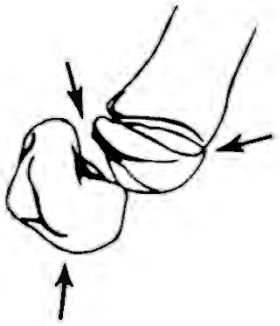

	EPIPHYSIS OF METACARPAL 1	TRAPEZIUM
Male Standards	*22 and 23*	*22 and 23*
Female Standards	*18 and 19*	*18 and 19*

X

Distinct osseous corner now separate the free, lateral (radial) margin of the trapezium from those facets which articulate with the scaphoid and the epiphysis of the first metacarpal.
The distal surface of the epiphysis follows closely the contour of the adjacent surface of the diaphysis. The articular surface of the epiphysis and the trapezium are reciprocally shaped.

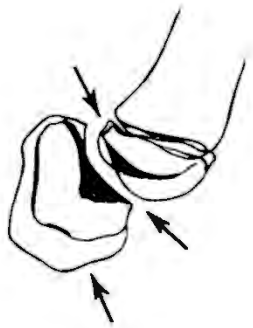

	EPIPHYSIS OF METACARPAL 1	TRAPEZIUM
Male Standards	*24 and 25*	*23 and 24*
Female Standards	*19 and 20*	*19 and 20*

XI

The trapezium has attained its young adult shape.
Epiphyseal-diaphyseal fusion has begun in the proximal end of the first metacarpal.

	PROXIMAL END OF METACARPAL 1	TRAPEZIUM
Female Standards	*22 and 23*	*22 and 23*

(Image adapted from Greulich and Pyle, 1959)

Figure 3.09.3 *Age related changes in the trapezium and the proximal epiphysis of the first metacarpal, for males (12.5 to 14 years) and females (10 to 14 years).*

I

Base of Metacarpal II: In the full-term newborn, the base is beginning to flare and its proximal margin is thin and slightly convex.

Male Standard *1*

Female Standard *1*

II

Base of Metacarpal II: The capitate portion of the margin begins to flatten. The trapezoid is still cartilaginous.

Male Standards *5 and 6*

Female Standards *4 and 5*

III

Base of Metacarpal II: The surface which will later articulate with the trapezoid begins to flatten. The trapezoid continues to be cartilaginous.

Male Standards *10 and 11*

Female Standards *9 and 10*

IV

Trapezoid: Ossification begins. The initial nodule is lateral to the distal half of the capitate. The position of the nodule now marks the centre of the trapezoid-metacarpal II joint.

Base of Metacarpal II: The base has broadened and its trapezoid facet has become relatively wider.

Male Standards *14 and 15*

Female Standards *11 and 12*

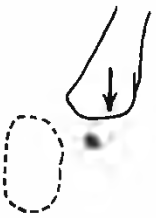

V

Trapezoid: The margin of the nodule is smooth and undifferentiated.

Base of Metacarpal II: There is a slight indentation in its trapezoid surface which foreshadows the future trapezoid-metacarpal II joint.

Male Standards *14 and 15*

Female Standards *12 and 13*

(Image adapted from Greulich and Pyle, 1959)

Figure 3.10.1 *Age related changes in the trapezoid and the base of the second metacarpal, for males (newborn to 6 years) and females (newborn to 5 years).*

VI

Trapezoid: Its capitate margin is beginning to flatten

Base of Metacarpal II: Its trapezoid facet has widened and the articular indentation has become distinct.

Male Standards *14 and 15*

Female Standards *12 and 13*

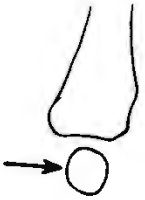

VII

Trapezoid: The trapezium overlaps the trapezoid. The articular facet of the trapezoid is visible as a thin, convex outline within the shadow of the trapezium. Its scaphoid margin begins to flatten; it forms a distinct osseous corner with the well-flattened capitate facet thereby giving the bone a squarish appearance.

Base of Metacarpal II: Its capitate process, medial to its trapezoid facet, projects toward the capitate. Reciprocal shaping of the trapezoid-metacarpal II joint surface is established. The blunted medial osseous corner on the trapezoid marks the corresponding border of that joint.

Male Standards *18 and 19*

Female Standards *15 and 16*

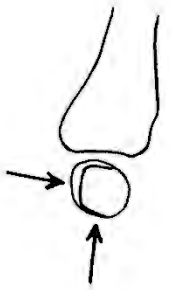

VIII

Trapezoid: Distinct osseous corners have formed at the junctions of its capitate, metacarpal II, and scaphoid facets. The arrow points to the lateral end of its proximal volar margin which is becoming visible at the junction of its trapezium and scaphoid facets.

Base of Metacarpal II: The articular surfaces of the trapezoid-metacarpal II joint are functionally equal in transverse dimension. If the capitate process on the base is prominent, it will now project proximally between the trapezoid and the base of Metacarpal III.

Male Standards *20 and 21*

Female Standards *18 and 19*

IX

Trapezoid: Its smooth convex trapezium margin is now distinctly visible within the shadow of that bone. Its metacarpal margin has become somewhat angular centrally. Blunted osseous corners mark off the four facets of the bone and give it a trapezoidal contour.

Female Standards *21 and 22*

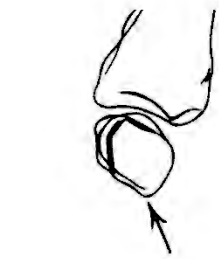

X

Young adult contours. The volar margins are most distinct along its medial, scaphoid and metacarpal borders

Female Standards *21 and 22*

(Image adapted from Greulich and Pyle, 1959)

Figure 3.10.2 *Age related changes in the trapezoid and the base of the second metacarpal, for males (9 to 11.5 years) and females (6.8 to 13.5 years).*

I

In the full-term new born, the shaft is slender and slightly constricted across the centre. Its distal margin, adjacent to the cartilaginous epiphysis, is relatively flattened. The proximal end is slightly rounded.

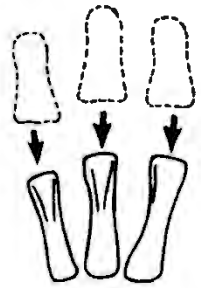

	SECOND	THIRD	FOURTH
Male Standard	*1*	*1*	*1*
Female Standard	*1*	*1*	*1*

II

Ossification begins from a single centre, or occasionally, from multiple centres. the initial nodule is seen close to the distal margin of the diaphysis.

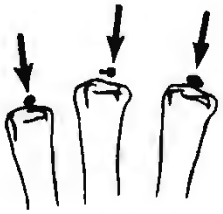

	SECOND	THIRD	FOURTH
Male Standard	*6 and 7*	*6 and 7*	*6 and 7*
Female Standard	*4 and 5*	*4 and 5*	*5 and 6*

III

The nodule is either round or slightly oval, and its margins are smooth and undifferentiated.

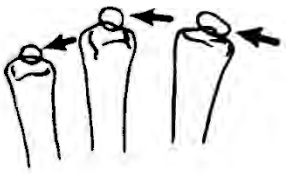

	SECOND	THIRD	FOURTH
Male Standard	*8 and 9*	*8 and 9*	*8 and 9*
Female Standard	*7 and 8*	*7 and 8*	*7 and 8*

IV

The proximal margin of the epiphysis begins to flatten, to conform to the shape of the adjacent surface of the diaphysis. The characteristic thickness of the growth cartilage plate begins to be visible centrally.

	SECOND	THIRD	FOURTH
Male Standard	*8 and 9*	*8 and 9*	*9 and 10*
Female Standard	*7 and 8*	*7 and 8*	*8 and 9*

(Image adapted from Greulich and Pyle, 1959)

Figure 3.11.1 *Age related changes in the epiphyses of the second, third and fourth metacarpals, for males (newborn to 5 years) and females (newborn to 5 years).*

[The epiphysis of the third metacarpal is used to illustrate these successive changes, which are similar in all three metacarpals]

V

The radial, ulnar, and distal margins of the epiphysis have become dissimilar in shape as the joint surface begins to differentiate

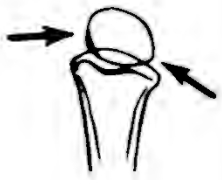

	SECOND	THIRD	FOURTH
Male Standard	*13 and 14*	*13 and 14*	*13 and 14*
Female Standard	*10 and 11*	*10 and 11*	*12 and 13*

VI

Parts of the volar surface of the epiphysis are now visible as thin, white linear markings just within its radial and ulnar margins.

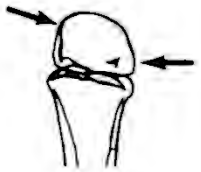

	SECOND	THIRD	FOURTH
Male Standard	*19 and 20*	*20 and 21*	*20 and 21*
Female Standard	*16 and 17*	*16 and 17*	*16 and 17*

VII

The epiphysis is now as wide as the distal end of the diaphysis and their adjacent margins conform closely in shape. There is as yet no reduction in the thickness of the growth cartilage plate.

	SECOND	THIRD	FOURTH
Male Standard	*21 and 22*	*22 and 23*	*22 and 23*
Female Standard	*18 and 19*	*18 and 19*	*18 and 19*

VIII

Epiphyseal-diaphyseal fusion begins.

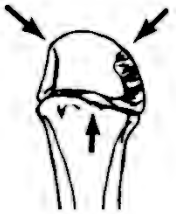

	SECOND	THIRD	FOURTH
Female Standard	*22 and 23*	*22 and 23*	*23 and 24*

(Image adapted from Greulich and Pyle, 1959)

Figure 3.11.2 *Age related changes in the epiphyses of the second, third and fourth metacarpals, for males (10 to 13.5 years) and females (7.8 to 15 years).*

[The epiphysis of the third metacarpal is used to illustrate these successive changes, which are similar in all three metacarpals]

I

In the full-term newborn, the shaft is slender and slightly constricted across its centre. Its distal margin, adjacent to the cartilaginous epiphysis, is relatively flattened. The proximal end is slightly rounded.

Male Standard *1*

Female Standard *1*

II

Ossification begins from a single centre, or occasionally, from multiple centres. The nodule first appears near the distal margin of the diaphysis.

Male Standards *8 and 9*

Female Standards *6 and 7*

III

The nodule is either round or slightly oval, and its margins are smooth and undifferentiated.

Male Standards *8 and 9*

Female Standards *7 and 8*

IV

The proximal margin of the epiphysis begins to flatten, to conform to the shape of the adjacent surface of the diaphysis. The characteristic thickness of the growth cartilage plate begins to be visible centrally.

Male Standards *9 and 10*

Female Standards *8 and 9*

V

The radial, ulnar, and distal margins of the epiphysis have become dissimilar in shape as the joint surface begins to differentiate.

Male Standards *14 and 15*

Female Standards *12 and 13*

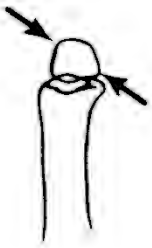

(Image adapted from Greulich and Pyle, 1959)

Figure 3.12.1 *Age related changes in the epiphysis of the fifth metacarpal, for males (newborn to 6 years) and females (newborn to 5 years).*

VI

Parts of the volar surface of the epiphysis are now visible as thin, white linear markings just within its radial and ulnar margins.

Male Standards *20 and 21*

Female Standards *17 and 18*

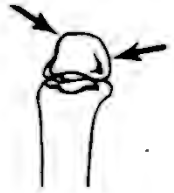

VII

The epiphysis is now as wide as the distal end of the diaphysis and their adjacent margins conform closely in shape. There is as yet no reduction in the thickness of the growth cartilage plate.

Male Standards *22 and 23*

Female Standards *18 and 19*

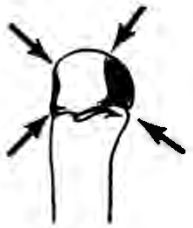

VIII

Epiphyseal-diaphyseal fusion begins.

Female Standards *23 and 24*

IX

Fusion of the epiphysis and diaphysis has recently been complete. The terminal line occasionally persists for a variable period.

Female Standards *23 and 24*

(Image adapted from Greulich and Pyle, 1959)

Figure 3.12.2 *Age related changes in the epiphysis of the fifth metacarpal, for males (11 to 13 years) and females (8.8 to 14 years).*

I

In the full-term newborn, the distal end of the shaft is convex and the proximal margin adjacent to the cartilaginous epiphysis is relatively quite flat.

Male Standard *1*

Female Standard *1*

II

Ossification begins in the epiphysis from a single centre or, occasionally, from multiple centres. The initial nodule is close to the margin of the diaphysis.

Male Standards *8 and 9*

Female Standards *7 and 8*

III

The epiphysis is thin and disk-shaped and its margins are smooth. Its longest axis is transverse. In the male standard, this epiphysis develops from two bone growth centres until it is more than half as wide as the adjacent margin of the shaft.

Male Standards *12 and 13*

Female Standards *8 and 9*

IV

The epiphysis is three-fourths as wide as its diaphysis, and it is as wide as the adjacent margin of the first metacarpal, with which it forms a joint. Its palmar side is thickened. the central portion of the growth cartilage plate has now attained its definitive thickness. The articular margin of the epiphysis is quite flat.

Male Standards *13 and 14*

Female Standards *9 and 10*

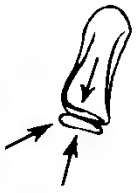

V

The epiphysis is as wide as its diaphysis. Its articular facet is slightly concave and thickened.

Male Standards *19 and 20*

Female Standards *16 and 17*

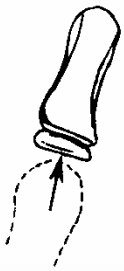

(Image adapted from Greulich and Pyle, 1959)

Figure 3.13.1 *Age related changes in the epiphysis of the proximal phalanx of the thumb, for males (newborn to 11 years) and females (newborn to 8.8 years).*

VI

The palmar extent of the articular surface is now visible; this border of the epiphysis extends beyond the edge of the shaft.. The articular surface has begun to shape to the contours of the distal end of the first metacarpal.

Male Standards *20 and 21*

Female Standards *17 and 18*

VII

The epiphysis is wider than the shaft. The sides of the epiphysis have thickened, and the shape and extent of the joint surface are now defined. Ossification of the adductor sesamoid of the thumb begins. The nodule is visible opposite the distal end of the first metacarpal.

Male Standards *22 and 23*

Female Standards *18 and 19*

VIII

The epiphysis caps the diaphysis. The flexor sesamoid has begun to ossify. It is close to the adductor sesamoid and is usually visible through the shadow of the distal end of the first metacarpal.

Female Standards *16 and 17*

IX

Epiphyseal-diaphyseal fusion begins.

Female Standards *22 and 23*

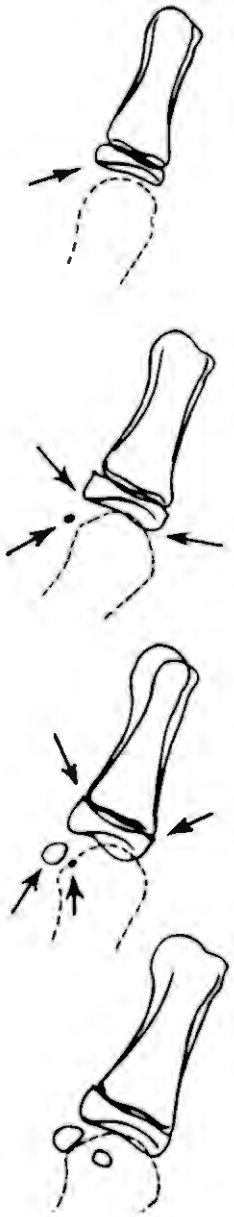

(Image adapted from Greulich and Pyle, 1959)

Figure 3.13.2 *Age related changes in the epiphysis of the proximal phalanx of the thumb, for males (11 to 13 years) and females (8.8 to 14 years).*

I

In the full-term newborn, the distal end of the diaphysis is convex, and its proximal end is flat. The epiphysis is as yet entirely cartilaginous.

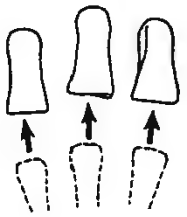

	SECOND	THIRD	FOURTH
Male Standard	*1*	*1*	*1*
Female Standard	*1*	*1*	*1*

II

Ossification begins in the epiphysis from a single centre, or occasionally, from multiple centres. The roundness of the distal end of the shaft has been somewhat reduced.

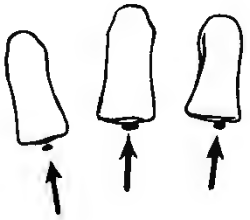

	SECOND	THIRD	FOURTH
Male Standard	*6 and 7*	*6 and 7*	*6 and 7*
Female Standard	*4 and 5*	*4 and 5*	*4 and 5*

III

The epiphysis is thin and disk-shaped and its margins are smooth. The nodule is as yet less than half as wide as the adjacent margin of the diaphysis. Its longest axis is transverse.

	SECOND	THIRD	FOURTH
Male Standard	*7 and 8*	*7 and 8*	*7 and 8*
Female Standard	*6 and 7*	*6 and 7*	*6 and 7*

IV

The epiphysis is as wide as the adjacent epiphyseal margin of the metacarpal with which it forms a joint. The central portion of the growth cartilage plate has attained its definitive thickness.
As the distal end of these phalanges, the future articular margin and the trochlear areas have begun to flatten.

	SECOND	THIRD	FOURTH
Male Standard	*10 and 11*	*10 and 11*	*10 and 11*
Female Standard	*7 and 8*	*7 and 8*	*7 and 8*

(Image adapted from Greulich and Pyle, 1959)

Figure 3.14.1 *Age related changes in the epiphyses of the proximal phalanges of the second, third and fourth digits, for males (newborn to 3.5 years) and females (newborn to 2 years).*

[The epiphysis of the proximal phalanx of the third digit is used to illustrate these successive changes, which are similar for all three digits.]

V

The articular surface of the epiphysis has become slightly concave and thickened. The sides of the epiphysis are now beginning to show the differences in shape and thickness which will later characterise them.

	SECOND	THIRD	FOURTH
Male Standard	*13 and 14*	*13 and 14*	*13 and 14*
Female Standard	*9 and 10*	*9 and 10*	*9 and 10*

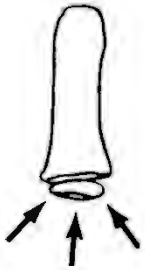

VI

The epiphysis is as wide as the adjacent margin of the diaphysis. The articular surface at the distal end of the shaft is becoming slightly concave.

	SECOND	THIRD	FOURTH
Male Standard	*19 and 20*	*19 and 20*	*20 and 21*
Female Standard	*16 and 17*	*16 and 17*	*16 and 17*

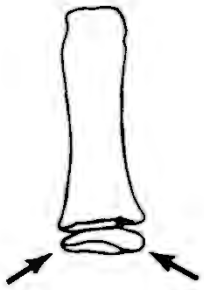

VII

The epiphysis begins to cap the shaft on the lateral (radial) side. The transverse extent of the articular surface, on both ends of the bone, is visible.

	SECOND	THIRD	FOURTH
Male Standard	*22 and 23*	*22 and 23*	*22 and 23*
Female Standard	*18 and 19*	*18 and 19*	*18 and 19*

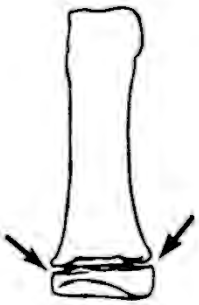

VIII

Epiphyseal-diaphyseal fusion begins

	SECOND	THIRD	FOURTH
Female Standards	*22 and 23*	*22 and 23*	*22 and 23*

(Image adapted from Greulich and Pyle, 1959)

Figure 3.14.2 *Age related changes in the epiphyses of the proximal phalanges of the second, third and fourth digits, for males (4.5 to 13 years) and females (2.7 to 14 years).*

[The epiphysis of the proximal phalanx of the third digit is used to illustrate these successive changes, which are similar for all three digits.]

I

In the full-term newborn, the distal end of the diaphysis is convex and its proximal end is flat. The epiphysis is entirely cartilaginous.

Male Standard *1*

Female Standard *1*

II

Ossification begins in the epiphysis from a single centre, or occasionally, from multiple centres. The roundness of the distal end of the shaft has been somewhat reduced.

Male Standards *7 and 8*

Female Standards *6 and 7*

III

The epiphysis is thin and disk-shaped and its margins are smooth. The nodule is as yet less than half as wide as the adjacent margin of the diaphysis. Its longest axis is transverse

Male Standards *7 and 8*

Female Standards *7 and 8*

IV

The epiphysis is as wide as the adjacent margin of the fifth metacarpal, with which it forms a joint. The central portion of the growth cartilage plate has attained its definitive thickness. At the distal end of this phalanx, the future articular margin and the trochlear areas have begun to flatten.

Male Standards *10 and 11*

Female Standards *7 and 8*

(Image adapted from Greulich and Pyle, 1959)

Figure 3.15.1 *Age related changes in the epiphysis of the proximal phalanx of the fifth digit, for males (newborn to 3.5 years) and females (newborn to 2 years).*

V

The articular surface of the epiphysis has become slightly concave and thickened. Its sides tend to remain symmetrical

Male Standards *13 and 14*

Female Standards *9 and 10*

VI

The epiphysis is as wide as the adjacent margin of the diaphysis. the articular surface at the distal end of the shaft is becoming slightly concave.

Male Standards *19 and 20*

Female Standards *16 and 17*

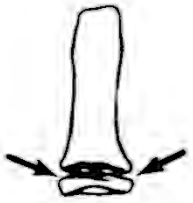

VII

The epiphysis begins to cape the shaft on the lateral (radial) side. The full transverse extent of the articular surface, on both ends of the bone, is visible.

Male Standards *22 and 23*

Female Standards *18 and 19*

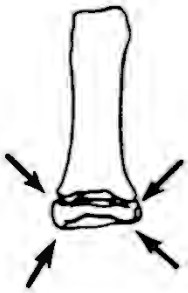

VIII

Epiphyseal-diaphyseal fusion begins.

Female Standards *22 and 23*

(Image adapted from Greulich and Pyle, 1959)

Figure 3.15.2 *Age related changes in the epiphysis of the proximal phalanx of the fifth digit, for males (4.5 to 13 years) and females (2.5 to 14 years).*

I

In the full-term newborn, the widest end of the shaft is its proximal end. The distal margin is rounded, the proximal margin is relatively flat. The centre of each diaphysis appears slightly constricted. The epiphysis is entirely cartilaginous.

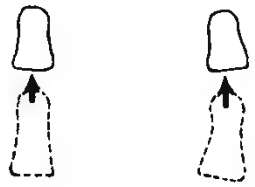

	THIRD	FOURTH
Male Standards	*1*	*1*
Female Standards	*1*	*1*

	SECOND	FIFTH
Male Standards	*1*	*1*
Female Standards	*1*	*1*

II

Ossification begins in the epiphysis from a single centre, or occasionally, from multiple centres. The initial nodule forms close to the proximal margin of the diaphysis.

	THIRD	FOURTH
Male Standards	*7 and 8*	*7 and 8*
Female Standards	*6 and 7*	*6 and 7*

	SECOND	FIFTH
Male Standards	*8 and 9*	*11 and 12*
Female Standards	*6 and 7*	*8 and 9*

III

The epiphyseal bone nodule is disk-shaped and its margins are smooth. Its longest axis is transverse.

	THIRD	FOURTH
Male Standards	*9 and 10*	*9 and 10*
Female Standards	*7 and 8*	*8 and 9*

	SECOND	FIFTH
Male Standards	*9 and 10*	*13 and 14*
Female Standards	*8 and 9*	*9 and 10*

(Image adapted from Greulich and Pyle, 1959)

Figure 3.16.1 *Age related changes in the epiphyses of the middle phalanges, for males (newborn to 5 years) and females (newborn to 3 years).*

[The middle phalanges of the third and fourth digits have been used to illustrate these successive changes, which are similar for digits two to five].

IV

The epiphysis is as wide as the adjacent trochlear surface of the proximal phalanx with which it articulates. The central portion of the growth cartilage plate has attained its definitive thickness.

	THIRD	FOURTH
Male Standards	*11 and 12*	*11 and 12*
Female Standards	*10 and 11*	*10 and 11*

	SECOND	FIFTH
Male Standards	*13 and 14*	*15 and 16*
Female Standards	*10 and 11*	*11 and 12*

V

The epiphysis has become the thickest centrally. The shape of its angular articular surface is becoming visible.

	THIRD	FOURTH
Male Standards	*13 and 14*	*13 and 14*
Female Standards	*11 and 12*	*11 and 12*

	SECOND	FIFTH
Male Standards	*14 and 15*	*16 and 17*
Female Standards	*11 and 12*	*13 and 14*

VI

The epiphysis is as wide as its diaphysis.

	THIRD	FOURTH
Male Standards	*21 and 22*	*22 and 23*
Female Standards	*16 and 17*	*16 and 17*

	SECOND	FIFTH
Male Standards	*22 and 23*	*22 and 23*
Female Standards	*16 and 17*	*16 and 17*

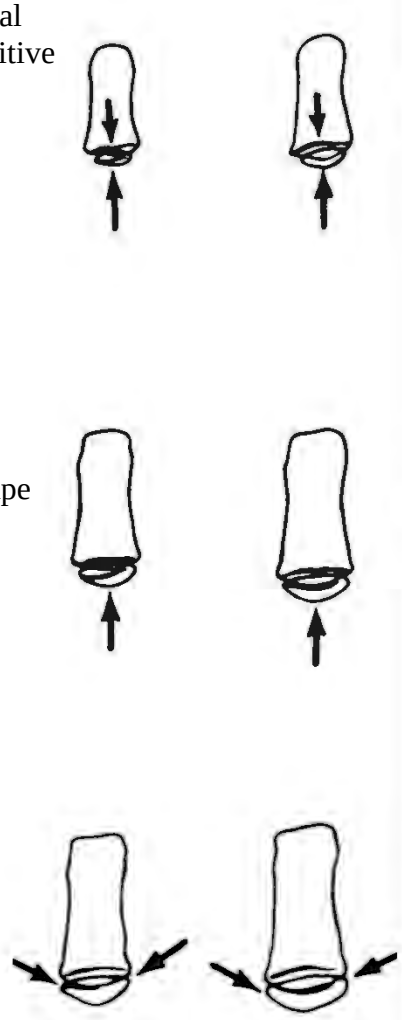

(Image adapted from Greulich and Pyle, 1959)

Figure 3.16.2 *Age related changes in the epiphyses of the middle phalanges, for males (3.5 to 13 years) and females (3 to 8.8 years).*

[The middle phalanges of the third and fourth digits have been used to illustrate these successive changes, which are similar for digits two to five].

VII

The epiphysis caps its diaphysis. The sides of the epiphysis have become thicker and are shaping to the contours of the sides of the shaft.

	THIRD	FOURTH
Female Standards	*18 and 19*	*18 and 19*

	SECOND	FIFTH
Female Standards	*19 and 20*	*19 and 20*

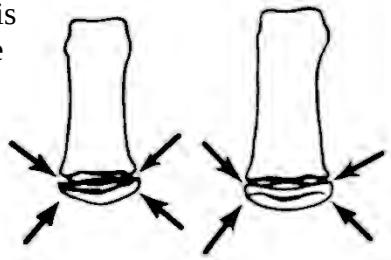

VIII

The epiphysis begins to fuse with its shaft.

	THIRD	FOURTH
Female Standards	*22 and 23*	*22 and 23*

	SECOND	FIFTH
Female Standards	*22 and 23*	*22 and 23*

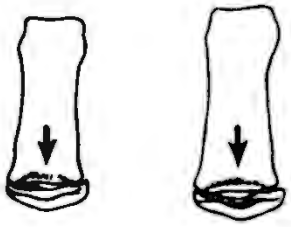

(Image adapted from Greulich and Pyle, 1959)

Figure 3.16.3 *Age related changes in the epiphyses of the middle phalanges, for females (10 to 14 years).*

[The middle phalanges of the third and fourth digits have been used to illustrate these successive changes, which are similar for digits two to five].

I

In the full-term newborn, the proximal end of the shaft is the widest portion. Its proximal margin, adjacent to the cartilaginous epiphysis, is well flattened. The distal end of the shaft is convex.

Male Standard *1*

Female Standard *1*

II

Ossification begins as a single centre or, occasionally, from multiple centres. The initial nodule forms close to the margin of the diaphysis.

Male Standards *6 and 7*

Female Standards *5 and 6*

III

The epiphysis is a single, oval nodule with smooth margins. Its longest axis is transverse.

Male Standards *7 and 8*

Female Standards *6 and 7*

IV

The inner bone margin of the epiphysis flattens to conform to the shape of the adjacent margin of the diaphysis. The central portion of the growth cartilage has attained its definitive thickness.

Male Standards *8 and 9*

Female Standards *7 and 8*

V

The epiphysis has become thickest centrally and the dorsal portion of its articular margin has flattened. Its palmar side is rounded.

Male Standards *10 and 11*

Female Standards *9 and 10*

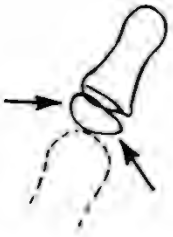

(Image adapted from Greulich and Pyle, 1959)

Figure 3.17.1 *Age related changes in the epiphysis of the distal phalanx of the thumb, for males (newborn to 3.5 years) and females (newborn to 3 years).*

VI

The shape and extent of the articular surface of the epiphysis are now defined. Its palmar side has begun to shape to the contours of the distal end of the proximal phalanx.

Male Standards *19 and 20*

Female Standards *17 and 18*

VII

The epiphysis caps the diaphysis

Female Standards *18 and 19*

VIII

Epiphyseal-diaphyseal fusion begins.

Female Standards *20 and 21*

IX

The epiphysis has recently fused with the diaphysis.

Female Standards *21 and 22*

(Image adapted from Greulich and Pyle, 1959)

Figure 3.17.2 *Age related changes in the epiphysis of the distal phalanx of the thumb, for males (10 to 11 years) and females (8.8 to 13.5 years).*

I

In the full-term newborn, the shaft has a rounded distal end and a relatively flat proximal end. The epiphysis is as yet cartilaginous.

	THIRD	FOURTH
Male Standards	*1*	*1*
Female Standards	*1*	*1*

	SECOND	FIFTH
Male Standards	*1*	*1*
Female Standards	*1*	*1*

II

Ossification begins in the epiphysis from a single centre or, occasionally, from multiple centres. The initial nodule forms close to the proximal margin of the diaphysis.

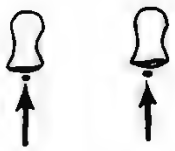

	THIRD	FOURTH
Male Standards	*8 and 9*	*8 and 9*
Female Standards	*7 and 8*	*7 and 8*

	SECOND	FIFTH
Male Standards	*8 and 9*	*8 and 9*
Female Standards	*8 and 9*	*8 and 9*

III

The epiphyseal bone nodule is disk-shaped and its margins are smooth. Its longest axis is transverse.

	THIRD	FOURTH
Male Standards	*10 and 11*	*10 and 11*
Female Standards	*8 and 9*	*8 and 9*

	SECOND	FIFTH
Male Standards	*11 and 12*	*11 and 12*
Female Standards	*9 and 10*	*9 and 10*

(Image adapted from Greulich and Pyle, 1959)

Figure 3.18.1 *Age related changes in the epiphyses of the distal phalanges of the second, third, fourth and fifth digits, for males (newborn to 4 years) and females (newborn to 3 years).*

[The distal phalanges of the third and fourth digits have been used to illustrated these successive changes, which are similar in digits two to five].

IV

The epiphysis is between one-half and two-thirds as wide as its diaphysis. The central portion of the growth cartilage plate has now attained its definitive thickness.

	THIRD	FOURTH
Male Standards	*11 and 12*	*11 and 12*
Female Standards	*9 and 10*	*9 and 10*

	SECOND	FIFTH
Male Standards	*14 and 15*	*14 and 15*
Female Standards	*10 and 11*	*10 and 11*

V

The epiphysis has become thickest centrally. The angular shape of its future articular surface is thus forecast.

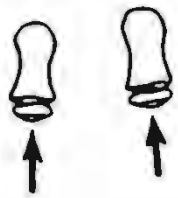

	THIRD	FOURTH
Male Standards	*13 and 14*	*13 and 14*
Female Standards	*12 and 13*	*12 and 13*

	SECOND	FIFTH
Male Standards	*15 and 16*	*16 and 17*
Female Standards	*13 and 14*	*13 and 14*

VI

The epiphysis is as wide as its diaphysis. Its articular surface is slightly wider than the adjacent surface of the middle phalanx with which it articulates.

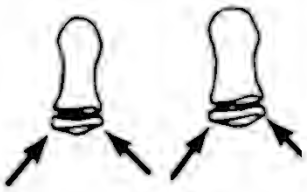

	THIRD	FOURTH
Male Standards	*16 and 17*	*16 and 17*
Female Standards	*12 and 13*	*12 and 13*

	SECOND	FIFTH
Male Standards	*17 and 18*	*17 and 18*
Female Standards	*14 and 15*	*14 and 15*

(Image adapted from Greulich and Pyle, 1959)

Figure 3.18.2 *Age related changes in the epiphyses of the distal phalanges of the second, third, fourth and fifth digits, for males (3.5 to 9 years) and females (2.5 to 6.8 years).*

[The distal phalanges of the third and fourth digits have been used to illustrate these successive changes, which are similar in digits two to five].

VII

The epiphysis caps the diaphysis.

	THIRD	FOURTH
Male Standards	*22 and 23*	*22 and 23*
Female Standards	*17 and 18*	*17 and 18*

	SECOND	FIFTH
Male Standards	*22 and 23*	*22 and 23*
Female Standards	*17 and 18*	*17 and 18*

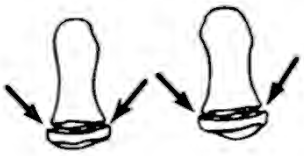

VIII

Epiphyseal-diaphyseal fusion begins.

	THIRD	FOURTH
Female Standards	*21 and 22*	*21 and 22*

	SECOND	FIFTH
Female Standards	*21 and 22*	*21 and 22*

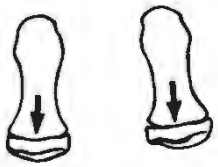

IX

Fusion of the epiphysis and shaft has been recently completed.

	THIRD	FOURTH
Female Standards	*21 and 22*	*21 and 22*

	SECOND	FIFTH
Female Standards	*21 and 22*	*21 and 22*

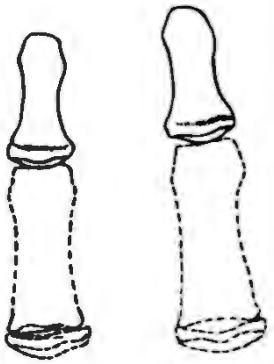

(Image adapted from Greulich and Pyle, 1959)

Figure 3.18.3 *Age related changes in the epiphyses of the distal phalanges of the second, third, fourth and fifth digits, for males (12.5 to 13 years) and females (8.8 to 13.5 years).*

[The distal phalanges of the third and fourth digits have been used to illustrate these successive changes, which are similar in digits two to five].

3.3 Statistical Analysis

3.3.1 Intra- and Inter-Observer Error Analysis

The primary researcher performed skeletal age estimates on all 1356 individuals in the sample, using the Atlas method of Greulich and Pyle (1959).
A sub-set of 46 radiographs (26 males and 20 females) was randomly selected, and a further two skeletal age estimates were performed on these data. At least 1 month elapsed between each assessment.

During this same time period, this identical sub-set was analysed by a second, independent observer, Kundisai Dembetembe, who is familiar with the GP method of skeletal age assessment. Performing multiple observations on the same sub-set of data intended to maintain a high degree of reliability and repeatability for the results of this research. Neither of the two researchers consulted the chronological ages of the sample when conducting their analysis.

The first level of statistical analysis tested for a significant difference between the three skeletal age estimates performed by the primary researcher; whereas the second level of analysis determined whether a significant difference existed between the skeletal age estimates of the primary and secondary researchers. The non-parametric, Kruskal-Wallis test was employed as the sample distribution deviated from normality. The first, second, third and secondary-observer age estimates were considered mutually exclusive.
These analyses were performed using *GraphPad Prism Version 5.01* (Graphpad Software, 2007).

3.3.2 Exploratory Data Analysis

Exploratory data analysis was performed to assess the correlation between chronological age and skeletal age. This was initially done on the sample as a whole, and thereafter each sex was analysed separately in order to determine if skeletal age estimation differed between the sexes, and whether there was a difference in correlation between chronological and skeletal age for males and females.

3.3.3 Regression Analysis

Regression analysis was used to determine the relationship between chronological age and skeletal age and nature thereof, as well as how this relationship changed depending on the sex of the subject. Regression analysis allows for the analysis of several variables, and is a statistical technique used in many of the comparative studies listed in *Chapter 2* (such as Thodberg, 2009; and Serinelli *et al.,* 2011). It is also used Greulich and Pyle (1959) for prediction of adult stature, using the GP Atlas.

For this research, two regression analysis models were selected. A model formalises relationships between variables in an equation format. The two models selected were the best-fit model and the mixed effect model. These models are used to predict chronological age, based on a given skeletal age.

Regression analysis was done using *Stata MP, Version 11* (Statacorp, 2009).

3.3.3.1 Best-Fit Model

(Reference for this section is Hill and Lewicki, 2006)

This regression analysis involved a model-building procedure, by a comparison of the Aikaikes and Bayesian Information criteria and the use of the likelihood ratio test where appropriate. The Aikaikes Information criteria (AIC) measure the goodness-of-fit of the model against the data. The addition of too many variables into the model may result in overfitting of the data, but by building the model whilst incorporating the Bayesian Information criteria (BIC), overfitting is prevented. The likelihood ratio test tests the likelihood that the data will fit within this specific model (as opposed to another model).

The model-building procedure resulted in a best-fit regression model. The best-fit regression model is considered to be a fixed-effect model. A fixed-effect model has only fixed-effect variables, which means that the relationship between the variables, as described by the model and resulting equation, applies to the whole sample, and the relationship remains constant across the whole sample. Fixed-effect variables in this case were sex and skeletal age.

This model included the skeletal age and sex of the subject, together with an age-sex interaction term, as predictor variables for chronological age. Each of the variables used to predict chronological age has a specific corresponding coefficient value ($\hat{\beta}_1$, $\hat{\beta}_2$ or $\hat{\beta}_3$), which

is provided as part of the output of the regression analysis, together with a $\hat{\beta}_0$ value for the Intercept. Together, they are incorporated into the equation:

$$\hat{CA}_i = \hat{\beta}_0 \text{ (Intercept)} + [\hat{\beta}_1 \text{ x Skeletal Age}] + [\hat{\beta}_2 \text{ x Sex}] + [\hat{\beta}_3 \text{ x Age-Sex Interaction Term}] + \hat{e}_i \text{ (Residual Error)}$$

The subscript i refers to 1,…,n number of subjects.

One can think of the above equation as similar to the regular regression equation $y = ax + b$, except in this case, y is the predicted CA ($\hat{CA}_i$); a (the slope) is replaced by $\hat{\beta}_1$; x is the skeletal age of the individual; and b is the Intercept value $\hat{\beta}_0$ (generated from the output of the analysis). In addition, the sex and age-sex interaction term are incorporated into the equation along with the residual error ($\hat{e}_i$).
The residual error can be thought of as the expected random error of the model, or 'statistical noise'.

By convention, sex is denoted as '0' for females and '1' for males, as these are binary variables. This is does not bias the results of predicted CA, because, given this notation: If predicted CA, using the best-fit model, was greater for females than for males, the model would output a negative co-efficient for sex; whilst if predicted CA using the model was greater for males than for females, this co-efficient would be a positive value. As the co-efficient for sex is calculated on the actual data (that is, the skeletal ages generated by this research), there is no bias towards either sex when using the best-fit model to predict chronological age, and the results of the analysis would not change if the denotation was switched (that is, males '0' and females '1').

The age-sex interaction term is simply the change in skeletal age multiplied by the sex (either '1' or '0') of the individual, and a significant coefficient for the age-sex interaction term ($\hat{\beta}_3$) indicates that the relationship between the predicted CA and the SA is dependent on the sex of the subject.

The model showed a reasonably good fit, but some variation (scatter) was still present. It was then re-run with the outliers removed to assess if variation decreased.

Other variables, besides the effect of sex, were added to the regression analysis to determine whether they would account for the variation observed, and thus improve the model. The

inclusion of the racial classification (Black, White and Coloured) and socio-economic status (SES) of the subject did not offer any improvement to this model, which was thus determined to be the final fixed-effect model.

3.3.3.2 Mixed-Effect Model

(References for this section are: Davidian and Giltinan, 1995; Pinheiro and Bates, 2000).

Although the best-fit model fit reasonably well, examination of the residual diagnostic plots and plots of the actual versus the predicted CA values indicated that the model becomes less accurate as age increases.

Since explanations for this increasing variance could not be determined by the inclusion of additional predictors (such as race and SES), and since the error did not appear to be consistently that of under- or over-prediction, further analysis was done using a mixed-effect model.

Whereas the best-fit model used only fixed-effects (that is, the relationship between the variables was 'fixed' and consistent across all age groups, for the entire sample), a mixed-effect model uses both fixed and random effects.
The fixed-effects, in this example, were variables such as skeletal age or sex, the relationship of which remains constant for the entire sample.
The random-effects are group-specific effects, in this case, age-category specific effects. They control for the basic correlation structure of the data, and they are not consistent across the entire sample, but change depending on the age category in question. The inclusion of random-effects allows for observations within a certain age-category to be more correlated than those between age-categories, as it assumes that observations within one age category are related.

The initial mixed-effect model used was a random intercept model. This model also uses skeletal age and sex of the subject, together with an age-sex interaction term, as predictor variables for chronological age; and their corresponding coefficients ($\hat{\beta}_1$, $\hat{\beta}_2$ or $\hat{\beta}_3$) are, once again, provided as output of the regression analysis.

They are incorporated into the following equation:

$$\hat{CA}_{ij} = \hat{\beta}_0 \text{ (Intercept)} + [\hat{\beta}_1 \text{ x Skeletal Age}] + [\hat{\beta}_2 \text{ x Sex}] + [\hat{\beta}_3 \text{ x Age-Sex Interaction Term}] + \hat{e}_i \text{ (Residual Error)} + \hat{b}_{0i} \text{ (Random Intercept Effect)}$$

Subscript i refers to 1,…32 GP age categories; j refers to 1,…,n subjects in the sample.

This model assumes that the relationship between the predicted chronological age and predictor variables is constant, regardless of the age-category, and thus the slope of the final regression equation will remain the same for all age categories. This is the fixed-effect portion of the model. It is only the intercept for each age category that changes, based on the random intercept effect value ($\hat{b}_{0i}$) which is calculated for each age category. This value is added to the $\hat{\beta}_0$ value to obtain the intercept value for the specific age group in question. The result is one 'population' regression line (applicable to the whole sample), which is based on the estimated parameters of the predictor variables (that is, the fixed-effects) and several age-group specific regression lines, which all have differing intercept values (that is, the random-effects). The residual error is still considered the 'statistical noise' due to inherent variation within the sample.

This model was able to capture most of the variation within the sample, but an additional mixed-effect model was used to determine if it would improve results.

This additional model, the random intercept-random slope model is based on the same principles as the random intercept model. It also has fixed- and random- effects, and uses the same predictor variables (sex, skeletal age and age-sex interaction term) to predict chronological age. The difference between these two models lies in the random-effects. Whereas the random intercept model allowed for a change in intercept value for each age category, with the slope value remaining constant across the sample, the random intercept-random slope model has differing intercept and slope values for each age group. The assumption under this model is that the relationship between chronological age and skeletal age is not constant, and thus allows both the intercept value and the relationship between the chronological and skeletal age to differ by age category.

The output of this model resulted in the following equation:

$$\hat{C}A_{ij} = \hat{\beta}_0 \text{ (Intercept)} + [\hat{\beta}_1 \text{ x Skeletal Age}] + [\hat{\beta}_2 \text{ x Sex}] + [\hat{\beta}_3 \text{ x Age-Sex Interaction Term}] + \hat{e}_i \text{ (Residual Error)} + \hat{b}_{0i} \text{ (Random Intercept Effect)} + \hat{b}_{1i} \text{ (Random Slope Effect)}$$

Subscript i refers to 1,…32 GP age categories; and j refers to 1,…,n subjects in the sample.

A random intercept effect value ($\hat{b}_{0i}$) and a random slope effect value ($\hat{b}_{1i}$) was calculated for each age category, and added to the $\hat{\beta}_0$ value.

The result of this model was one 'population' regression line (applicable to the whole sample), based on the estimated parameters of the predictor variables (that is, the fixed-effects) and several age-group specific regression lines, which all have differing intercept values and differing slopes (that is, the random-effects). The residual error is still considered the 'statistical noise' of the sample.

For both mixed effect models, sex is denoted as '0' for females and '1' for males, as these are binary variables. This notation does not bias the results, due to reasons previously mentioned.

The exploratory data analysis and regression analysis was completed with the help of Katya Mauff, a statistical consultant from the Department of Statistical Sciences at the University of Cape Town. These methods were considered the most appropriate to use, given the data set for this research project.

CHAPTER 4:
RESULTS

4.1 General Distribution of the Sample

The total sample of 1356 individuals comprised of 535 female and 821 male subjects. Analysis was more frequently performed using radiographs of the left hand than the right (see *Table 4.01* below). Although analysis of the left hand is preferred (Greulich and Pyle, 1959), this is not always possible, in which case the right hand is used.

Table 4.01 Distribution Profile of the Sample According to Sex and Side

Sex	Side		Total	
	Left	Right		
Female	429	106	535	1356
Male	672	149	821	

Results of the *Chi*-Square (χ^2) Test for Proportions shows no significant difference between the number of radiographs of the left and right side, at the 95% confidence level ($\chi^2 = 0.588$). The *Chi*-Square (χ^2) Test for Proportions does, however, indicate a significant difference in the number of males compared to females, at the 95% confidence level ($\chi^2 = 40.63$).

4.1.1 Distribution of the Sample According to Sex and Age Group

The age group distribution of the male and female samples can be seen in *Table 4.02*. These age groups are the same as those used in the GP Atlas, with one additional age category (1 to 3 months) which was created by the researcher, to incorporate those individuals who were not yet 3 months of age, but were older than 28 days, which is the threshold age to be considered a newborn (Bogin, 1999). The age category interval is not consistent, but instead changes depending on the category concerned. This reflects the amount of growth and skeletal change that occurs during the early infant growth years and at the onset of puberty (Greulich and Pyle, 1959). For this reason, there are more age categories (with a narrower age range) for newborn individuals up to approximately 5 years of age, and again after the age of 11 years, indicating the onset of puberty. The age categories differ between males and females. It is important to keep these factors in mind when interpreting *Figures 4.01 (a)* and *(b)*.

Table 4.02 Distribution Profile of the Sample According to Sex and Age Group

Male			Female		
Age Category	*Age Range (years)*	*N*	*Age Category*	*Age Range (years)*	*N*
Newborn	0 - 0.08	54	Newborn	0 - 0.08	56
1-3months *	0.09 - 0.24	42	1-3months *	0.09 - 0.24	31
3 months	0.25 - 0.49	35	3 months	0.25 - 0.49	26
6 months	0.50 - 0.74	27	6 months	0.50 - 0.74	18
9 months	0.75 - 0.99	16	9 months	0.75 - 0.99	11
1 year	1.00 - 1.24	10	1 year	1.00 - 1.24	10
1 year 3 months	1.25 - 1.49	9	1 year 3 months	1.25 - 1.49	6
1 year 6 months	1.50 - 1.99	17	1 year 6 months	1.50 - 1.99	15
2 years	2.00 - 2.66	40	2 years	2.00 - 2.66	16
2 year 8 months	2.67 - 2.99	25	2 year 6 months	2.67 - 2.99	18
3 years	3.00 - 3.49	29	3 years	3.00 - 3.49	29
3 year 6 months	3.50 - 3.99	33	3 year 6 months	3.50 - 4.16	33
4 years	4.00 - 4.49	32	4 year 2 months	4.17 - 4.99	28
4 years 6 months	4.50 - 4.99	40	5 years	5.00 - 5.74	24
5 years	5.00 - 5.99	50	5 years 9 months	5.75 - 6.82	49
6 years	6.00 - 6.99	66	6 years 10 months	6.83 - 7.82	39
7 years	7.00 - 7.99	76	7 years 10 months	7.83 - 8.82	40
8 years	8.00 - 8.99	59	8 years 10 months	8.83 - 9.99	32
9 years	9.00 - 9.99	40	10 years	10.00 - 10.99	14
10 years	10.00 - 10.99	46	11 years	11.00 - 11.99	23
11 years	11.00 - 11.49	22	12 years	12.00 - 12.99	16
11 years 6 months	11.50 - 12.49	34	13 years	13.00 - 13.49	1
12 years 6 months	12.50 - 12.99	14			
13 years	13.00 - 13.49	3			
13 years 6 months	13.50 - 13.99	2			
	TOTAL	*821*		*TOTAL*	*535*

** The 1-3 month age category was created by the researcher in order to include those individuals who were not yet 3months of age, but were older than 28 days which is outside the age range to be considered 'newborn' (Bogin, 1999)*

Figures 4.01 (a) and *(b)* provide a graphical representation of the age distribution of the male and female samples according to the GP age groups, based on the chronological age of each individual. The youngest individual in the male sample was 2 days old and the oldest was 13.7 years. The age range for the female sample was newborn (0 days) to 13.0 years.

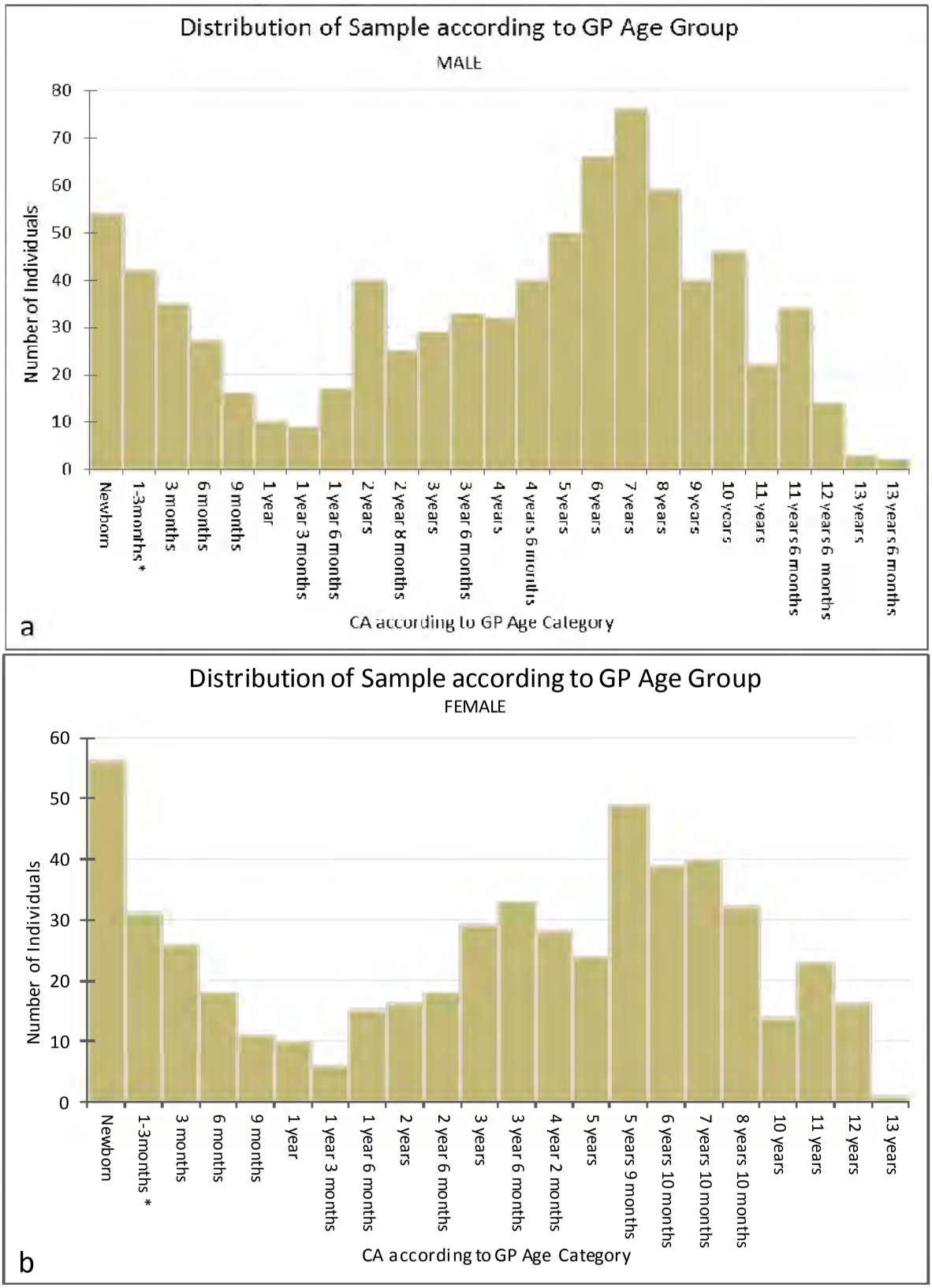

Figure 4.01 (a) and (b): *Distribution of the male (a) and female (b) samples according to the GP age groups, based on the chronological age of the samples. There are a large number of individuals in the 'Newborn' group, after which the numbers per age group decrease until approximately 2 years. Thereafter, the number of individuals per age group increases, peaking at 6 years in females and 7 years in males. Age range for the male sample is 2 days to 13.7 years, and for the female sample, newborn (0 days) to 13.0 years.*

There are a large number of individuals in the 'Newborn' age group for males and females. As age increases, the number of individuals per age group decreases until the age of 2 years, after which there is a steady increase, with values peaking at approximately 6 years in females and 7 years in males. As mentioned previously, this is mainly due to the distribution of the age categories, with more age groups (each with a narrower age range) for younger individuals, until 2 years, and the increase in age ranges for older children. The high number of newborn and 6-7 year old children is important, as these values are notably larger than for all other age categories.

The data are non-normally distributed, as can be seen in *Figure 4.02,* and confirmed by using the Shapiro-Wilks test ($p < 0.0001$). This is mainly due to the large number of individuals in the 'Newborn' age category. If one excludes this category, the data are approximately normal (which is seen by the green line in the graph).

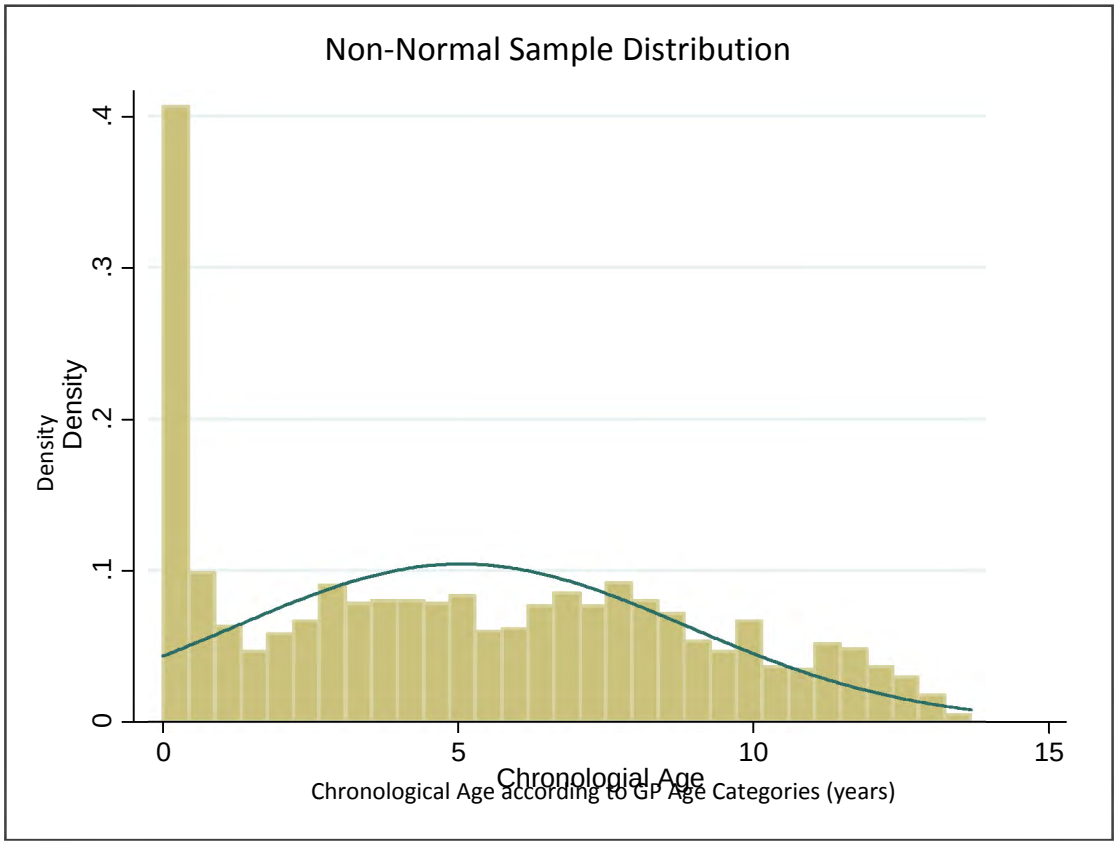

Figure 4.02 The sample is not normally distributed, due to the high number of individuals from the 'Newborn' age category. If this age category is excluded, an approximately normal distribution is present. This is shown by the green curve in the figure above.

4.2 Skeletal Age Estimation: GP Atlas Method

The results of skeletal age estimation using the GP Atlas method are presented in *Section 4.2*.

4.2.1 Intra- and Inter-observer Error

4.2.1.1 Intra-observer Error

As mentioned in *Chapter 3 Section 3.3.1*, a subset of 46 radiographs (26 males, 20 females) was analysed three times by the researcher, and once by an independent observer, Kundisai Dembetembe, who is well-practised in the GP age estimation method.

The non-parametric Kruskal-Wallis test was used to identify any significant differences between the three estimates of the researcher. The resulting *p*-values (females: $p = 0.892$ and males: $p = 0.732$) indicate that no significant differences exist between the three estimates performed by the primary researcher. This confirms a low intra-observer error, and, thus, the researcher was consistent in their skeletal age estimates using the GP Atlas method.

4.2.1.2 Inter-observer Error

This same test was used to identify significant differences between the three estimates of the researcher and the additional age estimate by the secondary observer. The inter-observer error is low for both sexes (females: $p = 0.958$ and males: $p = 0.892$). This indicates that the age estimates of the researcher are both consistent and reliable.

4.2.2 Exploratory Data Analysis

Table 4.03 details the estimation error range and the average estimation error (SA-CA) for each age group and sex. The 13 year age category for the female sample has been left blank, as there was only 1 individual in this age group, and thus, insufficient data to record average estimation error and error range. On average, estimation error increases from newborn to 13.5 years, but skeletal age is not consistently overestimated or underestimated, as can be seen by the negative and positive error ranges. On average, skeletal age is initially overestimated, for younger children (seen by a positive estimation error), and from approximately 3 years in females, and 4 years in males, skeletal age is underestimated (seen by a negative estimation error).

Table 4.03 Average Estimation Error (SA-CA) and Error Range

Male			Female		
Age Category	*Average Error (SA-CA)*	*Error Range*	*Age Category*	*Average Error (SA-CA)*	*Error Range*
Newborn	0.02	-0.08 to 0.42	Newborn	0.07	-0.08 to 0.61
1-3months *	0.09	-0.24 to 0.83	1-3months *	0.10	-0.17 to 0.58
3 months	0.10	-0.47 to 1.25	3 months	0.11	-0.38 to 0.55
6 months	0.15	-0.46 to 0.75	6 months	0.11	-0.25 to 0.38
9 months	0.08	-0.92 to 1.38	9 months	0.24	-0.23 to 1.09
1 year	0.07	-0.39 to 0.42	1 year	0.20	-0.46 to 1.00
1 year 3 months	0.43	-0.46 to 2.84	1 year 3 months	0.11	-0.37 to 0.42
1 year 6 months	-0.04	-1.04 to 1.11	1 year 6 months	0.16	-0.88 to 1.66
2 years	0.19	-1.54 to 2.12	2 years	0.34	-0.59 to 2.62
2 year 8 months	0.14	-1.49 to 2.61	2 year 6 months	0.20	-0.93 to 2.16
3 years	0.08	-2.44 to 2.80	3 years	-0.16	-0.79 to 1.01
3 year 6 months	0.04	-1.64 to 1.75	3 year 6 months	-0.25	-1.66 to 3.19
4 years	-0.12	-1.82 to 2.89	4 year 2 months	0.18	-2.50 to 2.49
4 years 6 months	-0.47	-3.01 to 2.00	5 years	0.30	-3.02 to 3.69
5 years	-0.64	-2.87 to 1.75	5 years 9 months	-0.02	-2.85 to 2.03
6 years	-0.58	-3.21 to 1.65	6 years 10 months	-0.23	-3.50 to 1.47
7 years	-1.03	-3.89 to 4.30	7 years 10 months	-0.37	-2.38 to 1.95
8 years	-0.98	-3.79 to 2.14	8 years 10 months	-0.20	-3.13 to 2.54
9 years	-0.92	-4.04 to 2.64	10 years	-0.48	-3.64 to 2.72
10 years	-0.80	-3.16 to 2.78	11 years	-0.83	-3.66 to 2.36
11 years	-0.91	-3.07 to 1.24	12 years	-0.52	-2.03 to 0.80
11 years 6 months	-1.14	-4.49 to 1.60	13 years	**	**
12 years 6 months	-1.96	-4.28 to -0.18			
13 years	-1.27	-2.68 to -0.19			
13 years 6 months	-2.16	-3.63 to -0.68			

** The 1-3 month age category was created by the researcher in order to include those individuals who were not yet 3months of age, but were older than 28 days which is outside the age range to be considered 'newborn' (Bogin, 1999)*

*** The 13 year age category for the female sample has been left blank, as there was only 1 individual in this age group, and thus, insufficient data to record average estimation error and error range.*

The correlation between chronological and skeletal age can be seen in *Figure 4.03*. Chronological age and skeletal age are positively and significantly highly correlated (Spearman $R = 0.96$). There is a non-systematic increase in the observed estimation error with an increase in age; that is, the estimation error for each individual is not the same, and skeletal age is not consistently underestimated or overestimated across the sample as a whole. This can be seen by the scatter which is present above and below the red dotted prediction line (CA = SA). Any data points above this line indicate underestimation of skeletal age (CA>SA); whereas any points below the line indicate overestimation of skeletal age (CA<SA). The blue trend line is calculated by the mean skeletal age estimate for each age group. It demonstrates the inconsistent overestimation and underestimation across all age groups and the increase in error as age increases.

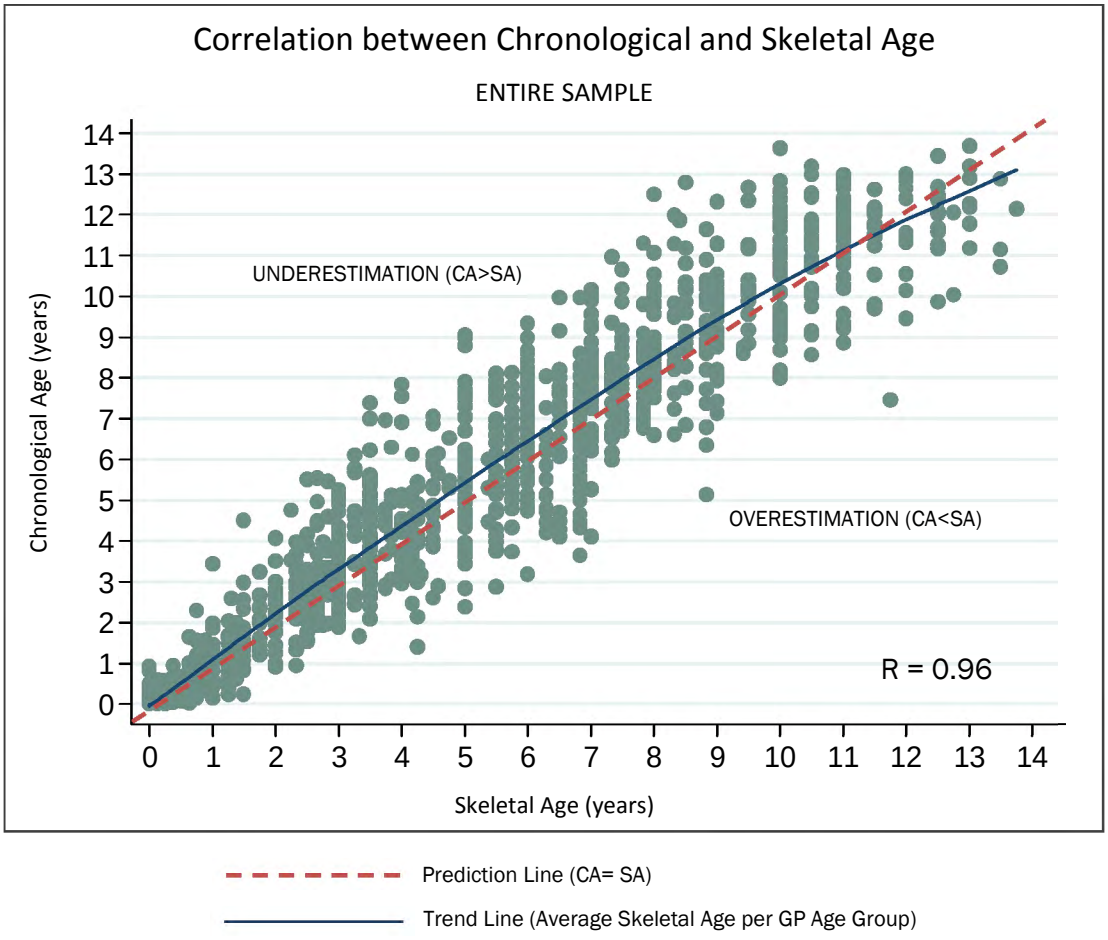

Figure 4.03 Correlation between chronological and skeletal ages for the entire sample. Chronological and Skeletal ages are positively and significantly highly correlated ($R = 0.96$). There is both underestimation and overestimation of skeletal age in all age categories.

4.2.2.1 Sex-specific Correlation

Figures 4.04 (a) and *(b)* detail this correlation by sex. A similar result is observed within each sex as for the entire sample. Chronological and skeletal ages are significantly and highly correlated (Spearman R for males = 0.96 and females = 0.97; $p < 0.0001$), with an increase in estimation error as age increases. Once again, this error is not consistent, and skeletal age is underestimated and overestimated for all age categories. The scatter around the blue trend line demonstrates the random inconsistency in age estimation for the sample. A comparison of the trend line and the prediction line illustrates the increase in error as age increases, and also shows that the male sample has a greater error compared to the female sample (there is a greater disparity between the trend line and prediction line for the male sample). This is further demonstrated in *Figure 4.05*.

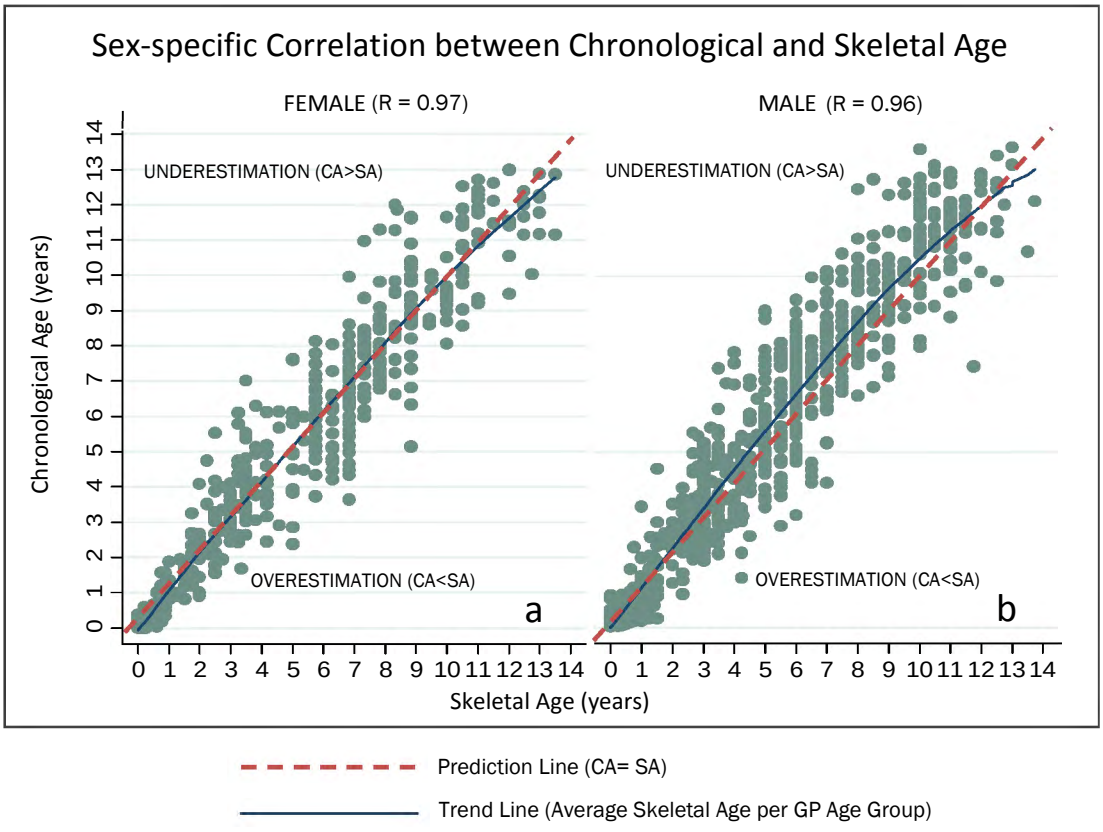

Figure 4.04 (a)* and *(b) Correlation between chronological and skeletal ages for the female (a) and male (b) samples. Chronological and Skeletal ages are positively and significantly highly correlated (Female R = 0.97; Male R = 0.96; $p < 0.0001$). For both sexes, there is both underestimation and overestimation of skeletal age in all age categories.

4.2.2.2 Error Distribution

Box-and-Whisker plots (*Figure 4.05 (a)* and *(b)*) demonstrate the distribution of the estimation error between SA and CA (that is, SA – CA), for the female and male samples, respectively.

When analysing the distribution of the estimation error (SA – CA) for each sex, females have a median estimation error which is close to zero, whilst the male sample has a more negative median estimation error, indicating a greater frequency of underestimation in the male sample. There appears to be little difference in the actual value of the median estimation error between the sexes, as both are close to zero. This is demonstrated by the overlapping boxes in *Figure 4.05*. However, when a more rigorous t-test analysis was performed, results showed that, although slight, the difference between the mean estimation error of each sex is significant ($p < 0.0001$ for both sexes), with a higher absolute mean error in the male sample.

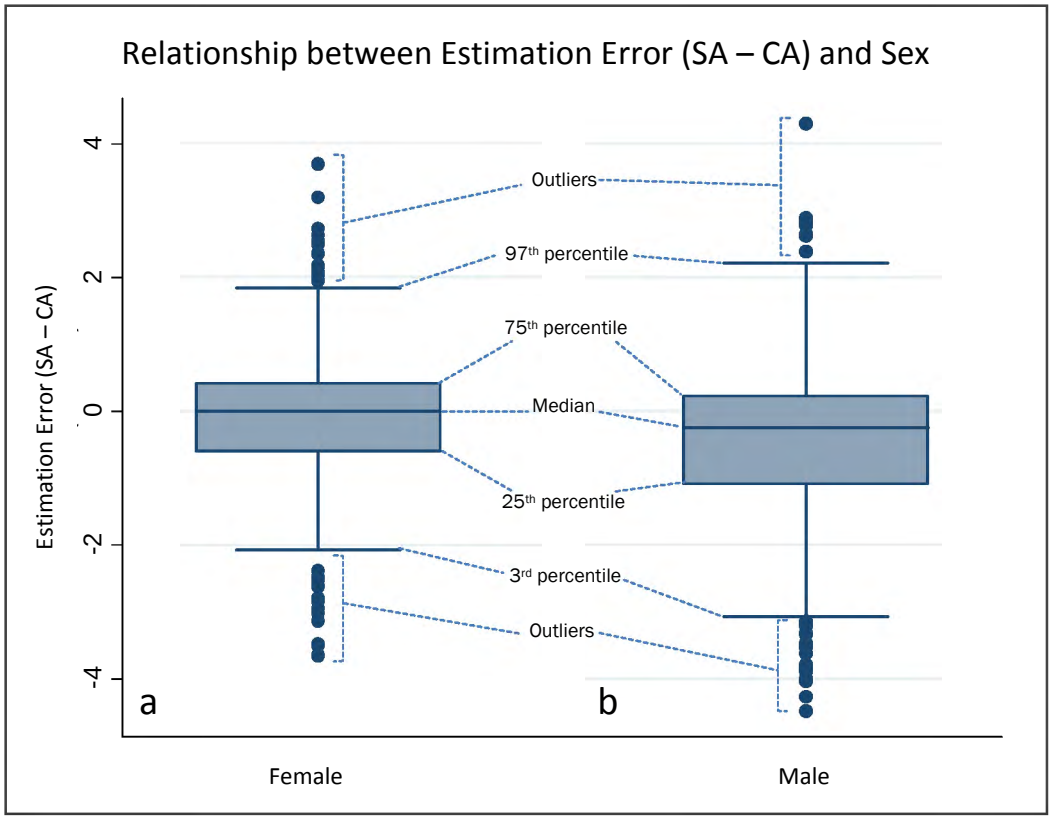

Figure 4.05 (a) and (b) Box-and-whisker plots demonstrate the relationship between estimation error (SA – CA) and sex. Males (b) exhibit a more negative median error, and a higher absolute error compared to females (a). There is a significant difference between the mean estimation error for males and females ($p < 0.0001$).

4.2.2.3 Error Type

The distribution of overestimation and underestimation of skeletal age by sex is described in *Table 4.04*. Individuals whose skeletal age estimate was greater or 'older' than their chronological age (as determined by their date of birth) were considered to have a skeletal age that was overestimated. Those whose skeletal age was less or 'younger' than their chronological age were said to be underestimated. There were a few individuals whose skeletal and chronological ages were the same – these individuals were considered to have an equal estimation of skeletal age.

Table 4.04 Incidence of Over-, Under- and Equal-Estimation of Skeletal Age

Error Type	*Sex*	
Overestimates (CA<SA)	Male	Female
N: Overestimated Individuals	284 (34.6 %)	258 (48.2 %)
N: Overestimated by more than 6 months	121 (42.6 %)	119 (46.1 %)
Maximum Overestimate (years)	4.3	3.7
Average Overestimate (years / months)	0.63 / 7.6	0.62 / 7.4
Underestimates (CA>SA)	Male	Female
N: Underestimated Individuals	529 (64.4 %)	266 (49.7 %)
N: Underestimated by more than 6 months	341 (64.5 %)	145 (54.5%)
Maximum Underestimate (years)	4.5	3.7
Average Underestimate (years / months)	1.02 / 12.2	0.77 / 9.2
Equal Estimates (CA=SA)	Male	Female
N: Individuals with Equal CA and SA	8 (1.0 %)	11 (2.0 %)

Table 4.04 shows that the GP Atlas Method tends to overestimate skeletal age in females more frequently than in males in this sample. Of the total female sample, 48.2% of individuals had an estimated skeletal age that was higher than their chronological age, when compared to only 34.6 % of males.

Results of the *Chi*-Square (χ^2) Test for Proportions shows that there is a significant association between sex and error type ($p < 0.0001$).

4.2.3 Regression Analysis – Best-Fit Regression Model

Regression analysis examined the relationship between chronological and skeletal age, based on the full data-set. Even though the data displayed slight non-normality, regression analysis remained relatively robust under these conditions, with only slightly skewed distribution of the residuals. Regression analysis aims to determine the cause of and account for sample variation. The first regression model chosen was the best-fit model, the results of which can be found in *Table 4.05*. The predictors of CA are skeletal age, sex, age-sex interaction, and the intercept value. The β values listed are the co-efficients for the predictors of CA.

Table 4.05 Regression Analysis: Best-Fit Model for Sex and Age

Predicted CA ($\hat{CA}_i$)	Coefficient	Std Error	P-Value
Skeletal Age	0.989 ($\hat{\beta}_1$)	0.013	<0.0001
Sex	0.102 ($\hat{\beta}_2$)	0.098	0.298
Age-Sex Interaction Term	0.057 ($\hat{\beta}_3$)	0.056	0.001
Constant / Intercept	0.122 ($\hat{\beta}_0$)	0.075	0.101

$\hat{CA}_i = \hat{\beta}_0$ (Intercept) + [$\hat{\beta}_1$ x Skeletal Age] + [$\hat{\beta}_2$ x Sex] + [$\hat{\beta}_3$ x Age-Sex Interaction Term] + $\hat{e}_i$ (Residual Error)

Subscripts: *i* in best-fit regression model refers to 1, …, n subjects

The regression equation for predicted chronological age ($\hat{CA}_i$) based on the best-fit model is as follows:

$$\hat{CA}_i \text{ (years)} = \hat{\beta}_0 \text{ (Intercept)} + [\hat{\beta}_1 \text{ x Skeletal Age}] + [\hat{\beta}_2 \text{ x Sex}] + [\hat{\beta}_3 \text{ x Age-Sex Interaction Term}] + \hat{e}_i$$

Sex is denoted as '0' for females and '1' for males, when calculating predicted CA using this equation. This is does not bias the results of predicted CA, because the given this notation: If predicted CA, using the best-fit model, was greater for females than for males, the model would output a negative co-efficient for sex; whilst if predicted CA using the model was greater for males than for females, this co-efficient would be a positive value, as it is in this case. As the co-efficient for sex is calculated on the actual data (that is, the skeletal ages generated for each individual in the sample), there is no bias towards either sex when using the best-fit model to predict chronological age, and the results of the analysis would not change if the denotation was switched (that is, males '0' and females '1').

Using the best-fit equation:

$$\hat{CA}_i \text{ (years)} = \hat{\beta}_0 \text{ (Intercept)} + [\hat{\beta}_1 \text{ x Skeletal Age}] + [\hat{\beta}_2 \text{ x Sex}] + [\hat{\beta}_3 \text{ x Age-Sex Interaction Term}] + \hat{e_i}$$

the average CA, predicted when SA is 0 (newborn) is 0.122 years for females. This is calculated by using the above equation and substituting the relevant values: $\hat{CA}_i = 0.122 + (0.989*0) + (0.102*0) + (0.057*0*0)$; therefore $\hat{CA}_i = 0.122$ years.
For males of the same SA, predicted average CA is 0.224 years, because $\hat{CA}_i = 0.122 + (0.989*0) + (0.102*1) + (0.057*0*1)$; thus $\hat{CA}_i = 0.224$ years.

Thus, predicted average CA is greater for males than for females, even at the newborn stage.

For a 1 unit increase in SA (SA = 1 year), the average predicted CA will increase by 0.989 years for females, because $\hat{CA}_i = 0.122 + (0.989*1) + (0.102*0) + (0.057*1*0)$; thus a female with SA of 1 year will have a predicted average CA of 1.11 years, using this equation.
A 1 unit increase in SA for males results in a 1.15 year increase in the predicted average CA, because $\hat{CA}_i = 0.122 + (0.989*1) + (0.102*1) + (0.057*1*1)$; thus on average, a male with a skeletal age of 1 year will have a predicted chronological age of 1.27 years.

Although the sex coefficient ($\hat{\beta}_1$) is not significant ($p = 0.298$), the coefficient for the age-sex interaction term ($\hat{\beta}_3$) is ($p = 0.001$) (See *Table 4.04*). A significant $\hat{\beta}_3$ value indicates that the relationship between the predicted CA and the SA is dependent on the sex of the subject.
When SA is zero, the small difference between the predicted CA of females compared to males is of little importance. The impact on predicted CA when SA increases by 1 unit, however, is significant, because the age-sex interaction term now has an influence. As SA increases further, this effect becomes even more compounded.
The example below illustrates this:

For females:

SA = 0: $\hat{CA}_i = 0.122 + (0.989*0) + (0.102*0) + (0.057*0*0) = 0.122$ years

SA = 1: $\hat{CA}_i = 0.122 + (0.989*1) + (0.102*0) + (0.057*1*0) = 1.11$ years

SA = 2: $\hat{CA}_i = 0.122 + (0.989*2) + (0.102*0) + (0.057*2*0) = 2.10$ years

For males:

SA = 0: $\hat{CA}_i = 0.122 + (0.989*0) + (0.102*1) + (0.057*0*1) = 0.224$ years

SA = 1: $\hat{CA}_i = 0.122 + (0.989*1) + (0.102*1) + (0.057*1*1) = 1.27$ years

SA = 2: $\hat{CA}_i = 0.122 + (0.989*2) + (0.102*1) + (0.057*2*1) = 2.32$ years

With further increases in SA, one can see the impact that sex and the interaction between sex and age has on predicted CA.

The distribution of the residuals (actual CA - predicted CA), can be seen in *Figure 4.06.* Examination of the histogram shows that the residuals follow a relatively normal distribution pattern, with the distribution only very slightly skewed to the left. The three highest bars indicate a large number of overestimated values.

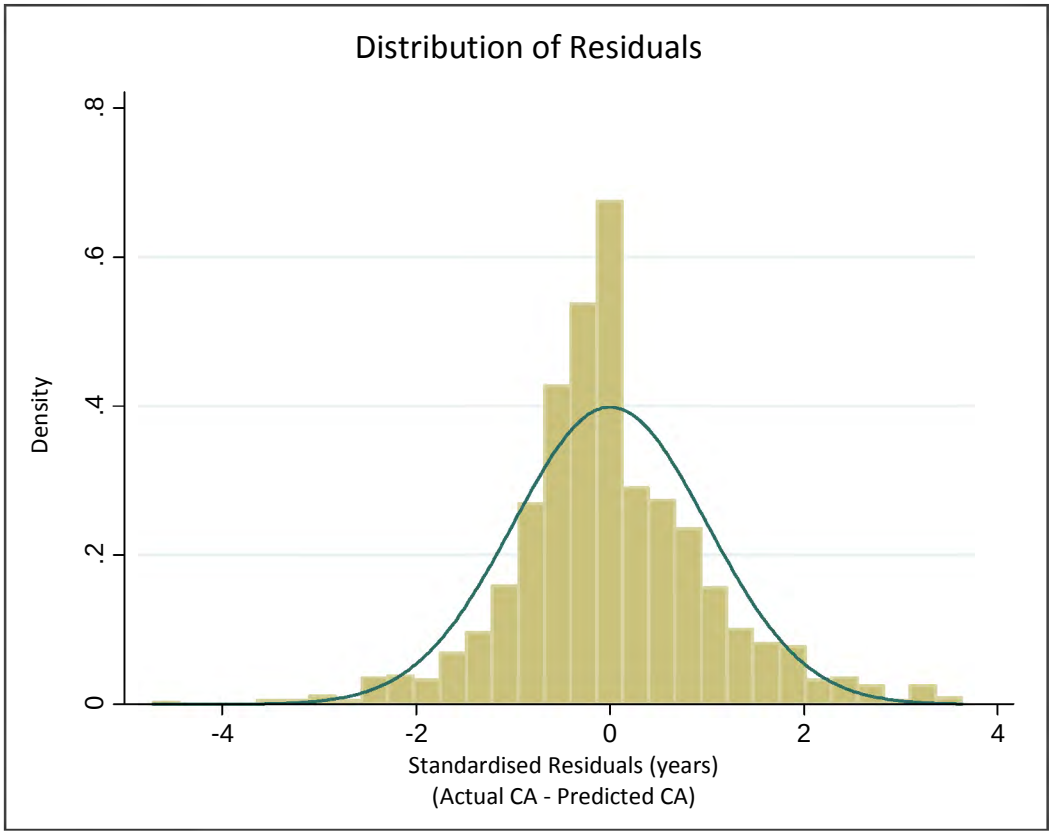

Figure 4.06 Residual distribution graph. Normal distribution of residuals, except for the highest 3 bars, which indicate a significant overestimation of chronological age

The plot of residuals against predicted chronological age (see *Figure 4.07 (a)*) follows a heteroskedastic distribution (characterised by the outward 'fanning' of the scatter). This fanning occurs mostly after the predicted age of 2 years, and increases with age.

Observations *1283* and *1312* are two potential outliers (marked in red in *Figures 4.07 (a)* and *(b)*). The Cook's *D* Statistic was used to determine the influence of these outliers on the results of the regression analysis. *Figure 4.07 (b)* shows how these two outliers skew the results of the regression.

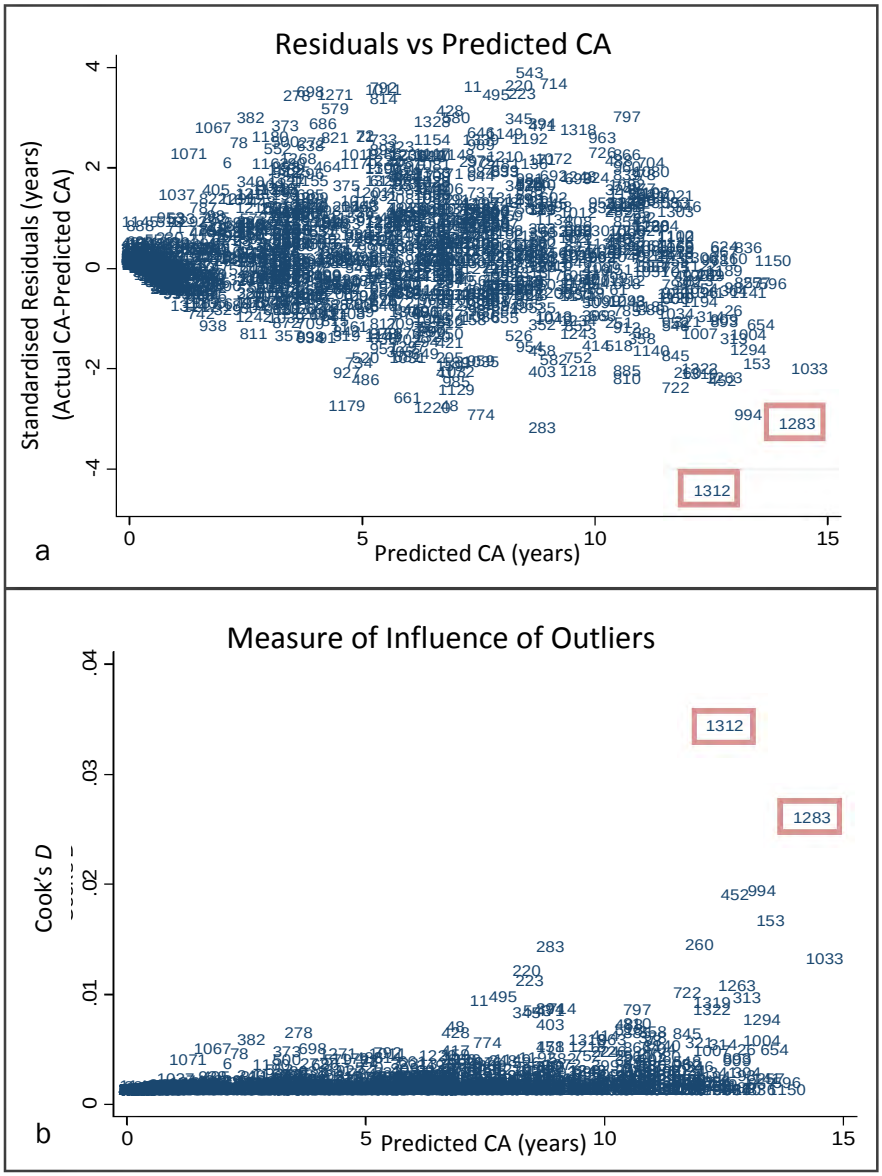

Figure 4.07 (a) and (b) Standardised residuals vs predicted CA reveals a heteroskedastic distribution, and two potential outliers (marked by rectangles). Cook's *D* measures the influence of these outliers, showing their skewing effect on the results of the regression analysis,

4.2.3.1 Analysis without Outliers

Performing the analysis again after removing observations *1283* and *1312*, resulted in changes in the coefficients for sex and the age-sex interaction term (see *Table 4.05*). The estimated coefficient for the age-sex interaction term increased from 0.057 to 0.063, and remains significant.

Table 4.05 Regression Analysis: Results after removal of Outliers

Predicted CA ($\hat{CA}_i$)	Coefficient	Std Error	P-Value
Skeletal Age	0.989 ($\hat{\beta}_1$)	0.012	<0.0001
Sex	0.081 ($\hat{\beta}_2$)	0.097	0.405
Age-Sex Interaction Term	0.063 ($\hat{\beta}_3$)	0.016	0.001
Constant	0.122 ($\hat{\beta}_0$)	0.074	0.096

$\hat{CA}_i = \hat{\beta}_0$ (Intercept) + [$\hat{\beta}_1$ x Skeletal Age] + [$\hat{\beta}_2$ x Sex] + [$\hat{\beta}_3$ x Age-Sex Interaction Term] + $\hat{e_i}$ (Residual Error)

The subscript i refers to 1,…,n number of subjects.

Using the same best-fit equation, but with the recalculated coefficients (from *Table 4.05*) substituted:

$$\hat{CA}_i \text{ (years)} = \hat{\beta}_0 \text{ (Intercept)} + [\hat{\beta}_1 \text{ x Skeletal Age}] + [\hat{\beta}_2 \text{ x Sex}] + [\hat{\beta}_3 \text{ x Age-Sex Interaction Term}] + \hat{e_i}$$

the predicted average CA, when SA is 0 (newborn) remains unchanged at 0.122 years for females and 0.224 years for males.

When there is a 1 unit increase in SA, however, the new coefficients calculated after removal of the outliers, have an effect. This effect is only for male individuals, as the coefficients which have changed are those for sex and the age-sex interaction term. Thus, predicted CA for females when SA increases by 1 unit will remain unchanged at 1.11 years; but for males, predicted CA will be 1.26 years ($\hat{CA_i} = 0.122 + [0.989*1] + [0.087*1] + [0.063*1*1]$).

Predicted CA for males before the removal of outliers, where SA = 1 year, was 1.27 years. Predicted CA for males after the removal of outliers, where SA = 1 year, was 1.26 years. Thus, recalculation with the outliers removed improves the best-fit model only slightly, with an improvement of 0.01 years on prediction of CA for males of 1 year. This will have a greater impact as age increases, thereby improving prediction of CA for older individuals.

Distribution of the residuals remains normal, with the over-prediction of chronological age remaining (represented by the three highest bars in the distribution), although somewhat decreased, compared to the distribution in *Figure 4.06*. The three highest bars decreased in height, once outliers were removed from analysis (see *Figure 4.08*).

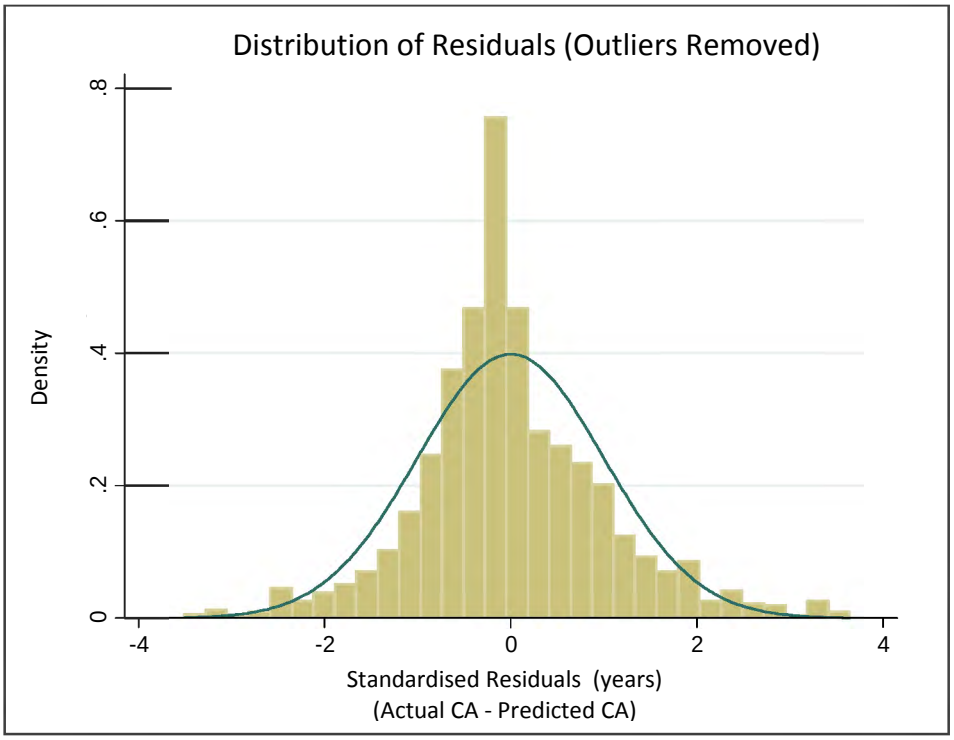

Figure 4.08 Distribution of residuals remains normal after outliers have been removed from analysis. There is still over-prediction of chronological age, although somewhat decreased after excluding the outliers from analysis

The plot of residuals against predicted chronological age in *Figure 4.09* still exhibits a heteroskedastic distribution (characterised by the outward 'fanning' of the scatter), even after the outliers have been removed from analysis. The 'fanning' of the scatter is only slightly decreased compared to analysis with the outliers included. As predicted CA increased, there is a significant 'fanning' of the residuals (because the residuals are increasing). This levels out for the older age groups (from approximately 10 years).

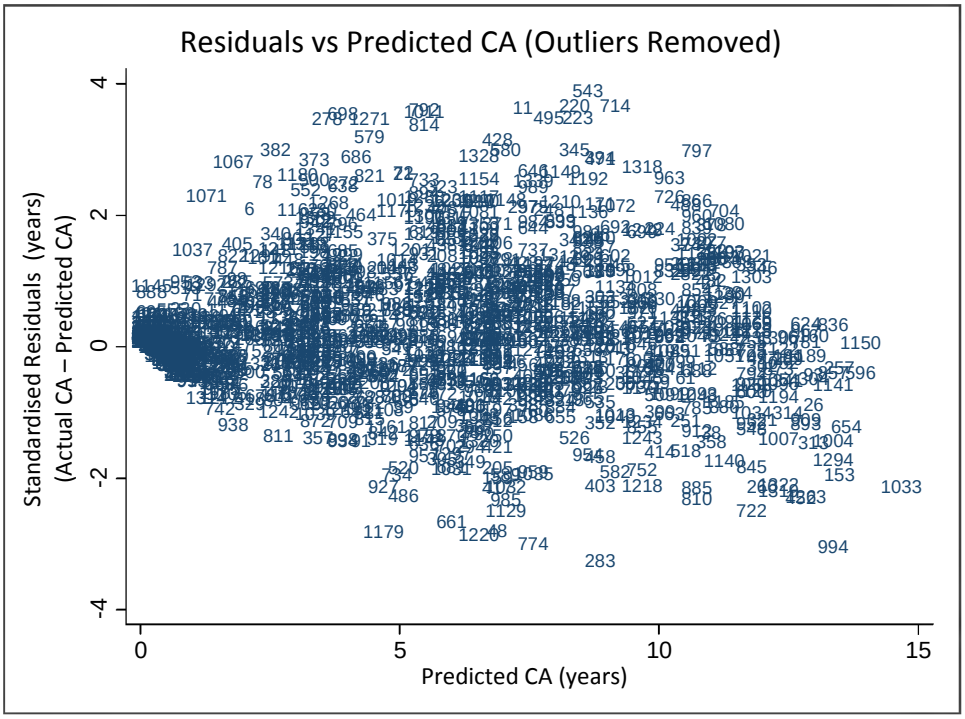

Figure 4.09 Heteroskedastic distribution remains, after outliers have been excluded from analysis. The 'outward fanning' is very slightly decreased, but still significant.

Using the best-fit regression equation, substituted with the values from *Table 4.05*, the plot of predicted chronological age and actual chronological age continues to show a fair degree of scatter (see *Figure 4.10*). Thus, there is variation within the sample that has not been sufficiently captured by the best-fit model of regression analysis, even after removal of outliers.

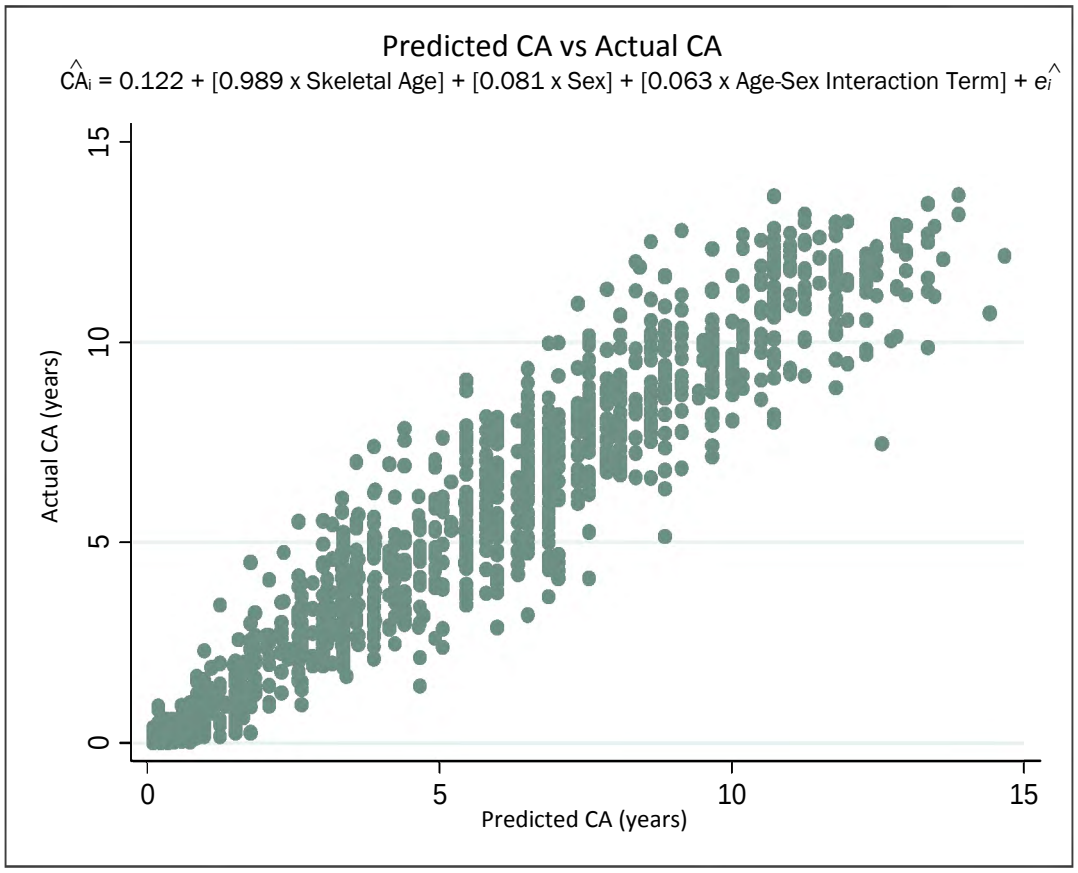

Figure 4.10 Predicted vs Actual CA for the sample results in correlated, but scattered values. This indicates variation in the sample which has not been accounted for by the best-fit regression analysis. Regression equation on graph.

4.2.3.2 Factors Influencing Sample Variation

Regression analysis has shown that sex has an influential role in the prediction of chronological age, but not all sample variation is accounted for by sex differences alone. Other factors may include racial classification or socio-economic status.

4.2.3.2.1 Variation due to Racial Classification

Identification by race was not possible for the entire data-set, but instead extended only to the mortuary sample, a subset of 338 individuals. *Table 4.07* outlines the distribution of this sub-set according to racial classification.

Table 4.07 Distribution of Sub-Sample according to Racial Classification

Sex	Racial Classification		
	Black	White	Coloured
Male	101	6	75
Female	100	2	54
Total	201	8	129

The sample is underpowered for White males and females, and this should always be taken into consideration when interpreting results related to racial classification.

Using 'Black' as an arbitrary base-line, racial classification was incorporated into the regression analysis to quantify its influence on predicted chronological age. This was done by comparing the differences in regression (if any) between Black children versus White children, and Black children versus Coloured children. The results of this analysis are presented in *Table 4.08.*

Table 4.08 Effect of Racial Classification on Regression Analysis

Parameters	Coefficient	Std Error	*P*-value
Skeletal Age	0.997	0.025	<0.0001
Sex	0.032	0.053	0.547
Age-Sex Interaction Term	0.023	0.031	0.401
Coloured	0.021	0.048	0.670
White	0.204	0.155	0.187
Constant	- 0.089	0.043	0.039

From *Table 4.08* it is evident that racial classification has no significant influence on predicted average chronological age (p = 0.67 for Coloured individuals; p = 0.19 for White individuals, when compared to Black individuals). The results for White children should be viewed with caution due to the very small sample size; however, based on the large sample size of Black and Coloured individuals, these results show that there is no significant difference between predictions of CA for Black compared to Coloured children.

The effect of racial classification does not change depending on the sex of the individual and remains non-significant for both males and females. This is because variation due to sex has already been accounted for by the previous stage of regression analysis; and thus the coefficient for sex and the age-sex interaction term are not significant.

4.2.3.2.2 Variation due to Socio-economic Status (SES)

Although racial classification has no influence on prediction of chronological age, socio-economic status (SES) (based on area and average monthly household income) may influence this prediction. *Table 4.09* lists the Police station areas in order of average monthly household income, from lowest to highest. Median monthly household income range (generated by Lightstone ©) was used to calculate average monthly household income. Average monthly household income was then used as an indirect indicator of the SES of a specific area.

Areas with a lower average monthly household income are considered to have a low SES, and conversely, higher average monthly household income areas have a high SES.

Table 4.09 Average Monthly Household Income based on Police Station Area

	Key	Police Station	# Suburbs per Area	Median Household Income Range	Average Household Income per month*	Cases per Area F	M	Total
Lower Income	1	Harare	6	R 1 500 - R 3 000	R 2 250	3	2	5
	2	Delft	5	R 1 500 - R 3 000	R 2 250	7	12	19
	3	Khayelitsha	1	R 1 500 - R 3 000	R 2 250	3	7	10
	4	Kraaifontein	24	R 1 500 - R 3 000	R 2 250	5	9	14
	5	Mfuleni	3	R 1 500 - R 3 000	R 2 250	3	5	8
	6	Nyanga	4	R 1 500 - R 3 000	R 2 250	31	22	53
	7	Philippi	3	R 1 500 - R 3 000	R 2 250	7	7	14
	8	Philippi East	2	R 1 500 - R 3 000	R 2 250	9	12	21
	9	Lingelethu-West	3	R 1 500 - R 3 000	R 2 250	1	2	3
	10	Atlantis	3	R 3 000 - R 6 000	R 4 500	5	6	11
	11	Elsies River	13	R 3 000 - R 6 000	R 4 500	0	2	2
	12	Gugulethu	1	R 3 000 - R 6 000	R 4 500	11	10	21
	13	Langa	1	R 3 000 - R 6 000	R 4 500	7	6	13
	14	Manenberg	7	R 3 000 - R 6 000	R 4 500	5	8	13
	15	Mitchell's Plain	17	R 3 000 - R 6 000	R 4 500	12	11	23
	16	Ravensmead	7	R 3 000 - R 6 000	R 4 500	1	0	1
	17	Hout Bay	10	R 6 000 - R 9 000	R 7 500	1	1	2
	18	Ocean View	4	R 6 000 - R 9 000	R 7 500	4	1	5
	19	Belhar	2	R 9 000 - R 15 000	R 12 000	1	0	1
	20	Grassy Park	7	R 9 000 - R 15 000	R 12 000	0	6	6
	21	Kensington	2	R 9 000 - R 15 000	R 12 000	0	1	1
	22	Maitland	6	R 9 000 - R 15 000	R 12 000	3	4	7
	23	Steenberg	4	R 9 000 - R 15 000	R 12 000	3	7	10
	24	Strandfontein	2	R 9 000 - R 15 000	R 12 000	2	1	3
	25	Parow	11	R 15 000 - R 18 000	R 16 500	3	0	3
	26	Athlone	13	R 18 000 - R 24 000	R 21 000	5	4	9
	27	Bellville	29	R 24 000 - R 37 000	R 30 500	0	1	1
	28	Diep River	6	R 24 000 - R 37 000	R 30 500	0	1	1
	29	Kuils River	27	R 24 000 - R 37 000	R 30 500	2	3	5
	30	Lansdowne	5	R 24 000 - R 37 000	R 30 500	1	1	2
	31	Milnerton	17	R 24 000 - R 37 000	R 30 500	10	13	23
	32	Mowbray	3	R 24 000 - R 37 000	R 30 500	1	6	7
	33	Muizenberg	11	R 24 000 - R 37 000	R 30 500	2	3	5
	34	Table View	14	R 24 000 - R 37 000	R 30 500	3	1	4
	35	Woodstock	4	R 24 000 - R 37 000	R 30 500	2	1	3
	36	Wynberg	3	R 24 000 - R 37 000	R 30 500	0	1	1
	37	Fish Hoek	8	R 37 000 - R 43 000	R 40 000	0	1	1
	38	Pinelands	3	R 43 000 - R 51 000	R 45 500	0	1	1
	39	Cape Town	7	R 51 000 - R 67 000	R 59 000	1	2	3
	40	Seapoint	6	R 51 000 - R 67 000	R 59 000	2	0	2
Higher Income	41	Kirstenhof	15	R 75 000 +	R 75 000 +	1	1	2

** Average household income per month is from the median household income range, which was generated by Lightstone ©, 2011.*

Average house-hold income ranged from R 2 250 per month for lower-income/low SES areas, to over R 75 000 per month for higher income/high SES areas. These values are based on the median monthly income range per household for each suburb in a Police station area, and reflect the income earned by the majority of people within that area. The median income ranges were generated by Lightstone ©.

The areas with the highest number of cases tended to fall within the low SES bracket with the exception of Steenberg and Milnerton (Key numbers *23* and *31*, respectively, in *Table 4.09* and *Figure 4.11*). The suburb with the highest case number was Nyanga, which is a geographically large area, with an average monthly house-hold income of R 2 250.
There tends to be a decrease the number of cases as the average monthly household income increases (and thus, as SES improves).

Figure 4.11 is a graphical representation of the difference between skeletal and chronological age for each Police station area. Any points beneath the *Estimation Error = 0* (dotted) line indicate underestimation of skeletal age; where *Estimation Error = 0*, skeletal age and chronological age were equal; skeletal age was overestimated for any points above the *Estimation Error = 0* line.

There is a wider error range for the low SES areas, which decreases as average monthly household income (and, therefore, SES) increases. This difference is not significant, as the relationship between Estimation Error and Police Station area yields a correlation coefficient of $R = 0.127$, and may simply be due to the higher case-load for low SES areas. This non-significant correlation is demonstrated further by the flat slope of the regression on the graph in *Figure 4.11*.

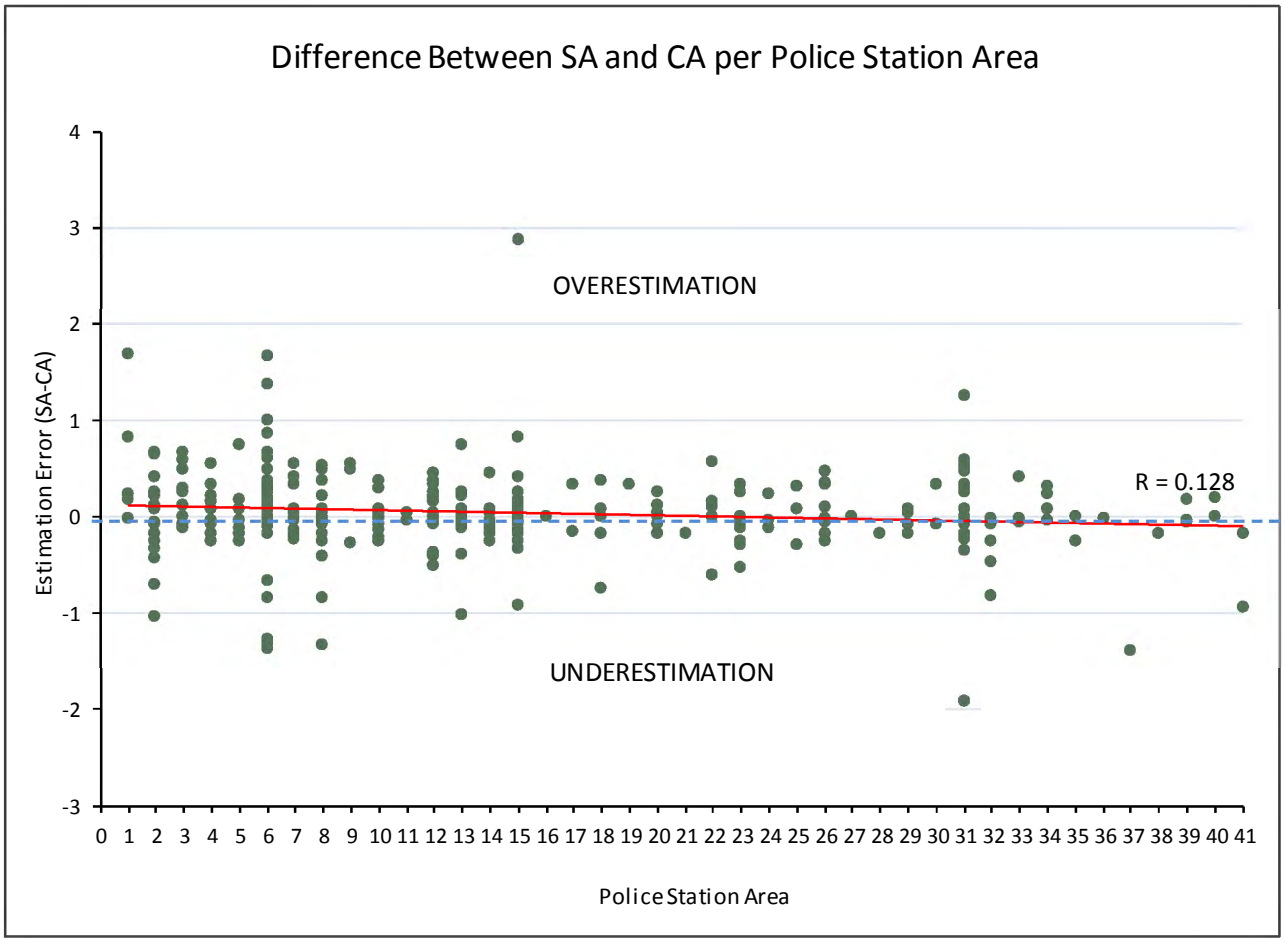

	Key	*Police Station*	*Key*	*Police Station*	*Key*	*Police Station*	
	1	Harare	15	Mitchell's Plain	29	Kuils River	
	2	Delft	16	Ravensmead	30	Lansdowne	
	3	Khayelitsha	17	Hout Bay	31	Milnerton	
	4	Kraaifontein	18	Ocean View	32	Mowbray	
	5	Mfuleni	19	Belhar	33	Muizenberg	
Lower Income	6	Nyanga	20	Grassy Park	34	Table View	*Higher Income*
	7	Philippi	21	Kensington	35	Woodstock	
	8	PhilippiEast	22	Maitland	36	Wynberg	
	9	Lingelethu-West	23	Steenberg	37	Fish Hoek	
	10	Atlantis	24	Strandfontein	38	Pinelands	
	11	Elsies River	25	Parow	39	Cape Town	
	12	Gugulethu	26	Athlone	40	Seapoint	
	13	Langa	27	Bellville	41	Kirstenhof	
	14	Manenberg	28	Diep River			

Skeletal Age = Chronological Age (Estimation Error = 0)

Regression Line

Figure 4.11 Difference between skeletal age and chronological age for each police station area. The low *R*-value ($R = 0.128$; $p = 0.5$) indicates no significant correlation between Estimation Error and Police Station area, which is also demonstrated by the 'flat' slope of the regression line (in red)

4.2.3.3 Summary of Results from the Best-Fit Model

The best-fit model of regression analysis was used to determine the relationship between skeletal age and chronological age, and to account for some of the variation seen in the data. Initial output from the analysis showed that sex and the interaction between sex and skeletal age had an effect on the prediction of chronological age. It was shown that from newborn, predicted chronological age for males was greater than for females, the effect of which was only slightly reduced once outliers had been removed from analysis. The impact of the interaction between age and sex became greater as age increased.

Other variables such as racial classification and SES were sought as possible predictors of chronological age, but they provided no improvement to the best-fit model.

Although a good fit, the final best-fit model did not sufficiently capture the variation within the sample.

4.2.4 Regression Analysis – Mixed-Effect Model

A mixed-effect model was used in an attempt to improve the results of the initial regression analysis. This model has both fixed- and random-effects, which are incorporated together to create a better model-fit for the data. Fixed-effects in this research are variables such as skeletal age and sex, the relationship of which is consistent across the entire sample. Random-effects are age-category specific effects. The inclusion of the random-effects accounts for difference correlation structures between observations, whilst assuming that observations within a specific age category are related.

The first mixed-effect model used was a random intercept model. This model assumes that the relationship between predicted chronological age and the predictor variables (sex, skeletal age and the age-sex interaction term) remains constant across the whole sample (this is the fixed-effect portion of the model), whilst the intercept value for each age category will change (this is the random-effect portion of the model). A second mixed-effect model was used to determine if it would improve the results of the prior model. This is the random intercept-random slope model. The fixed-effect portion of this model remains the same, that is, the relationship between predicted chronological age and the predictor variables remains constant across all age groups. The random-effect portion, however is made up of two random-effect parameters – the differing intercept and slope values for each age category, and thus allows more within-group variation to be accounted for.

This model uses a similar equation to that of the best-fit model. The regression analysis outputs coefficients for each of the predictor variables ($\hat{\beta}_1$, $\hat{\beta}_2$ or $\hat{\beta}_3$). For the random intercept model, the random-effect parameter, $\hat{b}_{0i}$, is calculated in the output of analysis. This is the random intercept effect value. For the random intercept-random slope model, a random intercept effect value ($\hat{b}_{0i}$) and a random slope effect value ($\hat{b}_{1i}$) are calculated. Both mixed-effect models have the additional residual error (e_{ij}).^

4.2.3.4 Random Intercept Effect

This mixed-effect model has both fixed-effects and age-group specific random intercept effects, and uses the equation:

$$\hat{CA}_{ij} = \beta_0 \text{ (Intercept)} + [\hat{\beta}_1 \text{ x Skeletal Age}] + [\hat{\beta}_2 \text{ x Sex}] + [\hat{\beta}_3 \text{ x Age-Sex Interaction Term}] + \hat{b}_{0i} + \hat{e}_{ij}$$

Subscript i refers to 1,…32 GP age categories; j refers to 1,…,n subjects in the sample.

Both $\hat{b}_{0i}$ (random-intercept effect parameter) and $\hat{e}_{ij}$ (residual error) are assumed to be normally distributed.

Table 4.10 outlines the estimated fixed-effect parameters, together with the estimated standard deviation (SD) of the random-effects for the random intercept model. These fixed-effect values have been adjusted for by the random-effect parameters, and thus the coefficient for sex is now negative. This does not change the relationship between sex and skeletal age.

Table 4.10 Parameters for Random Intercept Mixed Effect Model

Fixed-Effect Parameter	Coefficient	Std Error	P-Value
Skeletal Age	0.025 ($\hat{\beta}_1$)	0.006	<0.0001
Sex	- 0.013 ($\hat{\beta}_2$)	0.021	0.534
Age-Sex Interaction Term	0.007 ($\hat{\beta}_3$)	0.004	0.097
Constant/Intercept	5.758 ($\hat{\beta}_0$)	0.742	0.096

$$\hat{CA}_{ij} = \beta_0 \text{ (Intercept)} + [\hat{\beta}_1 \text{ x Skeletal Age}] + [\hat{\beta}_2 \text{ x Sex}] + [\hat{\beta}_3 \text{ x Age-Sex Interaction Term}] + \hat{b}_{0i} + \hat{e}_{ij}$$

Random-Effect Parameter	Estimate of Variation	Std Error
SD (Constant)	4.192	0.525
SD (Residual)	0.216	0.004

The estimated age category-specific $\hat{b}_{0i}$ values can be found in *Table 4.11*.

Table 4.11 Estimated Random Effect ($\hat{b}_{0i}$)* Values for GP Age Categories

GP Age Category	Estimated Random Effect ($\hat{b}_{0i}$)
Newborn	-5.704
1 - 3 months	-5.597
3 Months	-5.440
6 months	-5.195
9 months	-4.909
1 year	-4.671
1 year 3 months	-4.438
1 year 6 months	-4.040
2 years	-3.510
2 year 6 months	-3.114
2 years 8 months	-2.999
3 years	-2.615
3 years 6 months	-2.036
4 years	-1.621
4 years 2 months	-1.260
4 years 6 months	-1.124
5 years	-0.524
5 years 9 months	0.412
6 years	0.595
6 years 10 months	1.383
7 years	1.618
7 years 10 months	2.383
8 years	2.474
8 years 10 months	3.462
9 years	3.486
10 years	4.371
11 years	5.199
11 years 6 months	5.839
12 years	6.308
12 years 6 months	6.651
13 years	7.085
13 Years 6 months	7.530

**The* $\hat{b}_{0i}$ *value should be added to the* $\hat{\beta}_0$ *Intercept value when predicted chronological age is calculated*

The $\hat{\beta}_0$ intercept value for this model is 5.758, however, by adjusting the equation by the age-category specific random intercept effect value, $\hat{b}_{0i}$, (from *Table 4.11*), the predicted CA will be closer to the SA for that individual. This is reason for the distribution of the values in *Table 4.11*. For individuals under 5 years, the $\hat{b}_{0i}$ values are negative, and for individuals older than 5 years, the $\hat{b}_{0i}$ values are positive, as the $\hat{b}_{0i}$ for a specific SA is added to $\hat{\beta}_0$ to create a new intercept value for that age category.

Irrespective of sex, this model does not allow for the relationship between chronological age and skeletal age to change across the various age categories. Only the intercept is altered.

For example, using this model to predict chronological age, a female respondent with a skeletal age of 1 year will have a predicted chronological age of 1.11 years, which is obtained from the equation $\hat{CA}_{ij} = 5.758 - 4.671 + (0.025*1) - (0.013*0) + (0.007*0)$.

Figure 4.12 outlines the distribution of the residuals using this model. The distribution remains approximately normal, with a slight improvement on the distribution of residuals from the best-fit model, as the three highest bars have reduced in height somewhat. There remains a small degree of under- and –over prediction of chronological age.

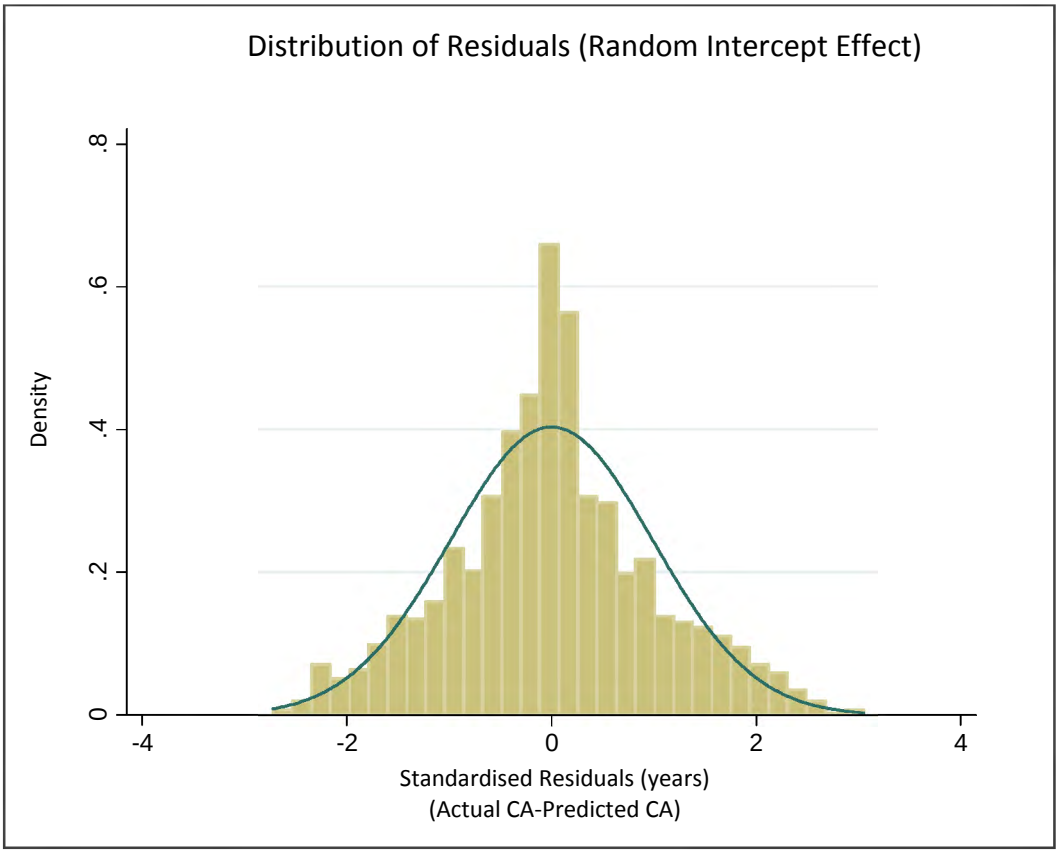

Figure 4.12 Residual distribution graph. Approximately normal distribution of residuals, with a slight improvement on the distribution from the previous regression model. There remains a small amount of under- and over-estimation of chronological age.

The plot of residuals against the fixed-effect portion of predicted chronological age in *Figure 4.13* continues to show a heteroskedastic distribution but compared to the distribution in *Figure 4.09,* the scatter is much improved, and there is considerably less 'fanning'.

The 'fanning' and scatter levels out after approximately 6 years (important to note, this is not the final predicted CA, as it is only the fixed-effect portion which has been plotted).

The predicted chronological age does not start at zero on the X-axis, as these values have not yet been adjusted by the random-effect parameters ($\hat{b}_{0i}$) for the age groups concerned. Instead the values start at the β_0 $\hat{}$value, 5.758 (from *Table 4.10*).

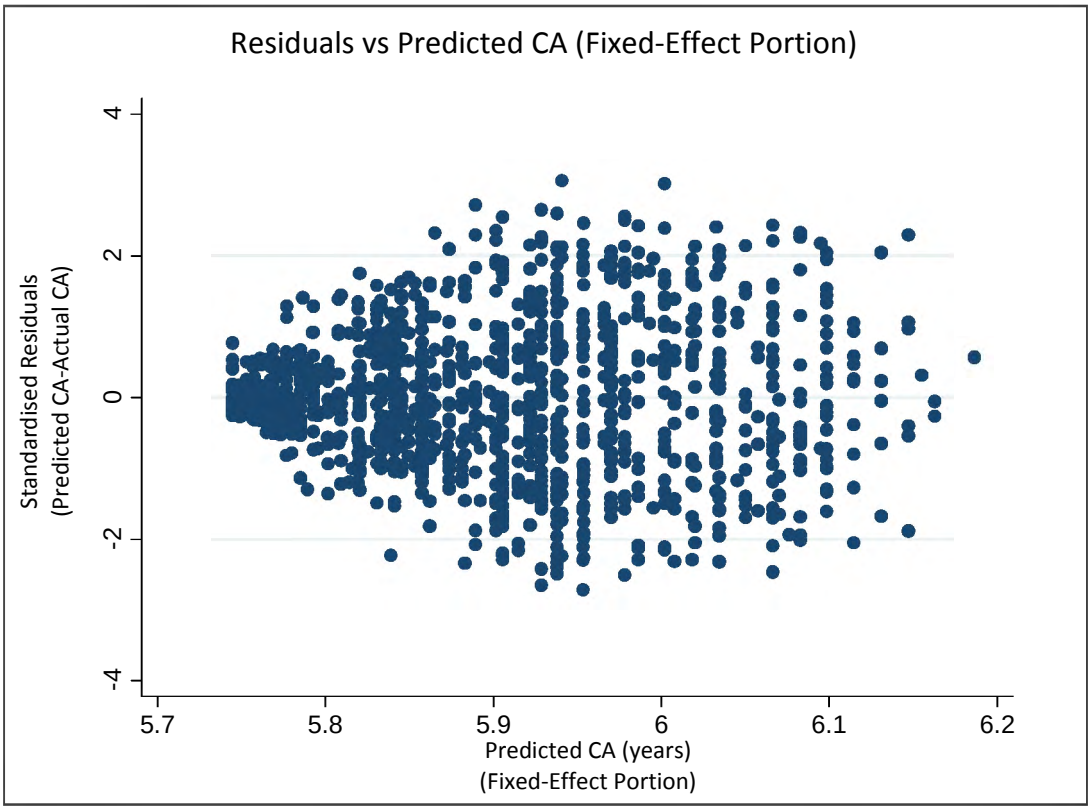

Figure 4.13 Heteroskedastic distribution remains, although the fanning of the scatter has improved considerably, using the random intercept model

The plot of the fixed-effect portion of the predicted chronological age against actual chronological age (*Figure 4.14 (a)*), using the equation:

$$\hat{}CA_{ij} = 5.758 + (0.025*\text{Skeletal Age}) - (0.013*\text{ Sex}) + (0.007*\text{Age-Sex Interaction Term})$$

shows a good model-fit for the data; however some variation can still be seen by the scatter on the graph. Note the intercept of the graph, which is greater than zero as these values are only the fixed-effect portion of the model, and $\hat{\beta}_0$ has not yet been adjusted by the random-effect parameters ($\hat{b_{0i}}$) for the age groups concerned.

If these values are adjusted by incorporating the random-effect parameters for each age category (*Figure 4.14 (b)*), the data cluster into age groups, and thus, the variation in the data becomes significantly reduced. There remains a small amount of outward dispersion within the middle age groups (5 to 10 years).

4.2.4.1.1 Summary of Random Intercept Model

The random intercept model is a mixed-effect model with both fixed- and random-effect parameters. The fixed-effect parameters are predictor variables such as sex and skeletal age, the effect of which is constant across the whole sample. The random-effects are age group specific, and for this analysis, the random-effect caused a change in the intercept value for each age category, whilst leaving the slope unchanged.

This model was an improvement on the best-fit model, as the variation in the sample was considerably reduced once the random-effect parameters were incorporated into the analysis and final regression plot. The addition of the random-effect parameters into the final regression line for the sample reduced the sample variation and scatter considerably.

The addition of random-effect parameters causes clustering of the data into age groups, and results in a strong correlation between actual and predicted chronological age. Comparing the plot of the fixed-effect portion of predicted CA to the fixed and random-effect portions, one can see that much of the variation in the sample can be considered ‘random’ variation, that is, not due to sex, or skeletal age, or the interaction between sex and skeletal age.

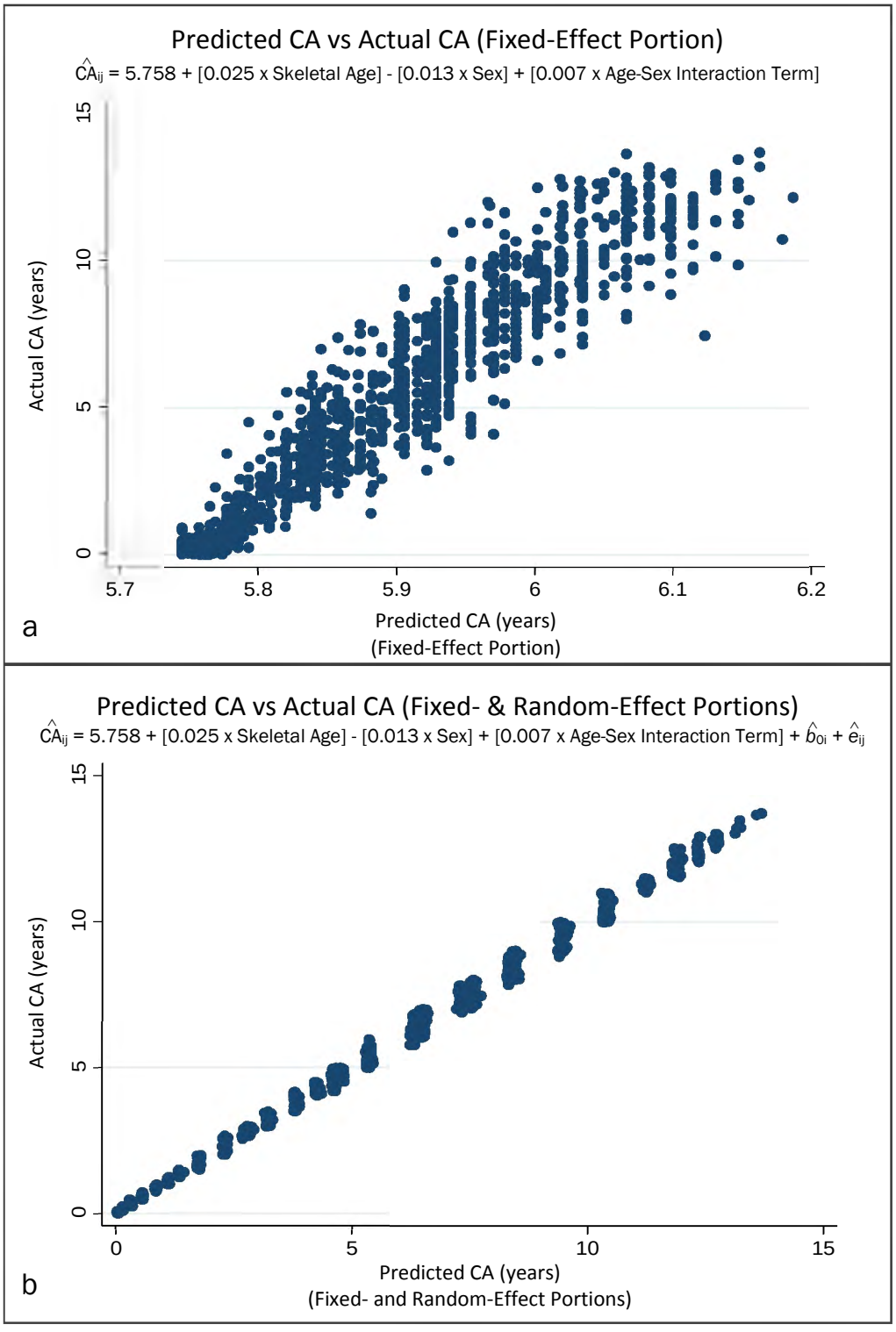

Figure 4.14 (a)* and *(b) The fixed-effect portion of predicted CA vs Actual CA for the sample shows a reduction on the variation within the data (a). By incorporating the random-effect parameters for each age category, the data cluster and the 'fit' is significantly improved (b).

4.2.4.2 Random Intercept-Random Slope Effect

The random intercept effect model in *Section 4.2.4.1* assumes that the relationship between chronological age and skeletal age remains constant across all age groups, irrespective of sex. The random intercept-random slope effect model questions whether this is, in fact, the case, or if the relationship between chronological age and skeletal age differs depending on the age group of the individual. This model seeks to improve on the previous model in *Section 4.2.4.1*.

The random intercept-random slope effect model is a mixed effect model, and thus, has both fixed- and random-effect parameters. The estimated standard deviation of the random-effects, together with the estimated fixed-effect parameters are outlined in *Table 4.12*. Added to the original equation are two age-group specific values: $\hat{b}_{0i}$ is the estimated intercept random-effect value; $\hat{b}_{1i}$ is the estimated slope random-effect value. These are listed for each GP age category in *Table 4.13*.

Table 4.12 Parameters for Random Intercept-Random Slope Mixed Effect Model

Fixed-Effect Parameter	Coefficient	Std Error	P-Value
Skeletal Age	0.025 ($\hat{\beta}_1$)	0.009	0.007
Sex	- 0.015 ($\hat{\beta}_2$)	0.021	0.471
Age-Sex Interaction Term	0.008 ($\hat{\beta}_3$)	0.004	0.076
Constant	5.752 ($\hat{\beta}_0$)	0.741	<0.0001

$\hat{CA}_{ij} = \hat{\beta}_0$ (Intercept) + [$\hat{\beta}_1$ x Skeletal Age] + [$\hat{\beta}_2$ x Sex] + [$\hat{\beta}_3$ x Age-Sex Interaction Term] + $\hat{b_{0i}} + \hat{b_{1i}} + \hat{e_{ij}}$

Random-Effect Parameter	Estimate of Variation	Std Error
SD (Constant)	4.188	0.008
SD (Skeletal Age)	0.030	0.525
SD (Residual)	0.214	0.004

The coefficients for the predictor variables (the fixed-effect parameters in *Table 4.12*) have changed from the output of the previous analyses. This is because each model is an improvement on the prior model, thus these values represent the most appropriate model.

Table 4.13 Estimated Intercept ($\hat{b}_{0i}$) and Slope ($\hat{b}_{1i}$) Random Effect Values

GP Age Category	Estimated Intercept Random Effect ($\hat{b}_{0i}$)	Estimated Slope Random Effect ($\hat{b}_{1i}$)
Newborn	-0.0002	-5.697
1 - 3 Months	-0.001	-5.590
3 months	0.001	-5.433
6 months	0.0003	-5.189
9 months	0.001	-4.904
1 year	0.002	-4.668
1 year 3 months	-0.002	-4.427
1 year 6 months	0.004	-4.041
2 years	0.002	-3.508
2 year 6 months	0.009	-3.133
2 years 8 months	0.0002	-2.994
3 years	-0.010	-2.578
3 years 6 months	-0.026	-1.931
4 years	-0.025	-1.511
4 years 2 months	-0.017	-1.170
4 years 6 months	-0.013	-1.060
5 years	-0.025	-0.392
5 years 9 months	0.054	0.079
6 years	0.009	0.548
6 years 10 months	-0.010	1.462
7 years	0.011	1.559
7 years 10 months	0.050	1.995
8 years	0.007	2.428
8 years 10 months	-0.030	3.747
9 years	0.010	3.402
10 years	0.020	4.184
11 years	-0.004	5.253
11 years 6 months	-0.030	6.169
12 years	0.010	6.201
12 years 6 months	-0.001	6.660
13 years	0.005	7.036
13 Years 6 months	0.003	7.503

$$\hat{CA}_{ij} = \hat{\beta}_0 \text{ (Intercept)} + [\hat{\beta}_1 \text{ x Skeletal Age}] + [\hat{\beta}_2 \text{ x Sex}] + [\hat{\beta}_3 \text{ x Age-Sex Interaction Term}] + \hat{b}_{0i} + \hat{b}_{1i} + \hat{e}_{ij}$$

Random effects for the intercept ($\hat{b}_{0i}$) *have subscript 0i, because they refer to the* $\hat{\beta}_0$*, and are age group specific.*
Slope effects ($\hat{b}_{1i}$) *have subscript 1i, since they are related to* $\hat{\beta}_1$*, and are age group specific.*
The residual error terms ($\hat{e}$) *have subscript ij, because they are the inner most level-subject specific.*

Using these values from, the residual diagnostics are vastly improved, with a distribution of the residual values that is close to normal (see *Figure 4.15*). The distribution is no longer skewed to the left, and the three highest bars have decreased in height from the previous analyses.

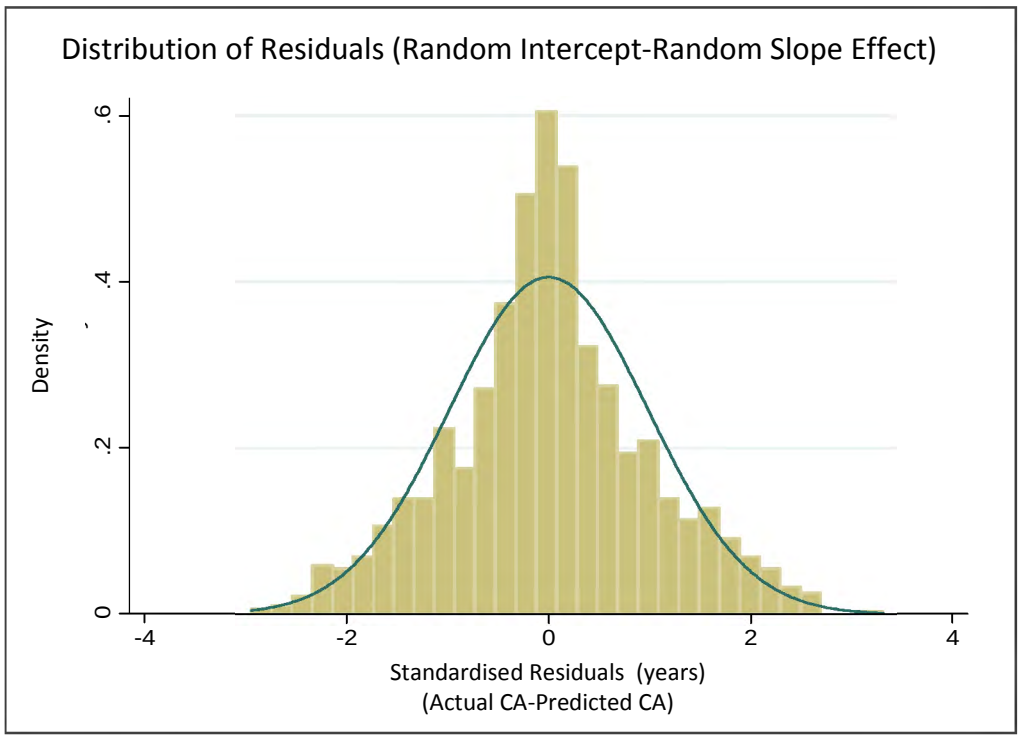

Figure 4.15 Residual distribution graph. Distribution is near-perfectly normal after applying the random intercept-random slope mixed effect model.

The distribution of predicted chronological age (using the fixed-effect parameters only) against actual chronological age (*Figure 4.16*) remains heteroskedastic but is more evenly distributed, especially for the older age groups (that is, the scatter no longer 'fans out' to the extent it did previous. Once again, after approximately 6 years, the scatter levels out. Note that this is the predicted CA based on the fixed-effect portion only.

The predicted chronological age does not start at zero on the X-axis, as these values have not yet been adjusted by the random-effect parameters ($\hat{b}_{0i}$) for the age groups concerned. Instead the values start at the β_0 ^ value, 5.752 (from *Table 4.12*).

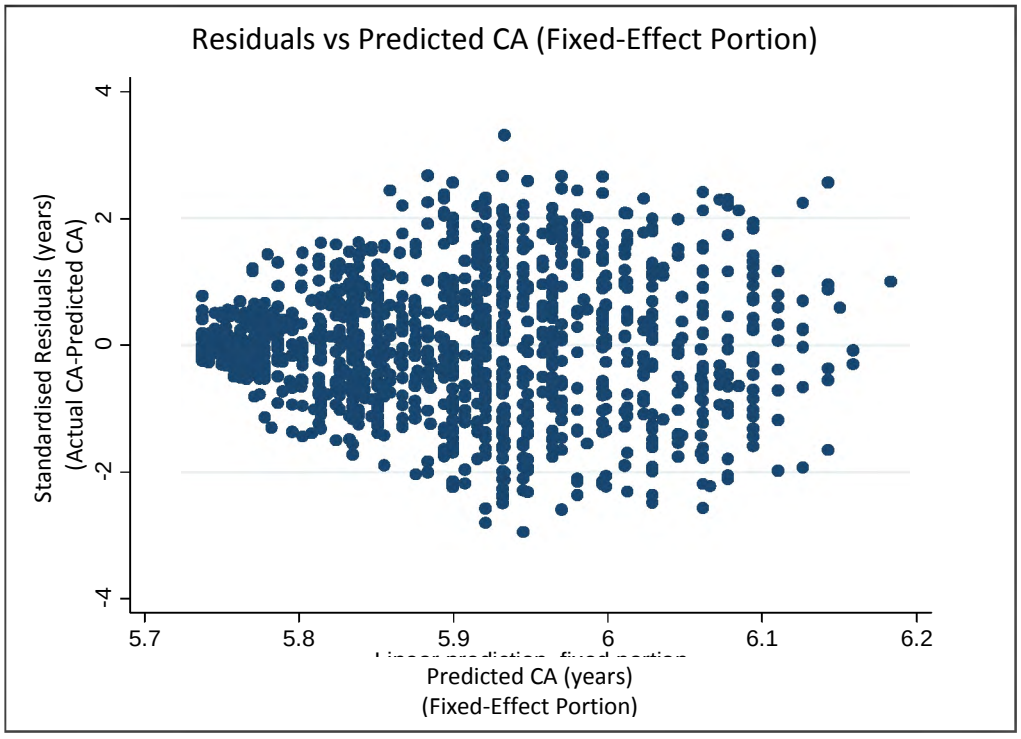

Figure 4.16 Heteroskedastic distribution has decreased, and there is far less scatter and fanning of the data after analysis by Random Intercept-Random Slope model

Figure 4.17 details the final plot of predicted chronological age (with both fixed- and random-effect parameters incorporated) using the random-effect parameters for each age category from *Table 4.13*, and the equation:

$$\hat{}CA_{ij} = 5.752 + [0.025 \times \text{Skeletal Age}] - [0.015 \times \text{Sex}] + [0.008 \times \text{Age-Sex Interaction Term}] + \hat{b}_{0i}\,(\text{estimated intercept random-effect})^{*} + \hat{b}_{1i}\,(\text{estimated slope random-effect})^{*} + \hat{e}_{ij}$$

** These values are age-group specific, and are found in Table 4.13*

By incorporating the random-effect parameters for each age category the data cluster into age groups, and thus, the variation in the data becomes significantly reduced. There remains a small amount of outward dispersion within the middle age groups (5 to 10 years), but it is an improvement on the random intercept model, as this dispersion is reduced.

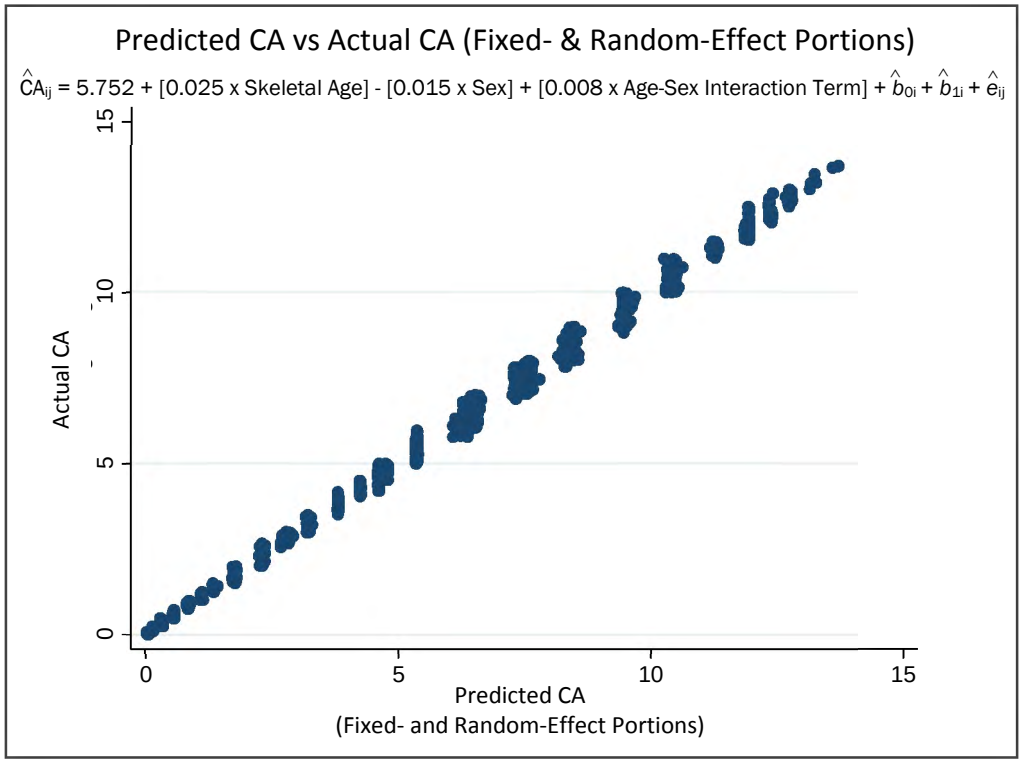

Figure 4.17 The final plot for predicted and actual chronological age, with the fixed- and random-effect portions incorporated. The data cluster into age categories and the 'fit' is significantly improved.

4.2.4.2.1 Summary of Random Intercept-Random Slope Model

The random intercept-random slope model is a mixed-effect model with both fixed- and random-effect parameters. The fixed-effect parameters are predictor variables such as sex and skeletal age, the effect of which is constant across the whole sample. The random-effects are age group specific, and for this analysis, the random-effect caused a change in the intercept and slopes values for each age category.

This model was an improvement on the random-intercept model, as the variation in the sample was considerably reduced once the addition random-effect parameter, the random-slope value, was incorporated into the analysis and final regression plot.
The addition of the random-effect parameters into the final regression line for the sample reduced the sample variation and scatter considerably.

Comparing the plot of the fixed-effect portion of predicted CA to the fixed- and random-effect portions, one can see that much of the variation in the sample can be considered 'random' variation, that is, not due to sex, or skeletal age, or the interaction between sex and skeletal age.

These mixed-effect models fit the data relatively well, although certain limitations remain, such as the possible inaccuracy of the GP age categories themselves. The increasing variance with an increase in age is still observed using these models, albeit somewhat lessened.

It is important to note that the outcome of these models does not result in a prediction tool as such, as there are still problems with the model. Even with the use of the model, the increasing variance remains, there are too many age categories which are unsatisfactory at best, and the model does not incorporate other potential variables which may account for the variance observed. This model does, however, illustrate the relationship between chronological age and skeletal age, determined by the GP Atlas, and that this relationship is not constant over all age categories. It accounts for the effect of sex, and the interaction of sex and age across the sample.

4.3 Anomalous Ossification Patterns

Whilst performing skeletal age estimates, anomalous ossification patterns were noted in 287 males and 111 females. These included delayed or advanced carpal, metacarpal and/or phalangeal development, and/or delayed or advanced formation of the radial and/or ulnar epiphyses. These features were not mutually exclusive, and one region may have been advanced whilst growth in another region was delayed. With reference to the carpal region specifically, it was found that, in some instances, only one carpal bone was delayed or advanced. These are specifically outlined in the table and do not form part of the general 'Delayed/Advanced Carpals' count.

The frequency of occurrence of these patterns is detailed in *Table 4.14. Figures 4.19* to *4.28* show examples of some anomalies. More than one anomaly may be represented by a single radiograph, thus, the number of anomalies are more than the number of individuals with anomalous ossification patterns.

Table 4.14 Type and Incidence of Anomalous Ossification Patterns

Anomaly	Male	Female
Delayed Carpals *	144	57
Advanced Carpals*	2	5
Delayed Triquetral	36	20
Advanced Triquetral	26	17
Advanced Trapezoid	10	11
Advanced Trapezium	6	9
Advanced Lunate	6	5
Advanced Scaphoid	32	12
Delayed Metacarpals	18	11
Advanced Metacarpals	5	3
Delayed Phalanges	6	5
Advanced Phalanges	9	4
Delayed Radial Epiphysis	6	5
Advanced Radial Epiphysis	5	0
Delayed Ulna Epiphysis	76	10
Advanced Ulna Epiphysis	12	11

** Delayed/Advanced Carpals refers to delayed or advanced development of the carpal region in general, or more specifically, to carpals not mentioned in the table.*

4.3.1 Delayed Carpal Development

The carpal bones are clearly visible on radiograph from approximately 3 months of age (0.25 years) in males and females. This process begins with the appearance of the Capitate and Hamate ossification centres.

In the female sample, carpal development was delayed from as early as 0.13 years, with delays in the formation of the Hamate ossification centre. Older individuals (up to the age of 6.83 years) were mostly delayed in the development of the Lunate and Scaphoid bones. The male sample was delayed from 1.25 to 10.5 years, with the ossification of the Lunate and Trapezium mostly affected. The older male individuals (from 10 years of age) were delayed in the growth of the Pisiform, which first appears at 10 years. Delayed carpal development was the most frequent anomaly seen on radiograph for the male and female samples.

Figure 4.18 provides an example of delayed carpal development in individual RXHM172. This individual was estimated as 4.25 years of age using the GP Atlas, and had a CA of 4.13 years: *(a)* GP Atlas standard for a 4 year old male; *(b)* radiograph of RXHM172, with Triquetral, Lunate and Trapezium absent (delayed); *(c)* GP Atlas standard for a 4.5 year old male.

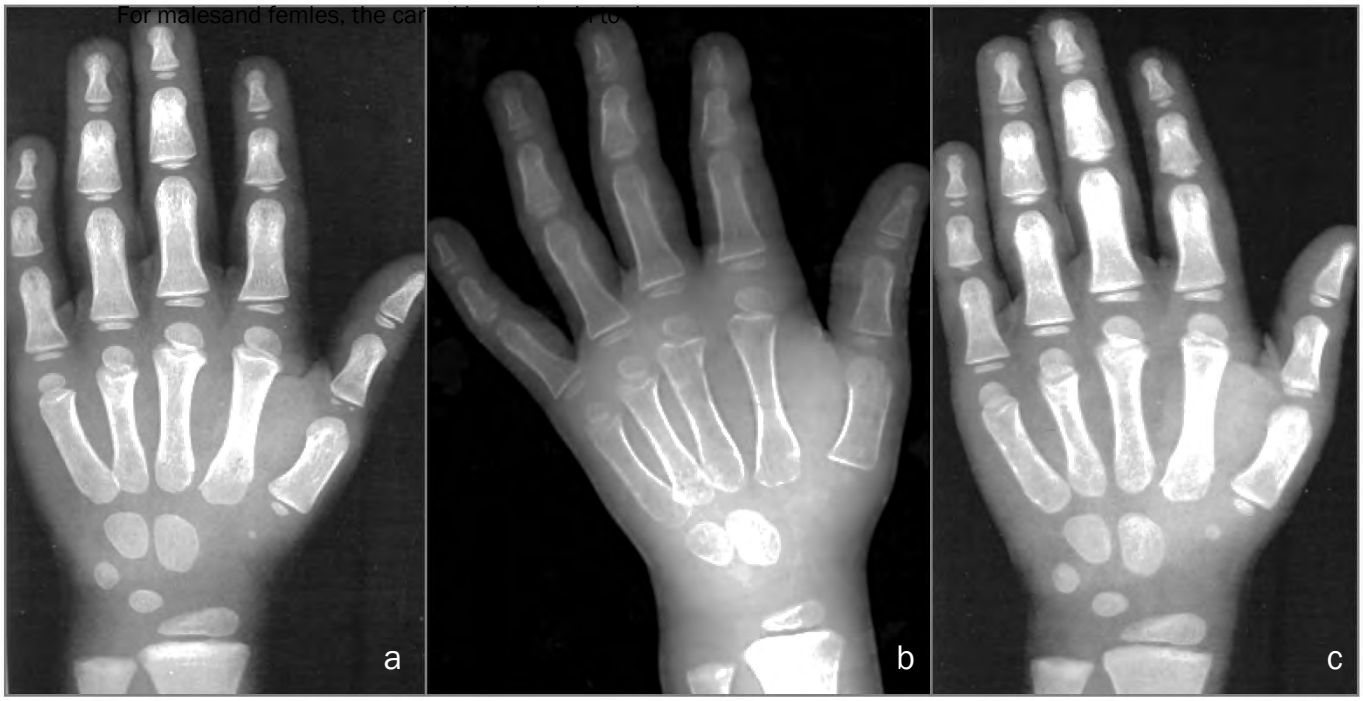

Figure 4.18 (a), (b) and (c) Delayed Carpal Development: Individual RXHM172 (b): skeletal age 4.25y; chronological age 4.13y. Delay in carpal formation (especially Triquetral, Lunate and Trapezium compared to the GP Atlas standards of 4y (a) and 4.5y (c)

4.3.2 Advanced Carpal Development

The female sample showed advanced carpal development from 0.75 years, with all cases having generally larger carpals than their corresponding GP standard. The male sample only had two cases of advanced carpal development, both involving early appearance of the Pisiform bone.

Figure 4.19 presents an example of advanced carpal development, specifically of the Pisiform, in individual RXHF122. The Pisiform appears at approximately 8.83 years in females, and 10 years in males. RXHF122 was estimated to be 6.29 years according to the GP Atlas, but had a CA of 4.13 years: *(a)* GP Atlas standard which most closely resembles RXHF122; *(b)* Radiograph of RXHF122, with the early appearance of the Pisiform indicated by an arrow; *(c)* GP Atlas standard for a female with SA 8.83 years, which is the usual age for the first appearance of the Pisiform.

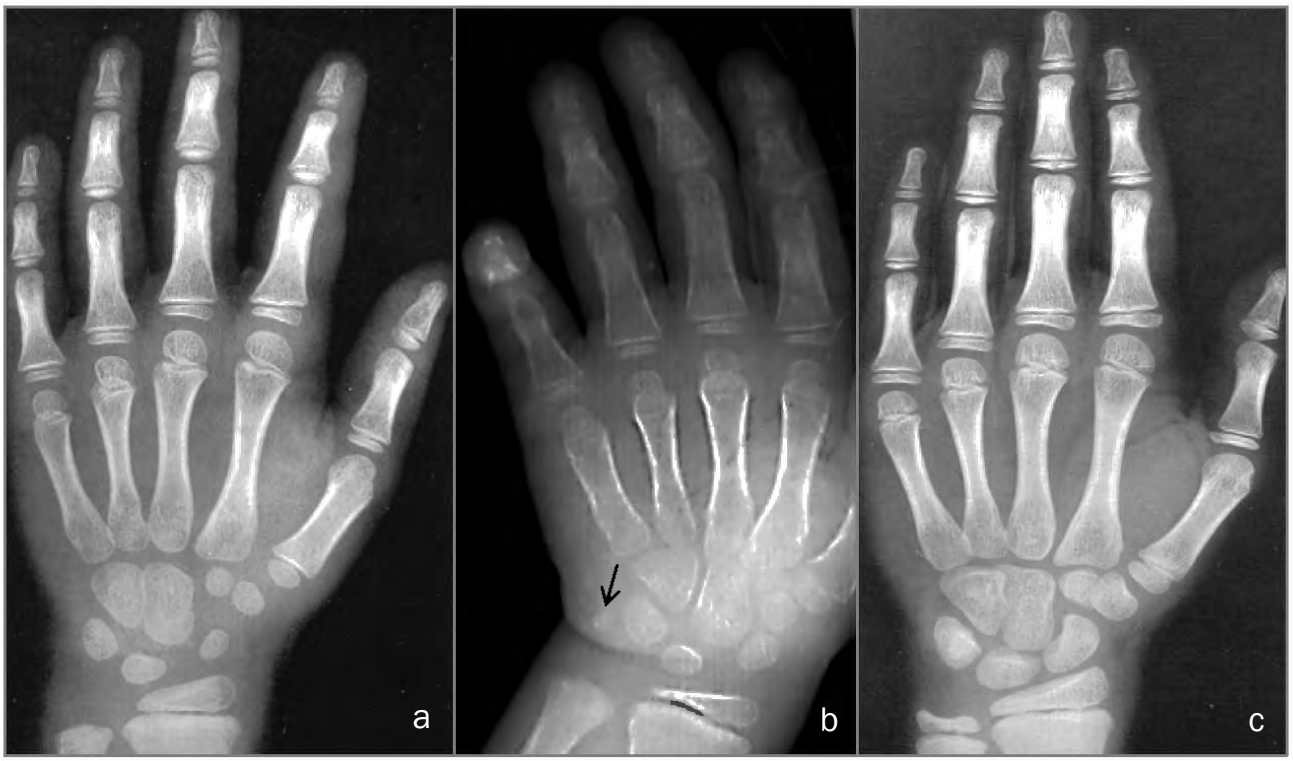

Figure 4.19 (a), (b) and (c) Advanced Carpal Development: Individual RXHF122 (b): skeletal age 6.29y; chronological age 4.21y. Advanced development of Pisiform bone (arrow), which only appears after 8.83y (c) in females. (a) GP Atlas standard which most closely resembles RXHF122.

4.3.3 Delayed Triquetral Development

The Triquetral first appears on radiograph after the age of 1.5 years in females, and 2 years in males. It is the third of the carpal bones to form.

Delays the development of the Triquetral occurred from 1.75 years in females and 2.33 years in males. The female sample had no formation of the bone in all but 1 case, where the Triquetral was present, but significantly reduced in size.

Individual RXHF71 is shown in *Figure 4.20 (a),* with a skeletal age of 3 years, and a chronological age of 3.09 years. The Triquetral is absent from this individual, as can be seen when compared to the GP Atlas standard for a female of 3 years *(b).* The Triquetral is indicated with an arrow in *(b).*

Figure 4.20 (a) and (b) Delayed Triquetral Development: Individual RXHF71 (a): skeletal age 3.0y; chronological age 3.09y. Triquetral absent when compared to corresponding GP Atlas standard (b). Triquetral indicated by arrow.

4.3.4 Advanced Triquetral Development

The female sample presented early formation of the Triquetral in 17 cases, from as early as 0.63 years. Individuals after the age of 3 years had enlarged Triquetral bones for their age. Development of the Triquetral in males occurred from 0.75 years, with males of up to 4 years showing enlarged Triquetral formation for their age.

Figure 4.21 presents an example of early development of the Triquetral. Individual SRMF14 *(b)* was newborn (CA 0.02 years), yet had already developed not only the ossification centre of the Triquetral (circled), but also the Capitate and Hamate, and hence was assigned a skeletal age of 0.63 years. *(a)* is the GP Atlas standard which most closely represents SRMF14, and *(c)* shows the GP Atlas standard in which the Triquetral is first visible in females.

Figure 4.21 (a), (b) and (c) Advanced Triquetral Development: Individual SRMF14 (b): chronological age 0.02y; skeletal age 0.63y. Advanced development of Triquetral (circled) which only develops after 2 y in females (c). (a) GP Atlas standard which most closely resembles SRMF14.

4.3.5 Delayed Metacarpal and Phalangeal Development

The epiphyses of the metacarpals first appear on radiograph from 1 year in females, and 1.5 years in males. Metacarpals II to V are first to appear, followed by the epiphysis of metacarpal I. This pattern of development and age of appearance is identical for the development of the epiphyses of the proximal phalanges in males and females.

Delays in metacarpal development affected individuals as young as 1 year (females), however, the majority of individuals showed delays in the development of metacarpal I epiphysis. This usually appears at 2 years in females, and 2.67 years in males, but individuals as old as 3 years showed complete absence of the metacarpal I epiphysis.
Epiphyses of the phalanges were delayed from younger ages in females (0.88 years) compared to males (2.33 years). The pattern of delay also differed, with females showing a more generalised delay of all epiphyses, and males delayed more specifically in the epiphysis of proximal phalanx I.

Individual RXHM99 (SA 3.0 years; CA 2.91 years) is represented by *Figure 4.22 (a),* and exhibits delays in the epiphysis of metacarpal I and proximal phalanx I. *(b)* is the GP Atlas standards closest in appearance to RXHM99, with the epiphyses of metacarpal I and proximal phalanx I indicated by arrows.

Figure 4.22 (a) and (b) Delayed Metacarpal and Phalangeal Development: Individual RXHM99 (a): skeletal age 3.0y; chronological age 2.91y. Delayed formation of the epiphysis of Metacarpal I and Proximal Phlanx I. (b): GP Atlas standard which most closely resembles RXHM99, with Metacarpal I and Proximal Phalangeal epiphyses present (arrow).

4.3.6 Advanced Phalangeal Development

Advanced development of the phalangeal epiphyses occurred in 13 cases, from 0.75 years. In younger individuals, the epiphyses of the proximal row of phalanges appeared earlier, mainly affecting proximal phalanx II, III and IV. Older individuals showed advanced growth of the intermediate and distal rows of epiphyses, as these only develop from 1.5 years in females, and 2 years in males.

The early appearance of the epiphyses of proximal phalanx II, III and IV can be seen in *Figure 4.23 (b)*. Individual RXHF7 *(b)* had a chronological age of 0.72 years, and a skeletal age of 0.75 years, yet already showed formation of the epiphyses of proximal phalanx II, III and IV (circled). *Figure 4.23 (a)* is the GP Atlas standard which most closely resembles RXHF7, whilst *(c)* shows the standard at which these features usually appear.

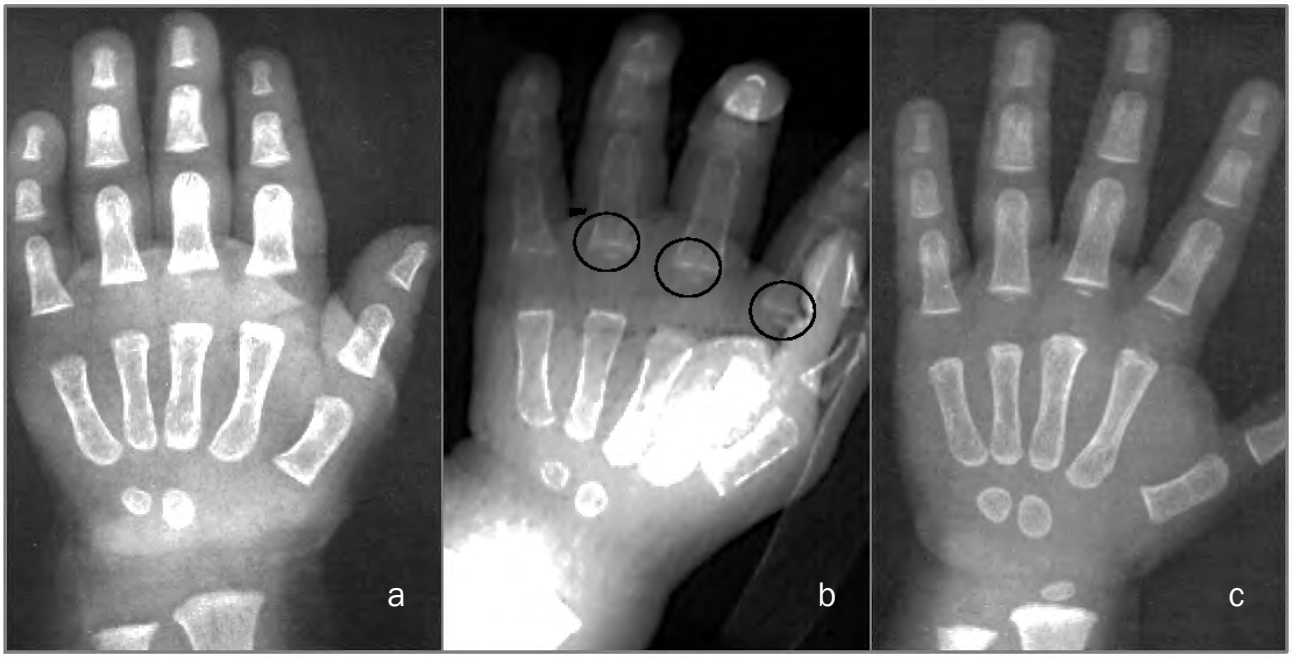

Figure 4.23 (a), (b) and (c) Advanced Phalangeal Development: Individual RXHF7 (b): skeletal age 0.75y; chronological age 0.72y. Advanced formation of epiphyses of proximal phalanges II – IV (circled), which only appear after 1y in females (c). (a): GP Atlas standard of 0.75y, which most closely resembles Individual RXHF7.

4.3.7 Delayed Development of the Radial Epiphysis

The radial epiphysis appears early in hand-wrist development. At 1 year in females, and 1.25 years in males it is very clearly visible on radiograph.

For some individuals in both sexes, there was a delay in the growth of this epiphysis from 1.5 years, with the epiphysis not having formed at all. In some older individuals (3.5 to 9 years), the epiphysis was smaller than is considered normal for that age.

Individual RXHM194 is shown in *Figure 4.24 (b)*. This individual had a chronological age of 4.51 years. Although RXHM194 was assigned a skeletal age of 1.5 years (shown by the GP Atlas standard in *(a)*), there is no formation of the radial epiphysis. *(c)* is the GP Atlas standard closest to the chronological age of this individual. It is clear that this individual is underdeveloped compared to both *(a)* and *(c)*.

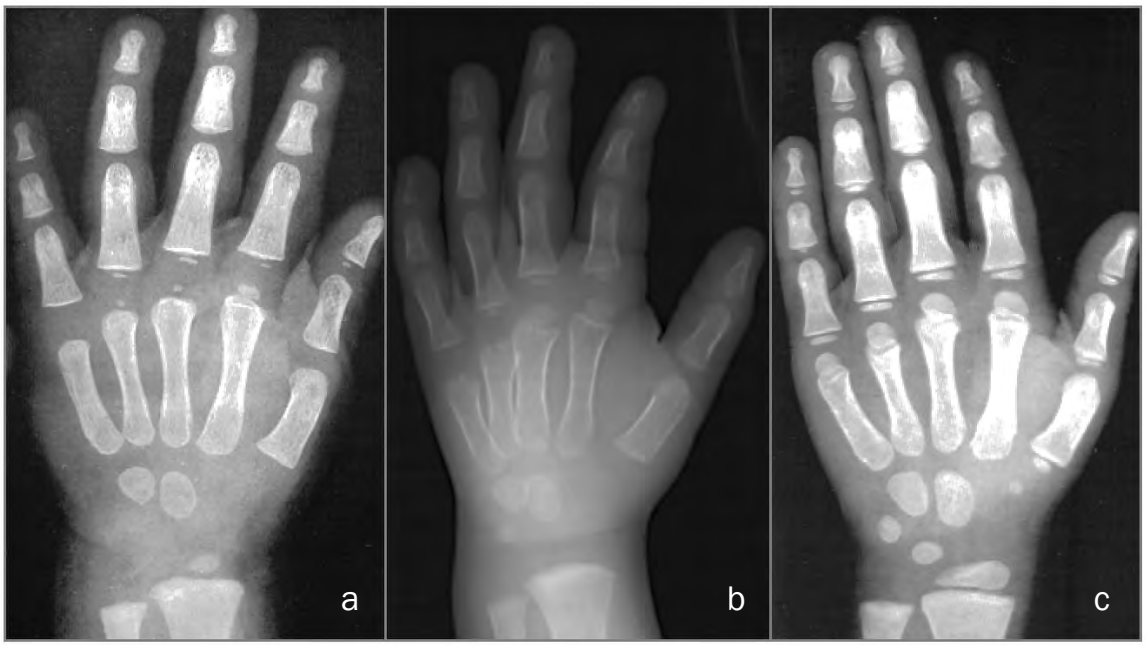

Figure 4.24 (a), (b) and (c) Delayed Development of Radial Epiphysis: Individual RXHM194 (a): GP Atlas standard closest in appearance to RXHM194. (b): skeletal age 1.5y; chronological age 4.51y, showing delay in development of radial epiphysis compared to (a). (c): GP Atlas standard closest to the chronological age of RXHM194 is greatly advanced in development compared to (b).

4.3.8 Advanced Development of the Radial Epiphysis

Development of the radial epiphysis was only advanced in the male sample, occurring between the ages of 1.25 and 3.5 years.

Individual RXHM19 (in *Figure 4.25 (a)*) showed advanced development in this region (circled) compared to the GP Atlas standard *(b)* which compared most closely to this individual.

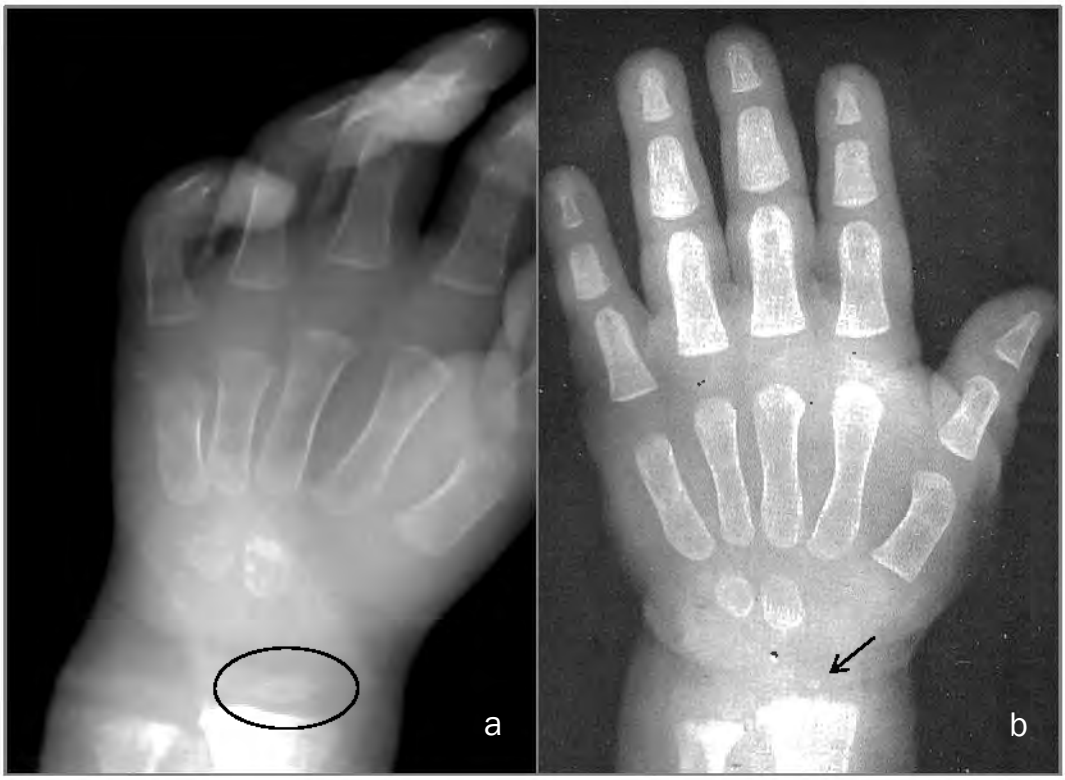

Figure 4.25 (a) and (b) Advanced Development of Radial Epiphysis: Individual RXHM19 (a): skeletal age 1.25y; chronological age 0.94y, showing advanced development of radial epiphysis (circled) compared to the GP Atlas standard which most closely resembled. This standard has smaller radial epiphysis (arrow) compared to (a).

4.3.9 Delayed Development of the Ulnar Epiphysis

The ulna epiphysis is one of the last ossification centres to form, appearing at 6 years in males, and 6.29 years in females. From the age of 5.5 to 10 years in males, and around 6.29 years in females, the ulna epiphysis was either not present, or was significantly reduced in size compared to the corresponding GP standard. The epiphysis was absent up to the age of 8.5 years in some cases.

Figure 4.26 (a) is the left hand of a male, aged 6.03 years (skeletal age 6.0 years), with no formation of the ulnar epiphysis. The GP Atlas standard for a 6.0 old male *(b)* shows the formation of this epiphysis clearly (indicted by the arrow).

Figure 4.26 (a) and (b) Delayed Development of Ulnar Epiphysis: Individual RXHM286 (a): skeletal age 6.0y; chronological age 6.03y, with delayed development of ulnar epiphysis compared to (b). (c): GP Atlas standard which most closely resembles RXHM286, with formation of the ulnar epiphysis (arrow) by 6.0y.

4.3.10 Advanced Development of the Ulnar Epiphysis

The epiphysis of the ulna appeared early in 12 males and 11 females, around the age of 3.5 years in both sexes. This is approximately 3 years earlier than the epiphysis usually appears. Older individuals showed epiphyses that were greater in size than was considered normal for their age.

One such case was individual RXHF229 (*Figure 4.27 (a)*), with a skeletal age of 6.83 years, and chronological age of 7.13 years. Compared to the GP Atlas standard *(b)* which most closely resembled this individual, the epiphysis of the ulna is considerably larger (indicated by the circle).

Figure 4.27 (a) and (b) Advanced Development of Ulnar Epiphysis: Individual RXHF229 (a): skeletal age 6.83y; chronological age 7.13y, showing advanced development of ulnar epiphysis (circled) compared to (b). (c): GP Atlas standard which most closely resembles RXHF229, with a smaller, less developed ulnar epiphysis compared to (a).

4.3.11 Summary of Anomalous Ossification Patterns

Anomalous ossification patterns were observed in 35% of males, and 21% of females. These included both advanced and delayed stages of development in the carpal, metacarpal or phalangeal regions, as well as in the development of the epiphyses of the radius and ulna. Both advanced and delayed stages of development were on radiograph of the same hand, but in different regions.

The purpose of documenting these anomalies was to bring to light the type of variation observed in this sample, compared to the GP sample. This variation has already been described in detail in *Section 4.2*, and by noting the anomalies the extent of variation within this South African sample can be shown radiographically.

CHAPTER 5

DISCUSSION

5.1 Summary of Results

The assessment of skeletal age (SA) in both the clinical and forensic settings serves to estimate the degree of development and biological maturation of a child (Büken *et al.,* 2009; Santos *et al.,* 2011). This is a suitable and frequently used technique, as skeletal age is the only indicator which can be analysed from birth until the attainment of the fully-developed adult body form (Tanner, 1978; Wheeler, 1991; Cox, 1997; Bogin, 1999; Uysal *et al.,* 2004).

The applicability of the GP Atlas method to assess skeletal age has been tested on various modern-day samples in recent years (see *Table 2.01* in *Chapter 2*), based on evidence that skeletal growth and development is affected by health status, access to water and suitable nutrition, secular trends in growth rate and height, genetic make-up and socio-economic status, amongst others (Cameron, 1992; Loder *et al.,* 1993; Schmeling *et al.,* 2000; Zhang *et al.,* 2009). It is believed that the effect of the above-mentioned factors may differ from one population to another, and thus the applicability of the GP Atlas may differ depending on the population in question (Dembetembe, 2010).

The current study examines these issues and tests the applicability of the GP Atlas on a sample of modern-day South African children, between the ages of 0 and 13 years.

Results showed a strong correlation between skeletal age and chronological age for males and females. There was, however, a large degree of variation within the sample, with underestimation and overestimation of skeletal age across all age groups and sexes. This variation increased as age increased.

Regression analysis was used in an attempt to determine the cause of the variation, and to create an equation whereby skeletal age could be used to predict chronological age. The best-fit fixed-effect model, random-intercept mixed-effect model and random intercept-random slope mixed effect model were used in the analysis, with the latter providing the best results. Variables for sex, race and socio-economic status were incorporated into the model to determine their effect on the prediction of chronological age. Based on this sample, the sex of the respondent (and its interaction with skeletal age) was the only variable which influenced the prediction of chronological age, based on its influence in reducing the amount

of variation within the sample when incorporated into the regression equation. This was shown by reduced scatter on the graphs.

As previously explained, the random intercept-random slope mixed effect model has both fixed- and random-effects parameters (see *Section 4.2.4.2, Chapter 4* for a detailed explanation). The fixed-effect parameters for this model are sex and skeletal age (and the interaction between these two). By incorporating the fixed-effect parameters into the regression analysis, variation was only slightly decreased; however when the random-effects parameters were incorporated into the analysis, the variation was almost completely reduced. The results of the regression analysis show that most of the variation within the sample can be considered to be random variation, that is, not due to sex, or skeletal age, or the interaction between sex and skeletal age.

The anomalous features observed on the radiographs (*Section 4.3, Chapter* 4) served to describe the type and extent of variation observed in this sample, compared to the GP Atlas sample.

This may mean that South African children are simply more variable than the GP Atlas sample, or that there is an addition variable which was not accounted for by this research which could be causing this variation.

5.2 Distribution of the Sample

The GP Atlas is constructed in such a way that there are more standards for the early developmental stages, with a 3 month interval between standards for the first year. Thereafter, the interval between the standards increases to 6 months on average, until the age of 5 years. During the period from 5 to 11 years, there is an interval of 1 year between the standards; and from 11.5 years, this interval decreases to 6 months once again, in order to accommodate the increase in growth and development which occurs at the onset of puberty.

The sample distribution was such that the highest numbers of individuals were from the ‘Newborn’ age category, relative to all other age categories. This age category is the shortest, and covers only the first 4 weeks after birth (Bogin, 1999). There was a decrease in the number of individuals per age group until approximately 1.25 years for both sexes; thereafter the number of individuals per age group began to increase again, peaking at around 6 years in females, and 7 years in males.

The reasons for this distribution according to age are varied. In this sample, the majority of children under the age of 2 were deceased children from the Tygerberg/Salt River mortuary sample, whereas those from the older age categories were radiographed as living individuals at Red Cross, predominantly during the investigation of injury; thus, for the first 2 years of development, the number of deceased children was considerably larger than the living subjects. All newborn individuals in this sample were deceased. It is thought that the most critical stage for survival is the first few weeks of birth, after which the child is able to build up immunity and stands a greater chance of survival. This may explain why the number of cases per age category decreases in the first year of development. Groenewald *et al.* (2010) identified the leading causes of mortality in Cape Town. Individuals under the age of 1 year accounted for approximately 6% of deaths of individuals between birth and 85+ years of age. This number dropped dramatically, to under 2% in children between the age of 1-4 years, and under 1% in children between the ages of 5-9 and 10-14 years. Approximately 50% of children under the age of 1 year died from communicable diseases, maternal causes, perinatal conditions or nutritional deficiencies, which are classified as one 'cause group' (Groenewald *et al.*, 2010). The other 50% died from any one of four other 'cause groups' such as HIV/AIDS, injuries, non-communicable diseases, or ill-defined causes. In general, this study found a high degree of infectious disease mortality amongst young children (Groenewald *et al.*, 2010).

The number of children per age category increases after 2 years. This is presumably due to the increase in interval between standards, from 2 years to 8 years. During this time, children also become more active, as they begin to walk and may become more prone to injury. The peak at ages 6 and 7 years for females and males respectively is partly due to the increase in interval between each standard, but may be because this age coincides with the time at which children begin primary school, where they are exposed to more contact with children, as well as contact sports. Considering that the majority of the individuals at this age were X-rayed due to injury, it may be such that the injuries occurred during sport activities or recreational time at school. According to the Child Accident Prevention Foundation of Southern Africa (CAPFSA), data from Red Cross shows that injuries due to falling had the highest incidence between 1999 and 2008. In 2008, injuries due to falling accounted for 39% of all injuries seen at the Red Cross Trauma unit, 14% of which were due to injuries on playground equipment (Childsafe Statistics, 2008).

Another reason for the sample distribution seen may be due to injuries sustained whilst commuting to school. As approximately 95% of patients from Red Cross are Government patients (that is, they are not funded by a private medical aid), it is possible that many of these children come from lower-income areas. According to Burrows *et al.* (2010), children in these areas are exposed to precarious living and commuting conditions, and the risk of injury is high. Injuries account for 23% of deaths in children between the ages of 5 and 14 years, with the leading cause being road traffic accidents (predominantly amongst pedestrians) (Burrows *et al.,* 2010). It has also been suggested that the older the child, the higher their risk of injury (Zwi, 1996; Krug *et al.*, 2000; Burrows *et al.*, 2010). According to CAPFSA, in 2008, injuries of pedestrians accounted for 72% of all transportation-related injuries (Childsafe Statistics, 2008). This may account for the higher number of older children from the Red Cross sample compared to the mortuary samples.

The number of individuals in each age category decreases after 11 years mainly because the interval between the GP standards becomes smaller.

There were significantly more males in the sample compared to females. This does not influence the results of this research as each sex was analysed independently and the GP Atlas is constructed in such a way that skeletal age estimates are performed separately for each sex.

5.3 Correlation between Skeletal and Chronological Age

The correlation co-efficient (in this case, the Spearman *R* value) is a measure of the strength of association, and not the agreement, between two variables; and in addition, the wider the range of values which are compared, the higher the degree of correlation between them (Bland and Altman, 1986; Bull, 1999).

Analysis of the sample as a whole yielded a Spearman *R* value of 0.96, indicating a significant and high correlation (and, therefore, association) between skeletal age and chronological age. Similar results are seen when each sex was analysed separately (Spearman *R* for females = 0.97; males = 0.96). This is to be expected, as both skeletal age and chronological age measure (to similar extents) the development of an individual over time.

Although there is a strong correlation between chronological and skeletal age, there is a large amount of variation within the sample, for both sexes. This variation is non-systematic in nature, that is, is it not consistently overestimating or underestimating. It increases with an increase in age.

One possible explanation for this is the increase in interval between the standards of the GP Atlas as age increases. By having many standards covering a small age range (as is the case for earlier standards in the GP Atlas), more of the variation is able to be accounted for by the method of skeletal age estimation. As the interval between standards increases, there is more time for developmental changes to take place. This is coupled with the fact that the onset of puberty does not occur at a fixed age, but rather over an age range, and is individual specific, allows for more variation within the sample (Bogin, 1999).

5.3.1 Error Distribution and Differences between Sexes

The GP Atlas standards are divided according to sex, and skeletal age estimates are performed separately for males and females, based on the understanding that males and females do not develop at the same rate (Greulich and Pyle, 1959).

The distribution of the estimation error (SA – CA) differs between the sexes, with males showing a lower median estimation error, and a higher absolute estimation error compared to females (see *Figure 4.05 (a)* and *(b)*). This suggests that the standards in the GP Atlas are more accurate in assessing skeletal age for females than for males, in this sample.

The frequency of under- and over-estimation of skeletal age also differed between the sexes, with the estimation error-type being significantly associated with the sex of subject (see *Table 4.03*). Skeletal age was underestimated more frequently in males (64%), whilst females showed a fairly even distribution of error type, with 48% of cases overestimated, and 50% underestimated. Equal estimates occurred in only 1% and 2% of cases for males and females respectively. This result corresponds with those of Roff (2008), in which skeletal age was underestimated most frequently in South African males.

It must be noted that, during analysis of this sample, it was more difficult to use the GP Atlas to assess skeletal age in the male sample, and analysis infrequently yielded a result that exactly matched a corresponding standard, but instead skeletal age was an average of two adjacent standards.

Results of the best-fit regression analysis reiterate these sex differences, with newborn males having a higher average predicted chronological age (0.224 years) than females (0.122 years). Thus, there is an inconsistency in skeletal age estimation using the GP Atlas, with high frequency of over- and under-estimation of skeletal age, which differs between the sexes. Other international studies (detailed in *Table 2.01, Chapter 2*) indicate similar findings, with high frequencies of over- and under-estimation and differing results of skeletal age estimates for each sex (Chan *et al.,* 1961; Loder *et al.,* 1993; Shaikh *et al.,* 1998; Koc *et al.,* 2001; Büken *et al.,* 2007).

These differences between sex and error type may be due to the construction of the GP Atlas itself. The standards and age categories are not consistent for both sexes, specifically between ages 2 to 9 years. Not only are the age categories different between this age range, but there is one additional age category for males which is not present in the female standards.

Another possible explanation for the differences between estimation error-type and sex is that females are able to resist environmental determinants of growth, particularly negative influences such as disease or under-nutrition, more easily than males (Bogin *et al.,* 1989; Bogin, 1999). This may be due to the action of the second X-chromosome as a potential added genetic 'buffer' against environmental factors, compared to the Y-chromosome of the male genome; coupled with the fact that females, in general, tend to have an earlier onset and more rapid phase of development than males. This results in females having a reduced amount of exposure to any environmental stresses which may be present during development, as well as less time to respond to these stresses (Bogin *et al.,* 1989). The growth of males, from prenatal life to adulthood, is thus more sensitive to environmental factors compared to females (Bogin, 1999).

The inconsistent age categories and genetic differences between males and females, coupled with the difficulty experienced in estimating age for males using the GP Atlas, provide possible explanations for the differences observed between the sexes in this sample.

5.4 Factors Affecting Growth and Development

Development may be affected by factors such as racial and genetic factors, socio-economic status, regional or climatic differences as well as an individual's state of health. As these factors are not consistent across all populations, skeletal maturation may show a striking variability depending on the sample being studied (Büken *et al.,* 2007).

Although the GP Atlas method is the suggested method for skeletal age estimation in many international protocols and is considered an acceptable standard (Cameriere *et al.,* 2008), extensive research has been conducted regarding the flexibility and applicability of this method to other race groups and children of varying socio-economic backgrounds worldwide (Varkkola *et al.,* 2011).

The genetic and environmental factors which may potentially affect development are discussed below.

5.4.1 Genetic Factors – The Impact of Race on Skeletal Age Estimation

Racial (and therefore, genetic) differences may impact the timing and order of skeletal development (Cameriere et al., 2008). *Table 2.1*, in *Section 2.3, Chapter 2*, provides a detailed list of comparative studies for different race groups and how they compare to the GP sample. The majority of these studies found that the GP method was not applicable in different countries or between races. Some key studies from *Table 2.1* are outlined in this section.

In a study based on children from the same geographic area as the original GP sample, Loder *et al.* (1993) showed that Black females were developmentally advanced by 0.4 – 0.7 years, except during the middle childhood period. White males were delayed by 0.9 years during middle childhood and 0.4 years in late childhood, although they became developmentally advanced by 0.5 years during adolescence. Shaikh *et al.* (1998), in a study of children from Pakistan, established a 1 year developmental delay in males between 8 and 15 years, and a 0.5 year delay in females between 8 and 13 years. Similar to Loder *et al.*, Shaikh *et al.* found children were skeletally advanced during adolescence.

American children of European (EA) and African (AA) descent, born after 1980, were the focus of a 2001 study by Mora *et al*., the results of which showed significant differences in development between these two groups. Prepubertal EA children were delayed compared to

AA, and postpubertal EA males are advanced compared to AA males, once again showing a difference between skeletal age estimates for the groups pre- and post-puberty. Mora *et al.* (2001) conclude that the GP method was imprecise for this sample.

A South African pilot study by Phillips and Thompson (2000) correlated skeletal age and dental age in South African children, to ascertain whether age determined by dental and hand-wrist development was in agreement with chronological age. The two methods assessed in this study were the GP Atlas method for skeletal age estimation, and the dental age estimation method of Moorees, Fanning and Hunt (1963). The applicability of these methods was tested on children from "Caucasian, Negroid and Mixed" population groups, living in the Western Cape region of South Africa (Phillips and Thompson, 2000). These categories most probably refer to White, Black and Coloured children from the Western Cape region, as used in this current study. The children in each group were assumed to come from similar genetic and socio-economic backgrounds.

Results showed that the GP Atlas method consistently under-estimated skeletal age for children from all three groups, with a difference between SA and CA of up to 1 year in some cases. Whilst dental age estimation remained fairly accurate for children of Coloured ancestry, the method was only fairly accurate for White children. The same method was deemed inaccurate for Black children (Phillips and Thompson, 2000).

Other South African studies by Roff (2008) and Dembetembe (2010) showed that the GP Atlas was not suitable for South African children, and in particular children of African descent (Dembetembe, 2010).

In the current study, race groups were compared, using the mortuary sub-sample. Coloured and White children were compared to Black children, who were used as an arbitrary baseline. There was not a large enough sample of White children for the comparison between White and Black children to be significant; however, it was shown that there was no significant difference in skeletal age estimates between Coloured and Black children.

Considering that no significant difference was found for skeletal age estimates between Coloured and Black children, it is possible to consider the mortuary sub-sample as one homogenous group, comprising mostly of Coloured and Black children. This may explain some of the variability seen in the sample, as this group differs racially from the original sample of White children used in the GP Atlas.

Genetic differences may, thus, be a contributing factor to the variation in this sample; however, due to the non-systematic nature of the variation, the extent of this potential effect of racial classification on skeletal age estimation cannot be determined, as it is overshadowed by the random variation within the sample

The variation seen in the current South African sample may, thus, be caused by the race and genetic differences between the South African sample and the GP sample; but, due to the fact that the variation is not systematic, and under and overestimation is observed across all age groups, the extent of this potential difference due to racial classification cannot be determined.

5.4.2 Environmental Factors – Socio-Economic Status (SES)

The standard of economic modernization of a population impacts the rate of ossification of the skeleton, and extreme conditions of poverty and malnutrition, due to low SES, are known to cause delays in skeletal maturation (Mora *et al.*, 2001; Büken *et al.*, 2007). This would cause an underestimation of skeletal age when using a reference population of a higher SES (such as the GP Atlas) (Schmeling *et al.*, 2000; Schmidt *et al.*, 2007).

The effect of SES on development was demonstrated by Bogin *et al.* (2007). The GP Atlas was used to assess skeletal age for three groups of South American children from different socio-economic backgrounds. Results indicated that children of low SES showed a significant delay in skeletal development, compared to their high SES counterparts; thus, SES plays an integral role during development, and SES-related deficits which occur during early childhood may continue into adolescence (Bogin *et al.*, 2007).

Similar results were found by Cameron (1992) and Cameron *et al.* (1992), when the effect of SES and urbanization was assessed for a sample of South African Black children. Both of these studies found that rural children of low SES experienced poorer growth rates compared to ‘well-off’ children from urban areas, but were more advanced than ‘average’ children from urban areas. Urbanisation is, thus, not necessarily conducive to perfect child development and improved health, but requires an improvement in SES to be most beneficial to the growth and development of children (Cameron, 1992; Cameron *et al.*, 1992).

For this research, SES was calculated for the mortuary sub-sample using average monthly household income values generated by Lightstone ©, 2011. The results for the effect of SES on skeletal development for this sample were inconclusive, in part due to the indirect method of assessing SES. Police station areas (noted from the mortuary records) were used to ascertain the average monthly household income, based on all the suburbs within the jurisdiction of each Police station. This was then used as an indirect indicator of SES.

There are several potential problems with this method of assessing SES, one being that the jurisdiction of a Police station may cover many suburbs of varying socio-economic levels. The Cape Town Metropole is a very heterogeneous region, with wide differences in income and housing standards between areas. The lower-income/low SES areas include suburbs with mostly informal settlements and Reconstruction and Development Program (RDP) housing, whereas residential property in higher-income, more affluent areas includes mostly sectional title and free-standing houses. Interspersed between these are rural farming areas (for example, Philippi) and mixed areas where affluent families live in close proximity to families in informal settlements (such as Hout Bay) (Heaton and Amoateng, 2007). There are wealthier suburbs which have very low income areas within their borders, such as Milnerton, with an average monthly household income of R 30 500. Contained within Milnerton Police station's jurisdiction is Dunoon, a low-income/low SES area, with RDP housing and shack dwellings. The death of an individual must be reported at and investigated by the Police station whose jurisdiction includes the area in which the death occurs. As the mortuary records contain only the Police station where the death was reported, it cannot be determined in which suburb, within a given Police station jurisdiction, the deceased child was residing at the time of his or her death.

Another potential problem is that the Police station where the death was reported may not encompass the residential area of the child. Examples of such instances would be a child from Nyanga (which is a low income/lower SES) who drowns at Muizenberg beach (jurisdiction of Muizenberg Police station, a high income/higher SES area) or a child who is hospitalized and later dies in a hospital which is outside of their residential area and is under the jurisdiction of a difference Police station to that of the residential area. In such cases, the death may be reported at a Police station which covers a higher SES area(s), but the deceased individual, in fact, came from a low SES area, and is thus not a true reflection of the environment in which the child was developing before they died.

All Police stations in this sample contained within their jurisdiction, lower SES areas; thus, there is a possibility that all individuals in the mortuary sample came from lower SES areas. This would explain the non-significant correlation between SES and the estimation error (SA-CA).

It was noted that the case-load for the lower SES areas was greater than the higher SES areas, and as average monthly household income increased, so the case-load decreased. Steenberg and Milnerton were an exception to this. Although these areas have a mid to high average monthly household income, they had higher case-loads than suburbs of similar SES. There are large, densely populated low SES suburbs within the Police station jurisdiction of Steenberg and Milnerton, which may account for the high case-loads of these two areas.

The differences in the case load between the low and high SES areas in this sample are a reflection of the disparities which exist between the classes in South Africa, resulting in different mortality rates among different SES groups.

Differences in health status have been observed between income groups, population groups, urban/rural groups, and groups with different levels of education (Bradshaw, 2008). Poor health is strongly association with low SES, and there is increasing evidence indicating that poor health is a result of inequalities between groups (Hargreaves *et al.,* 2004; Doolan *et al.,* 2007). The burden of disease in South Africa includes diseases and conditions of poverty and under-development, injuries, chronic disease, and HIV/AIDS which has a rapid and wide-spread impact, particularly among children and young adults. Other factors including access to health care, nutrition, and living and working conditions also affect health and development. Poor environments may cause children to be underweight and show stunted growth, thus causing children to not reach their full developmental potential (Grantham-McGregor *et al.,* 2007; Nannan *et al.,* 2007; Walker *et al.,* 2007).

Infant mortality rate (IMR) is an indicator of health which reflects not only the prevalence of low birth-weights of children but also the degree of poverty experienced by mothers and their children and their access to healthcare (Bachmann, London and Barron, 1996). One outstanding characteristic of the South African social structure is its inequality. IMR differs between SES groups, rural/urban areas and between race groups. This may be because living conditions and dwelling types reflect racial segregation, a repercussion of South Africa's Apartheid history (Bachmann, London and Barron, 1996).

The highest IMR occurs amongst children from informal settlements, which tend to have only low income/lower SES households. These children also tend to be mostly South African Black children (and in some cases, Coloured children), who are the most common residents of informal settlements (Heaton and Amoateng, 2007).

Lifestyle in informal settlements is vastly different from more affluent areas. Household size in these areas is often large, and it may be challenging for the demands placed on such families to be met due to widespread impoverishment. A child's health may become compromised in a large family, through malnourishment, unsanitary living conditions, inadequate attention, failure to recognise illness, and failure to seek medical attention. Furthermore, there is a heightened risk for spread of diseases and cross-contamination whenever a large number of people live within close proximity to one another (Heaton and Amoateng, 2007). This leads to the spread of diseases such as gastroenteritis, pneumonia, HIV and Tuberculosis which are the leading causes of infant deaths in informal settlements (Bachmann, London and Barron, 1996).

The association between SES, area and income, and thus, child health status and access to resources suggest that higher income/higher SES families are also more easily able to spend money to ensure children are kept clothed, warm and fed, reducing the potential of malnutrition and exposure to illness (Heaton and Amoateng, 2007).

In a study that examined the factors influencing infant and child survival among Black and Coloured children in South Africa, Anderson *et al.* (2002) noted a striking contrast between the overall living conditions of Black and Coloured children, with Coloured children enjoying a better-off and healthier lifestyle than their Black counterparts in all aspects of life. They found that a substantially larger proportion of Coloured households (93%) had access to running tap water in the residential dwelling or on site, as opposed to 42% of Black households.

IMR is affected by exposure to disease, household size, sanitation and nutrition, all of which are consequences of SES and the inequality that exists between racial and income groups within South Africa. This explains the difference in case number between the low income/lower SES and the high income/higher SES groups in this sample and the high number of Black and Coloured children compared to White children.

5.5 Regression Analysis

Regression analysis was used to account for the non-systematic variation seen in the sample, and to create an equation whereby skeletal age, as determined by the GP Atlas, could be used as a predictor of chronological age.

The random intercept-random slope mixed-effect model has both fixed- and random-effects parameters (see *Section 4.2.4.2, Chapter 4* for a detailed explanation). The fixed-effect parameters are the variables for sex and skeletal age (and the interaction between the two). The random-effects parameters are age category specific and account for the random variation within the sample. Incorporating the fixed-effect parameters into the regression analysis decreased variation only slightly; however when the random-effects parameters were incorporated into the analysis, the variation was almost completely reduced.

The results of the regression analysis show that most of the variation within the sample can be considered random variation (or 'statistical noise'), which is not due to sex or skeletal age.

The outcome of this regression analysis does not result in a fool-proof prediction tool. It does illustrate, however, that although SA and predicted CA are measuring age and development over time, the relationship between SA and predicted CA is not constant across all age categories and sexes. It also demonstrates the degree of variation within the South African sample compared to the GP sample, and how much of this variation is random. This may mean that South African children are simply more variable than the GP Atlas sample, or that there is an addition variable which was not accounted for by this research, which could be causing the variation.

5.6 Anomalous Ossification Patterns

The anomalous ossification patterns noted from the radiographs (*Section 4.3, Chapter 4*) served to quantify the type and extent of variation observed in this sample, compared to the GP Atlas sample. An anomaly was any feature considered to be delayed or advanced when compared to the corresponding GP Atlas standard for each individual, and was most often the advanced or delayed appearance of an ossification centre. These are listed in *Table 5.01*, based on the affected region of the hand-wrist, in order of the frequency observed.

Table 5.01 Anomalous Ossification Patterns (in order of frequency)

Anomalous Region	Male		Female		Total
	Observations	%	Observations	%	%
Hamate/Capitate/Pisiform	146	18	62	12	30
Ulna Epiphysis	88	11	21	4	15
Triquetral	62	8	37	7	15
Scaphoid	32	4	12	2	6
Metacarpals	23	3	14	3	6
Phalanges	15	2	9	2	4
Radial Epiphysis	11	1	5	1	2
Trapezoid	10	1	11	2	3
Trapezium	6	<1	9	2	<3
Lunate	6	<1	5	1	<2

Anomalous ossification patterns were observed in 35% of males and only 21% of females. Anomalies in the Capitate, Hamate, Pisiform, Ulna epiphysis, Triquetral and Scaphoid were more prominent in males, whereas anomalies in the Metacarpals, Phalanges and Radial epiphyses showed equal frequency for both sexes. Females showed a slightly higher frequency of anomalies in the Trapezoid, Trapezium and Lunate.

From the above table, it is also evident that the appearance of ossification centres of the Hamate, Capitate and Pisiform bones was the most variable. In most cases, the ossification centres of the Hamate and Capitate did not appear at 3 months, the age indicated in the GP Atlas, and the individual was classified as Newborn, although their chronological age was older. The ossification centre of the Pisiform, however, appeared earlier than is stipulated in the GP Atlas.

The variation in development between males and females has already been demonstrated by regression analysis and differences in error-type between the sexes. As previously explained, this variation may be due to inherent sex differences due to genetics, and also because the GP Atlas standards are not consistent for both sexes. The difference in frequency of the observed anomalous features between males and females demonstrates the potential differences in development between the sexes and also serves to quantify the variation seen between South African children and the GP Atlas sample.

5.7 Limitations

5.7.1 Limitations of the GP Atlas Method

Previous research by international authors has questioned the applicability of the GP Atlas to other race, population and SES groups, with the majority of studies concluding that the GP Atlas is no longer an applicable skeletal age estimation method for these groups. There are also drawbacks to the GP Atlas itself.

5.7.1.1 The GP Atlas Standards

Assigning skeletal age to an individual was often problematic as some standards were difficult to interpret. This was mainly due to poor image and printing quality of the radiographs in the Atlas, which are from the 1940s.

The construction of the GP Atlas standards may be a potential cause of the variation observed in the South African sample. The age interval between each standard is not consistent, which may be a cause of the variation seen in the South African sample. By having many standards covering a small age range (as is the case for earlier standards in the GP Atlas), more of the variation is accounted for by the method of skeletal age estimation. As the interval between standards increases, there is more time for developmental changes to take place, and for the influence of genetics and environment to have an effect on skeletal development. This is coupled with the fact that the onset of puberty does not occur at a fixed age, but rather over an age range, and is individual specific, allows for more variation within the sample (Bogin, 1999). It may be that the GP Atlas sample experienced the onset of puberty at a different age to the South African sample, impacting development and causing some of the variation seen. The standard age categories are also different for each sex, between the ages of 2 and 9 years, with an additional standard included for males. This may be another reason for the variation seen between the male and female South African sample, when using the GP Atlas for skeletal age assessments.

To improve the GP Atlas, age categories should be standardized for both sexes and more standards should be included for individuals between the ages of 2 to 9 years. Instead of 1 year age ranges between standards, a more appropriate range of 6 months may aid in accounting for some sample variation.

Digital methods, such as BoneXpert™, based on the GP Atlas, seek to improve skeletal age estimates by reducing observer error and decreasing the time taken per assessment. As yet, BoneXpert™ cannot be used as a replacement method to the GP Atlas as it was designed to be equal, on average, to the GP Atlas, and is not an improved method.

5.7.1.2 Use of the Method in Clinical and Forensic Settings

The use of the GP Atlas in clinical and forensic settings may be less accurate than initially intended by the authors of the method. The method, as originally described by Greulich and Pyle (1959), involves the complex comparison of all the bones in the hand-wrist region of a sample radiograph against the standards in the GP Atlas. In most cases nowadays, a more rapid and modified version of the method is used, whereby the overall appearance of a sample radiograph is compared to the standards in the GP Atlas, and a skeletal age is hence assigned. Although skeletal age estimates using this approach may be considerably quicker, they may not be as accurate (Bull, 1999).

5.7.1.3 Standard Deviation (SD) Values

Another drawback of the GP Atlas is the variability tables, with standard deviation (SD) values for each sex, which are included in the GP Atlas (on pages 51 and 53 – See *Appendix F*). The SD values are sex and age category specific values, intended to provide an age range for each skeletal age estimate. One SD value above and below a given skeletal age is said to include two-thirds (66%) of the population, whereas two SD values will include 94% of the population (Greulich and Pyle, 1959).

For young individuals, the SD values are sufficiently small (for example, the SD for a 1 year old male is 1.97 months, and 1.77 months for a female of the same age); but as the SD values increase with each subsequent age standard, practical use of the SD values becomes problematic for older children, as the age range is wide. According to the GP Atlas, females as young as 4.5 years, and males of 11 years have a SD value 10 months or greater.

Within a forensic context, the use of the SD values is critical, especially in cases where the age of a child is in question (for example if the child is unidentified or if there is no supporting documentation which accurately indicates the age of the child). To determine the age of such a child using the GP Atlas, with any degree of certainty, one would need to use two SD values above and below the assigned skeletal age, to include 94% of all children in the population.

Using the SD values from the GP Atlas, a 10 year old female would have an estimated skeletal age between 8 and 12 years. In a legal and forensic context, this age range is too wide, as many physiological changes occur between 8 and 12 years of age. These developmental and physiological changes have implications in terms of search criteria in criminal cases, validity of evidence and correct identification of missing persons, and provide yet another reason why the GP Atlas is no longer suitable for skeletal age estimation of South African children.

5.7.2 Research Limitations

As with any scientific research, this project was not without limitations. These involved mostly data-capturing and the samples themselves.

The sample was divided into two groups: radiographs from deceased children at Tygerberg and Salt River Mortuaries, and living, injured children from Red Cross Children's Hospital. No medical history was available for any of the subjects, thus, no information regarding pre-existing developmental abnormalities was available. The information that was available for each subject differed depending on the source of the radiographs (mortuary or hospital). On the whole, the sample was underpowered for the older age groups.

For the hospital sub-sample, no information regarding the race of the child or the reason for hospitalization was provided. Although patients at Red Cross are predominantly Government funded (and therefore assumed to have a lower SES), SES could not be determined as no residential information was available. This would have been used as an indirect indicator of SES. The hospital sub-sample could not, therefore, be used in the statistical analysis of the effect of race and SES on skeletal age estimation. This hospital sub-sample was also underpowered for certain age groups, specifically between 0 and 2 years of age, and consisted mainly of older children.

The mortuary sample contained only deceased children, predominantly between the ages of 0 and 2 years. For most of the children in this sample, cause of death was listed as Sudden Unexpected Death in Infancy (SUDI) or Sudden Infant Death Syndrome (SIDS).
SUDI is an umbrella term which refers to any unexpected death of a seemingly healthy child (Krous, 2010). A case is classified as SIDS if the child dies whilst asleep, within their first year of life, and if no conclusive cause of death is determined by a complete post-mortem and investigation into circumstance surrounding their death (Burger, 2011).

The diagnosis for SIDS is one of exclusion and little is known about its causes. Its definition is imprecise at best as there are no definitive and easily identifiable post-mortem markers for SIDS (Krous, 2010). This may become problematic as it is not know how the development of a child who dies of SUDI or SIDS is affected, and it could be that these children had pre-existing developmental abnormalities which went undetected.

Racial classification was only available for the mortuary sub-sample, provided by the mortuary records. The majority of the sample consisted of Black and Coloured children. Not only was this sample significantly underpowered for White children, but the three racial categories are not representative of all race groups in South Africa. Classification of race for this sample was highly subjective, and information regarding the race of the deceased was provided by family, mortuary technicians or police officials, and may have differed from the race group to which the deceased most identified themself. These racial classifications are also based on the old Apartheid race groups, which are no longer legislated, but are still frequently used in our democratic society.

SES was determined for the mortuary sample only, based on the Police station at which the death was reported and the average monthly household income, generated by Lightstone © 2011. This was an indirect method, and may not have been as accurate as other methods (such as actual monthly income per household for each deceased individual). Because of the Police station jurisdiction covering suburbs of differing SES, it is possible that all individuals came from low SES backgrounds, and thus, the impact of SES on development could be listed as a possible cause for the variation observed in the sample.

CHAPTER 6

CONCLUSION

6.1 Conclusion

The current study aimed to determine whether this method is still applicable to modern, South African children between the ages of 0 and 13 years.

The results of this study concur with similar international studies which tested the applicability of the GP Atlas method. More specifically, these results also agree with other South African studies by Phillips and Thompson (2000), Roff (2008) and Dembetembe (2010), who indicated a significant difference between chronological age and skeletal age as estimated by the GP Atlas method. The current study revealed a large degree of variation within the sample, with overestimation and underestimation of skeletal age across all age groups and sexes. This variation was further quantified by the variety and number of anomalous features observed on the sample radiographs.

The GP Atlas itself exhibits some fundamental flaws in its construction and the sample on which it is based, causing its applicability to be questioned. The standards are difficult to interpret, and are often unclear as they are old and the printing is of a poor quality. The standards are not consistent across the sexes, and the age categories are not uniform, often with a range between categories that is too wide.

South Africa is a country which is racially diverse, and due to its Apartheid history, there are major inequalities between classes, resulting in a population with socio-economic levels of opposite extremes. The GP Atlas is based on a sample of White children, from high socio-economic backgrounds, born in the first half of the twentieth century – vastly different to the children from the modern South African society.

Methods which assess skeletal age are required to be both rapid and accurate, and the GP Atlas does not meet this requirement for South African children. The degree of random variation observed in this sample, which could not be accounted for by sex, race or socio-economic status, as well as the discrepancies in the GP Atlas itself, cause this method to no longer be sufficiently accurate or applicable for use in clinical or forensic settings to estimate skeletal age of South African children between the ages of 0 and 13 years.

Other more accurate methods should be used to assess development in South African children. A method such as that of Phillips (2008) which assesses dental maturation and is based on a South African sample should be sought as an alternative when the chronological age of a child is in question.

REFERENCES

Andersen E. 1971. Comparison of the Tanner-Whitehouse and Greulich-Pyle methods in a large scale Danish survey. Am J Phys Anthropol 35: 373 – 376.

Anderson M. 1971. Use of the Greulich-Pyle "Atlas of skeletal development of the hand and wrist" in a clinical context. Am J Phys Anthropol 35: 347 – 351.

Anderson BA, Romani JH, Phillips H, van Zyl J. 2002. Environment, access to healthcare and other factors affecting infant and childe survival among the African and coloured populations of South Africa, 1989 – 1994. Population and Environment 23 (4): 349 – 364.

Bachmann M, London L, Barron P. 1996. Infant mortality rate inequalities in the Western Cape province of South Africa. Int J Epidemiol 25 (5): 966 – 972.

Beresowski A, Lundie JK. 1952. Sequence in the time of ossification of the carpal bones in 705 African children from birth to six years of age. S Afr J Med Sci 17: 25 – 31.

Bilgili Y, Hizel S, Kara SA, Sanli C, Erdal HH, Altinok D. 2003. Accuracy of skeletal age assessment in children from birth to 6 years of age with the ultrasonographic version of the Greulich-Pyle atlas. 22 (7): 683 – 690.

Bogin B. 1999. Patterns of human growth. Second Edition. Cambridge University Press.

Bradshaw D. 2008. Determinants of health and their trends. South African Heath Review. 51 – 69.

Buikstra JE, Ubelaker DH. 1994. Standards of data collection from human skeletal remains. Arkansas Archaeological Survey Research series No. 44.

Büken B, Şafak AA, Yazici B, Büken E, Mayda AS. 2007. Is the assessment of bone age by the Greulich-Pyle method liable at forensic age estimation for Turkish children?. Foren Sci Int 173: 146 – 153.

Büken B, Erzengin ÖU, Büken E, Şafak AA, Yazici B, Erkol Z. 2009. Comparison of the three age estimation methods: Which is more reliable for Turkish children?. Foren Sci Int 183: 103.e1 – 103.e7.

Bull RK, Edwards PD, Kemp PM, Fry S, Hughes IA. 1999. Bone age assessment: a large scale comparison of the Greulich and Pyle, and Tanner and Whitehouse (TW2) method. Arch Dis Child 81: 172 – 173.

Burger MC. 2011. Profiling the approach to the investigation of viral infections in cases of Sudden Unexpected Death in Infancy (SUDI) in the Western Cape Province. Unpublished Thesis. University of Stellenbosch, South Africa.

Burrows S, van Niekerk A, Laflamme L. 2010. Fatal injuries among urban children in South Africa: risk distribution and potential for reduction. Bull World Health Organ 88: 262 – 272.

Cameriere R, Ferrante L, Mirtella D, Cingolani M. 2006. Carpals and epiphyses of radius and ulna as age indicators. Int J Legal Med 120: 143 – 146.

Cameriere R, Ferrante L. 2008. Age estimation in children by measurement of carpals and epiphyses of radius and ulna and open apices in teeth: A pilot study. Foren Sci Int 174: 59 – 62.

Cameriere R, Ferrante L, Ermenc B, Mirtella D, Štrus K. 2008. Age estimation using carpals: Study of a Slovenian sample to test Cameriere's method. Foren Sci Int 174: 178 – 181.

Cameron N. 1984. In the measurement of human growth. Croom Helm Ltd, Kent. pp 113 – 141.

Cameron N, Kgamphe JS, Leschner KF, Farrant PJ. 1992. Urban-rural differences in the growth of South African children. Ann Hum Biol 19: 23 – 33.

Cardoso HFV. 2008a. Epiphysial union at the innominate and lower limb in a modern Portuguese skeletal sample, age estimation in adolescent and young adult male and female skeletons. Am J Phys Anthropol 135: 161 – 170.

Castriota-Scanderberg A, Sacco MC, Emberti-Gialloreti L, Fraracci L. 1998. Skeletal age assessment in children and young adults: comparison between newly developed sonographic method and conventional methods. Skeletal Radiol 27: 271 – 277.

Childsafe Statistics. 2008. Child Accident Prevention Foundation of Southern Africa (CAPFSA). Available at http://www.childsafe.org.za/research.htm.

Corlett JT. 1986. Growth of urban schoolchildren in Botswana. Ann Hum Biol 13: 73 – 82.

Corlett JT, Woollard E. 1988. Growth patterns of rural children in the Kgalagadi region of Botswana. Ann Hum Biol 15: 153 – 159.

Cox LA. 1997. The biology of bone maturation and ageing. Acta Paediatr Suppl 423: 107-108

Chan ST, Chang KSF, Hsu FK. 1961. Growth and skeletal maturation of Chinese children in Hong Kong. Am J Phys Anthropol 19: 289 – 300.

Children's Hospital Trust – Frequently Asked Questions. 2008. http://www.childrenshospitaltrust.org.za/frequently-asked-questions

Criminal Procedure Act 51 of 1977. Section 337. South Africa.

Davidian M, Giltinan DM. 1995. Nonlinear models for repeated measurement of data. Monographs on statistics and applied probability, Volume 62. London: Chapman and Hall.

Dembetembe KA. 2010. Age estimation using epiphyseal closure at the wrist joint: an investigation of individuals of African origin, 14 to 22 years [unpublished thesis]. Cape Town (Western Cape): University of Cape Town. Available from Department of Human Biology, University of Cape Town.

Deutero-Malay Definition. 2011. http://www.asianinfo.org/asianinfo/malaysia/pro-history.htm.

Doolan K, Ehrlich R, Myer L. 2007. Experience of violence and socioeconomic position in South Africa: a national study. PLoS ONE 2 (12): e1290.

Douglas TS, Pitcher RD, van As AB. 2010. Full-body radiographic imaging of the injured child. CME 28 (3): 108, 110-112.

Dunham EC, Jeness RM, Christie AU. 1939. A consideration of race and sex in relation to the growth and development of infants. J Pediatr 14: 156 – 160.

du Toit, MK. 1992. A Life-Span Developmental Orientation: The Relevance of Chronological Age in Life-Span Developmental Psychology: A Theoretical Observation. SA J Psych 22: 21-26.

Garn S, Sandusky ST, Nagy JM, McCann MB. 1972. Advanced skeletal development in low-income Negro children. J Pediatr 80: 965 – 969.

Gertych A, Zhang A, Sayre J, Pospiech-Kurkowska S, Huang HK. 2007. Bone age assessment of children using a digital hand atlas. Compu Med Imag Grap 31: 322 – 331,

Gilli G. 1996. The assessment of skeletal maturation. Horm Res 45 (2): 49 – 52.

Giordano D, Leonardi R, Maiorana F, Scarciofalo G, Spampinato C. 2007. Epiphysis and metaphysic extraction and classification by adaptive thresholding and DoG filtering for automatic skeleton bone age analysis. 29th Annual International conference of the IEEE Engineering in Medicine and Biology Society. EMBS pp 6551 – 6556.

Giordano D, Spampinato C, Scarciofalo G, Leonardi R. 2010. An automatic system for skeletal bone age measurement by robust processing of carpal and epiphysial/metaphysical bones. IEEE T. Instrumentation and Measurement 59 (10): 2539 – 2553.

Grantham-McGregor S, Cheung YB, Cueto S, Glewwe P, Richter L, Strupp B and the International Child Development Steering Group. 2007. Child development in developing countries: development potential in the first 5 years for children in developing countries. Lancet 369 (9555): 60 – 70.

Graphpad Prism. 2007. Graphpad Software Incorporated. San Diego, CA.

Greulich WW. 1957. A comparison of the physical growth and development of American-born and native Japanese children. Am J Phys Anthropol, 15: 489-516.

Greulich WW, Pyle SI. 1959. Radiographic atlas of skeletal development of the hand and wrist. Standford: Standford University Press.

Greulich WW. 1960. Skeletal features visible on the roentgenogram of the hand and wrist which can be used for establishing individual identification. Am J Roentgenol Radium Ther Nuc Med 83: 756 – 764.

Groell R, Lindbichler F, Riepl T, Gherra L, Roposch A, Fotter R. 1999. The reliability of bone age determination in central European children using the Greulich and Pyle method. Br J Radiol 72: 461 – 464.

Groenewald P, Bradshaw D, Daniels J, Zinyakatira N, Matzopolous R, Bourne D, Shaikh N, Naledi T. 2010. Local-level mortality surveillance in resource-limited settings: a case study of Cape Town highlights disparities in health. Bull World Health Organ 88: 444 – 451.

Haiter-Neto F, Kurita LM, Menezes AV, Casanova MS. 2006. Skeletal age assessment: A comparison of 3 methods. Am J Orthod Dentofacial Orthop 130: 435 e15 – 435 e20.

Hargreaves J, Collinson MS, Kahn K, Clark SJ, Tollman SM. 2004. Childhood mortality among former Mozambican refugees and their hosts in rural South Africa. Int J Epidemiol 33 (6): 1271 – 1278.

Heaton TB, Amoateng AY. 2007. Families and households in post-Apartheid South Africa. Chapter 8: The family context for racial differences in child mortality in South Africa: 171 – 187. HSRC Press.

Heredahl S, Kase BF, Stake G. 1994. Skeletal maturation during thyroxin treatment in children with congenital hyperthyroidism. Acta Pediatr 83: 618 – 622.

Hill K, Punsent PB. 1994. A fully automated bone-aging system. Acta Pediatr 83: 81 – 83.

Hill T, Lewicki P. 2006. Statistics: methods and applications: a comprehensive reference for science, industry, and data mining. StatSoft Inc.

Hsieh C, J T, Tiu C. 2007. Bone age estimation based on phalanx information with fuzzy constrain of carpals. Med Bio Eng Compu 45: 283 – 295.

Hsieh C, Jong T, Chou Y, Tiu C. 2007. Computerized geometric features of carpal bone for bone age estimation. Chinese Med J 120 (9): 767 – 770.

Johnston FE. 1963. Skeletal age and its prediction in Philadelphia children. Hum Biol 35: 192–202.

Khan KM, Miller BS, Hoggard E, Somani A, Sarafoglou K. 2009. Application of ultrasound for bone age estimation in clinical practice. J Pediatr 154 (2): 243 – 247.

Kim J, Oh I, Lee E, Choi K, Choe B, Yoon T, Lee C, Moon J Shin S Choi J. 2008. Anthropometric changes in children and adolescents from 1965 to 2005 in Korea. Am J Phys Anthopol 136: 230 – 236.

Koç A, Karaoğlanoğlu M, Erdoğan M, Kösecik M, Cesur Y. 2001. Assessment of bone ages: Is the Greulich-Pyle method sufficient for Turkish boys?. Pediatr Int 43: 662 – 665.

Krogman WM, Işcan MY. 1986. The human skeleton in forensic science. Second Edition. Illinois: Charles C Thomas. pp 480 – 492.

Krous HF. 2010. Sudden unexpected death in infancy and the dilemma of defining the sudden infant death syndrome. Current Pediatric Reviews 6: 5 – 12.

Krug EG, Sharma GK, Lozano R. 2000. Global burden of disease. Am J Public Health 90: 523 – 526.

Lee MC. 1971. Maturation disparity between hand-wrist bones in Hong Kong Chinese children. Am J Phys Anthropol 34: 385 – 396.

Levine E. 1972. Carpal fusions in children of four South African populations. Am J Phys Anthropol 37: 75 – 84.

Lin P, Zhang F, Yang Y, Zheng C. 2004. Carpal-bone feature extraction analysis in skeletal age assessment based on deformable model. JCS & T 4 (3): 152 – 156.

Loder RT, Estle DT, Morrison K, Eggleston D, Fish DN, Greenfield ML, Guire KE. 1993. Applicability of the Greulich and Pyle skeletal age standards to black and white children of today. Am J Dis Child 147: 1329 – 1333.

Lynnerup N, Belard E, Buch-Olsen K, Sejrsen B, Damgaard-Pedersen K. 2008. Intra- and interobserver error of the Greulich-Pyle method as used on a Danish forensic sample. Foren Sci Int 242 e.1 – 242 e.6.

Malaysia's History and Background, AsianInfo.org. 2010. http://www.asianinfo.org/asianinfo/malaysia/pro-history.htm

Martin DD, Stahl K, Schweizer R, Thodberg HH, RankeMB. 2008. Validation of BoneXpert in children with precocious puberty. Proc 47th Annual Meeting of European Society for Paediatric Endocrinology, Istanbul, Turkey (Abstract) Horm Res 70 (1):73.

Martin DD, Deusch D, Schweizer R, Binder G, Thodberg HH, Ranke MB. 2009. Clinical application of automatic Greulich-Pyle bone age in children with short stature. Pediatr Radiol 39 (6): 598 – 607.

Martin DD, Neuhof J, Jenni OG, Ranke MB,Thodberg HH. 2010. Automatic determination of left- and right-hand bone age in the first Zurich longitudinal study. Horm Res Paediatr 74 (1): 50 – 55.

Meadows L, Jantz RL. 1995. Allometric changed in the long bones from 1800s to the present. J Forensic Sci 40: 762 – 767.

Mellits ED, Dorst JP, Cheek DB. 1971. Bone age: its contribution to the prediction of maturational or biological age. Am J Phys Anthropol 35: 381 – 384.

Michael DJ, Nelson AC. 1989. HANDX: A model-based system for automatic segmentation of bones from digital hand radiographs. IEEE Trans Med Imag 8 (1): 64 – 69.

Moorrees CFA, Fanning EA, Hunt EE Jnr. 1963. Age cariation of formation stages for ten permanent teeth. J Dent Res 42: 1490 – 1502.

Mora S, Boechat MI, Pietka E, Huang HK, Gilsanz V. 2001. Skeletal age determination in children of European and African descent: Applicability of the Greulich and Pyle standards.

Nannan N, Norman R, Hendricks M, Dhansay MA, Bradshaw D. 2007. South African Comparative Rish Assessment Collaborating Group.

Niemeijer M, van Ginneken B, Maas CA, Beek FJA, Viergever MA. 2003. Assessing the skeletal age from a hand radiograph: Automating the Tanner-Whitehouse method. SPIE Medical Imaging 5032: 1197 – 1205.

Ontell FK, Ivanovic M, Ablin DS, Barlow TW. 1996. Bone age in children of diverse ethnicity. AJR 167: 1395 – 1398.

Phillips VM, Thompson IOC. 2000. A correlation between dental age and bone age. Forensic Odontology: Proceedings of the European IOFOS Millennium Meeting, Leuven (Belgium). pp 55 – 58. Leuven University Press, Leuven, Belgium.

Pietka E. 1995. Computer-assisted bone age assessment based on features automatically extracted from a hand radiograph. Comput Med Imag Grap 19(3): 251 – 259.

Pietka E, Gertych A, Pospiech S, Cao F, Huang HK, Gilsanz V. 2001. Computer-assisted bone age assessment: Image pre-processing and epiphyseal/metaphyseal ROI extraction. IEEE Trans Med Imag. 20 (8): 715 – 729.

Pietka E, Pospiech-Kurkowska S, Gertych A, Cao F. 2003. Integration of computer assisted bone age assessment with clinical PACS. Comput Med Imag Graph 27: 217 – 218.

Pietka E, Gertych A, Pospiech-Kurkowska S, Cao F, Huang HK, Gilsanz V. 2004. Computer assisted bone age assessment: graphical user interface for image processing and comparison. J Digit Imag 17 (3): 175 – 188.

Pinheiro JC, Bates DM. 2000. Mixed-effects models in S and S-PLUS. Statistics and Computing Series. Springer-Verlag, New York, NY.

Pitcher RD, van As AB, Sanders V, Douglas TS, Wieselthaler N, Vlok A, Paverd S, Kilborn T, Rode H, Potgieter H, Beningfield SJ. 2008. A pilot study evaluating the "STATSCAN" digital X-ray machine in paediatric polytrauma. Emerg Radiol 15: 35-42.

Pryor JW. 1928. Difference in the ossification of male and female skeletons. J Anat 62: 499 – 506.

Richter L, Norris S, Pettifor J, Yach D, Cameron N. 2007. Cohort Profile: Mandela's children: The 1990 birth to twenty study in South Africa. Int J Epidemiol 36 (3): 504 – 511.

Roche AF, Roberts J, Hamill PVV. 1975. Skeletal maturity of children 6-11 years: racial, geographic area and socioeconomic differentials, United States. (Vital and health statistics - series 11. no. 149). U.S. Government Printing Office, Washington, D.C.

Santos C, Ferreira M, Alves FC, Cuhna E. 2011. Comparative study of Greulich and Pyle Atlas and Maturos 4.0 program from age estimation in a Portuguese sample. Foren Sci Int 212: 276.e1 – 276.e7

Satoh M, Tanaka T, Hibi I. 1997. Analysis of bone maturation and growth velocity in isolated growth hormone deficient boys with and without gonadal suppression treatment in GH deficient boys with associated gonadotropin deficiency. J Pediatr Endocrinol Metab 10: 615 – 622.

Serinelli S, Panetta V, Pasqualetti P, Marchetti D. 2011. Accuracy of three age determination X-ray methods on the left ahnd-wrist: A systematic review and meta-analysis. Legal Med 13: 120 – 133.

Schaefer MC, Black SM. 2007. Epiphyseal union sequencing: aiding in the recognition and sorting of commingled remains. J Forensic Sci 52: 277 – 285.

Scheuer L, Black S. 2000. Developmental Juvenile Osteology. Academic Press. London

Schmeling A, Kaatsch HJ, Marré B, Reisinger W, Riepert T, Ritz-Temme S, Rösing FW, Rötzscher K, Geserick G. 2000. Guidelines for age estimation in living individuals in criminal proceedings. Study Group of Forensic Age Estimation of the German Association for Forensic Medicine. Available at: http://agfad.uni-muenster.de/english/empfehlungen/empfehlung_strafverfahren_eng.pdf

Schmeling A, Reisinger W, Lorreck D, Vendura K, Markus W, Geserick G. 2000. Effect of ethnicity on skeletal maturation: consequences for forensic age estimations. Int J Legal Med 113: 254 – 258.

Schmeling A, Schulz R, Reisinger W, Muhler M, Wernecke KD, Geserick G. 2004. Studies on the time frame for ossification of the medial clavicular epiphysial cartilage in conventional radiography. Int J Legal Med 118: 5 – 8.

Schmidt S, Koch B, Schulz R, Reisinger W, Schmeling A. 2007. Comparative analysis of the applicability of the skeletal age determination methods of Greulich-Pyle and Thiemann-Nitz for forensic age estimation in living subjects. Int J Legal Med 121: 193 – 296.

Schmidt S, Koch B, Schulz R, Reisinger W, Schmeling A. 2008. Studies in use of the Greulich-Pyle skeletal age method to assess criminal liability. Legal Med 10: 190 – 195.

Schmidt S, Nitz I, Schult R, Tsokos M, Schmeling A. 2009. The digital atlas of skeletal maturity by Gilsanz and Ratib: a suitable alternative for age estimation of living individuals in criminal proceedings?. Int J Legal Med 123: 489 – 494.

Schulz R, Muhler M, Mutze S, Schmidt S, Reisinger W, Schmeling A. 2005. Studies on the time frame for ossification of medial epiphysis of the clavicle as revealed by CT scans. Int J Legal Med 119: 142 – 145.

Shaikh Ah, Rikhasor RM, Qureshni Am. 1998. Determination of skeletal age in children aged 8 – 18 years. J Pal Med Assoc 48: 104 – 106.

Soegiharto BM, Cunningham SJ, Moles DR. 2008. Skeletal maturation in Indonesian white children assessed with hand-wrist and cervical vertebrae methods. Am J Orthod Dentofacial Orthop 134: 217 – 226.

South African Law Commission. 1997. Juvenile Justice. Paper 9, Project 106. ISBN: 0-621-27335.

StataCorp. 2009. Stata Statistical Software: Release 11. College Station, TX: StataCorp LP

Sutow WW. 1953. Skeletal maturation in healthy Japanese children, 6 to 19 years of age. Comparison with skeletal maturation in American children. Hiroshima J Med Sci 2: 181 – 193.

Tanaka T. 2006. Annual research reports of The Foundation for Growth Science 30:261. Available at www.fgs.or.jp/public/05/2006_08.html

Tanner JM, Whitehouse RH, Marshal WA. 1975. Assessment of skeletal maturity and prediction of adult height (TW2 Method). London: Academic Press.

Tanner JM. 1978. Foetus into man: physical growth from conception to maturity. London: Open Books.

Tanner JM,. Gibbons RD, Bock RD. 1992. An image analysis system for TW skeletal maturity. Hormone Res 37: 11

Thiemann HH, Nitz I (1991) Radiographic Atlas of the normal hand in childhood. Second Edition. Leipzig: Thieme.

Thodberg HH, Sävendahl L. 2008. Validation of automated bone age determination in healthy American children of four ethnicities. Proc 47th Annual Meeting of European Society for Paediatric Endocrinology, Istanbul, Turkey (Abstract) Horm Res 70 (1): 88.

Thodberg HH. 2009. An Automated Method for Determination of Bone Age. J Clin Endocrinol Metab 94: 2239 – 2244.

Thodberg HH, Kreiborg S, Juul A, Pedersen KD. 2009. The BoneXpert method for automated determination of skeletal maturity. IEEE Trans Med Imaging 28 (1):52–66

Tisè M, Mazzarinin L, Fabrizzi G, Ferrante L, Giorgetti R, Taglibracci A. 2011. Applicability of Greulich and Pyle method for age assessment in forensic practice on an Italian sample. Int J Legal Med 125: 411 – 416.

Todd TW. 1937. Atlas of skeletal maturation. St Louis: CV Mosby.

Uysal T, Sari Z, Ramoglu SI, Basciftci FA. 2004. Relationships between dental and skeletal maturity in Turkish subjects. Angle Orthodontist 74 (5): 657 – 664.

van Rijn RR, Lequin MH, Robben SGF, Hop WCJ, van Kuijk C. 2001. Is the Greulich and Pyle atlas still valid for Dutch children today?. Pediatr Radiol 31: 748 – 752.

van Rijn, Lequin MH, Thodberg HH. 2009. Automatic determination of Greulich ahd Pyle bone age in healthy Dutch children. Pediatr Radiol 39 (6): 598 – 607.

Varkkola O, Ranta H, Metsäniitty M, Sajantila A. 2011. Age assessment by the Greulich and Pyle method compared to other skeletal X-ray and dental methods in data from Finnish child victims of the Southeast Asian Tsunami. Forensic Sci Med Pathol 7 (4): 311 – 316.

Walker SP, Wachs TD, Gardner JM, Lozoff B, Wasserman GA, Pollitt E *et al.* 2007. Child development: risk factors for adverse outcomes in developing countries. International Child Development Steering Group. Lancet 369 (9556): 145 – 157.

Wheeler MD. 1991. Physical changes of puberty. Endocrin Metab Clin 20 (1): 1-14.

Zhang A, Gertych A, Liu BJ. 2007. Automatic bone age assessment for young children from newborn to 7-year-old using carpal bones. Comput Med Imag Grap 31: 299 - 310

Zhang A, Sayre JW, Vachon L, Liu BJ, Huang HK. 2009. Racial differences in growth patterns of children assessed on the basis of bone age. Radiology 250 (1): 228 – 235.

Zwi AB. 1996. Injury control in developing countries – Context more than content is critical. Inj Prev 2: 91 – 92.

APPENDIX A:

Definitions and Terminology

Definitions and Terminology (adapted from du Toit, 1992 and Bogin, 1999)

Term	Definition
Growth	Changes in size, composition and proportions of biological structures
Maturation	The progression towards attaining complete and maximal development
Chronological Age	The period of time which has elapsed from the date of birth to the date in question
Adolescence	The period of physical and psychological transition between the onset of puberty and the mature, adult state
Skeletal Development	The development of the human skeletal system from the early days of pregnancy until the bones have reached their fully-mature form
Skeletal Maturity	How far a child has advanced in the development of its skeleton
Skeletal Maturation	The process of bone development towards a fully developed adult skeleton
Skeletal/Bone Age	A measure of the degree of skeletal maturity
Skeletal Age Assessment/ Skeletal Age Estimation	The use of various techniques (eg X-rays of the hand-wrist, clavicle, long bones) to assess age in terms of the degree of bone growth and development
Biological/Physiological Maturity	The process of growth and development of the body and body structures through specific stage (eg post-natal period, puberty) toward the attainment of maximal growth and development
Adult Bone Structure	A skeletal system that is fully developed, with complete epiphysial union of all bones and cessation of bone growth
Mature Adult Body Form	The attainment of complete development of the body and body structures, with cessation of growth in these regions

APPENDIX B:

GP Atlas Standards for Males (Newborn – 4 Years 6 Months)

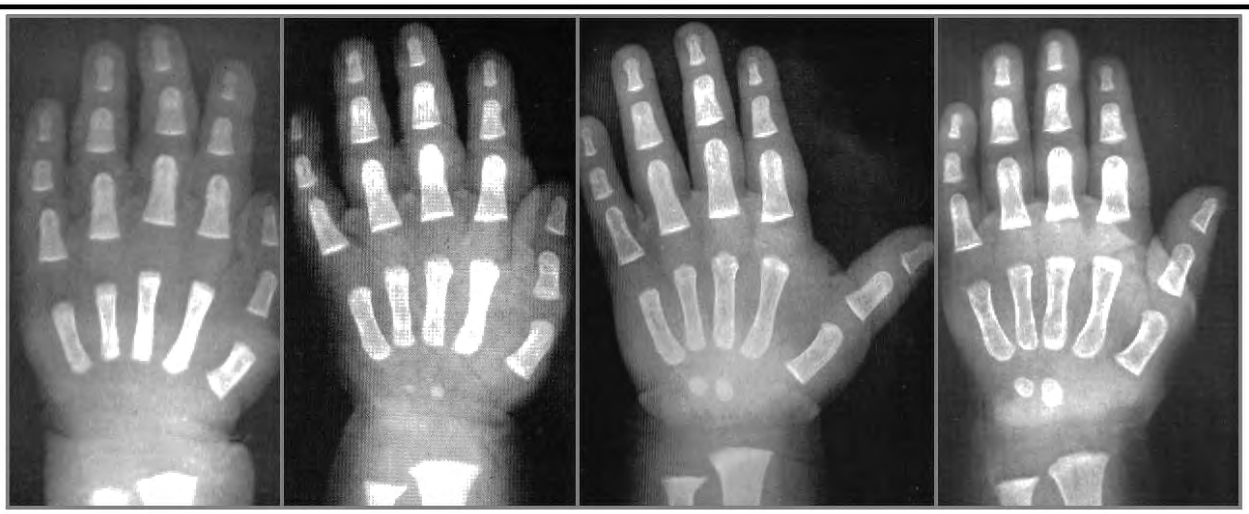

Newborn | 3 Months | 6 Months | 9 Months

1 Year | 1 Year 3 Months | 1 Year 6 Months | 2 Years

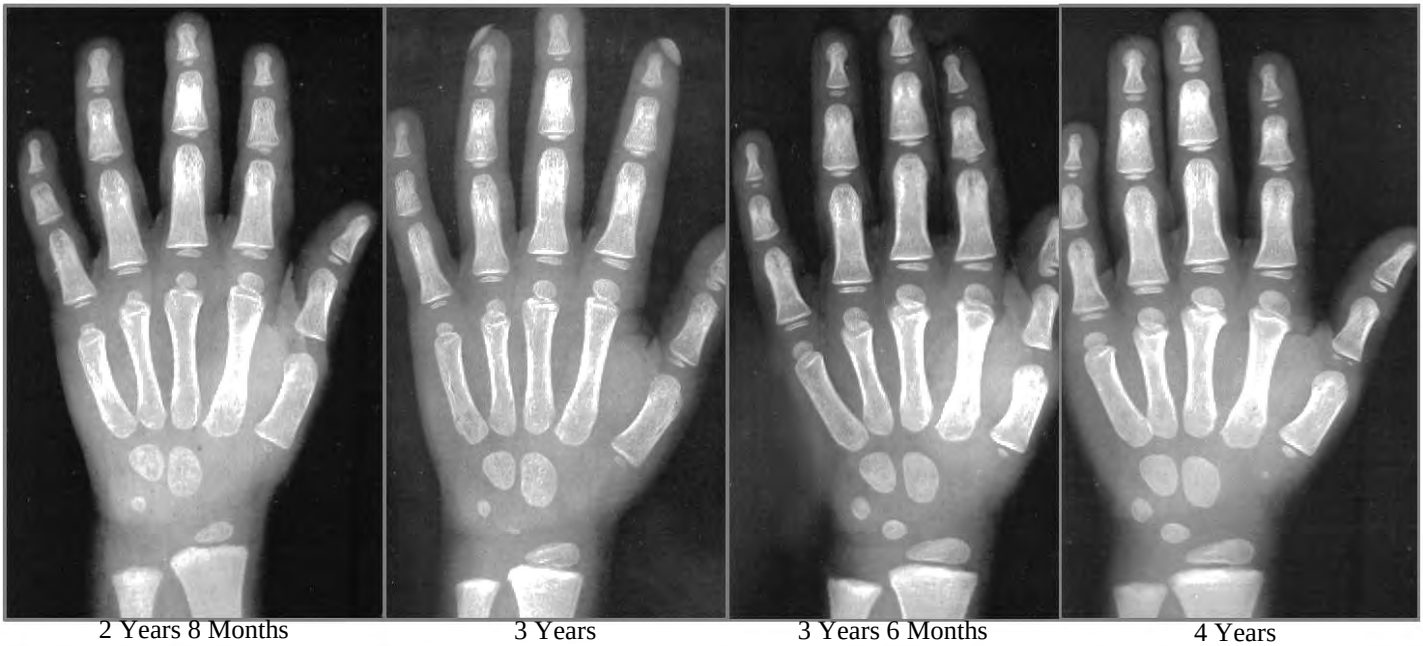

2 Years 8 Months | 3 Years | 3 Years 6 Months | 4 Years

APPENDIX B:

GP Atlas Standards for Males (5 Years – 13 Years 6 Months)

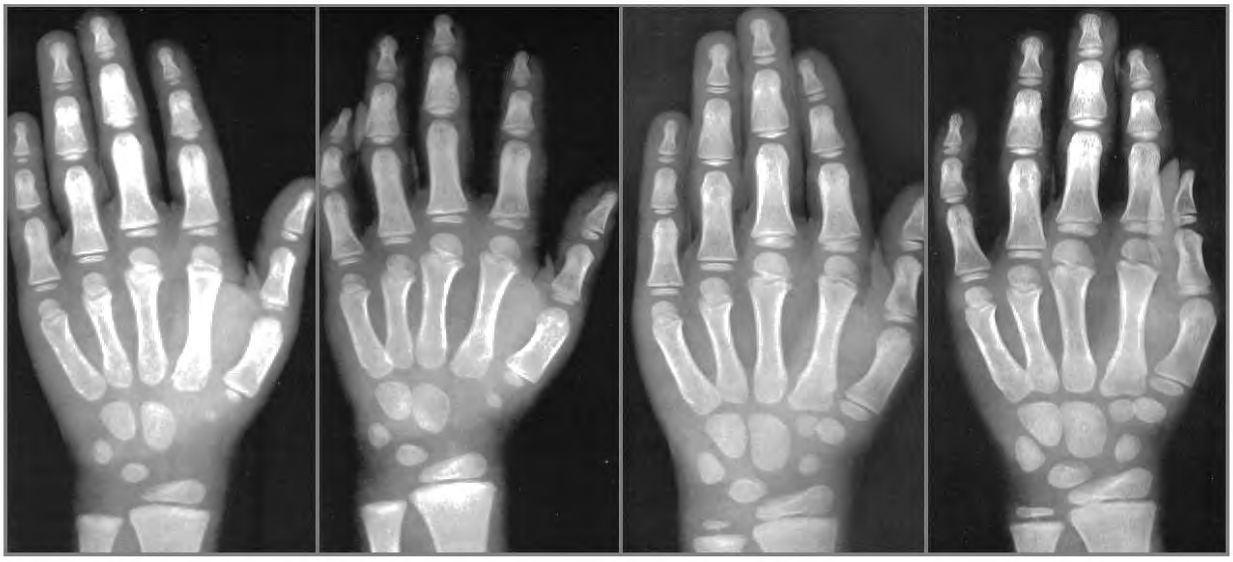

4 Years 6 Months | 5 Years | 6 Years | 7 Years

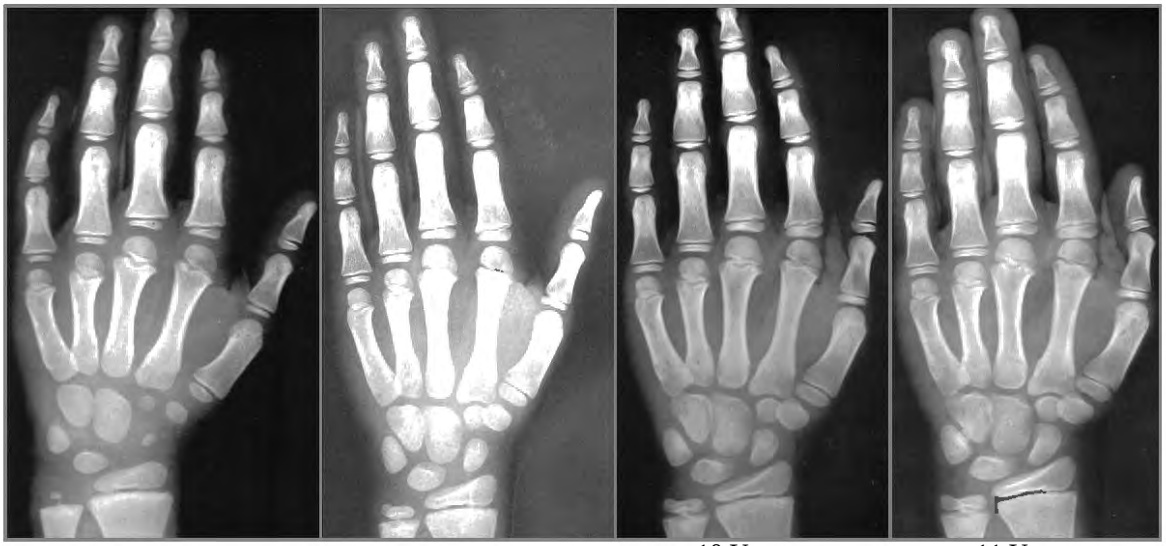

8 Years | 9 Years | 10 Years | 11 Years

11 Years 6 Months | 12 Years 6 Months | 13 Years | 13 Years 6 Months

APPENDIX B:

GP Atlas Standards for Females (Newborn – 4 Years 2 Months)

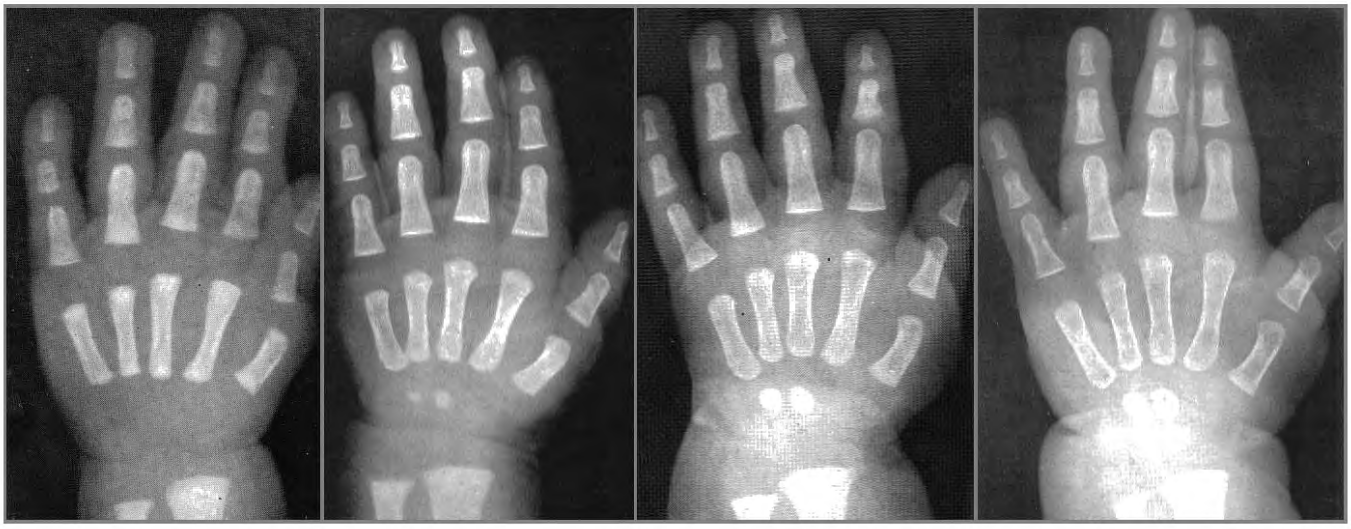

Newborn | 3 Months | 6 Months | 9 Months

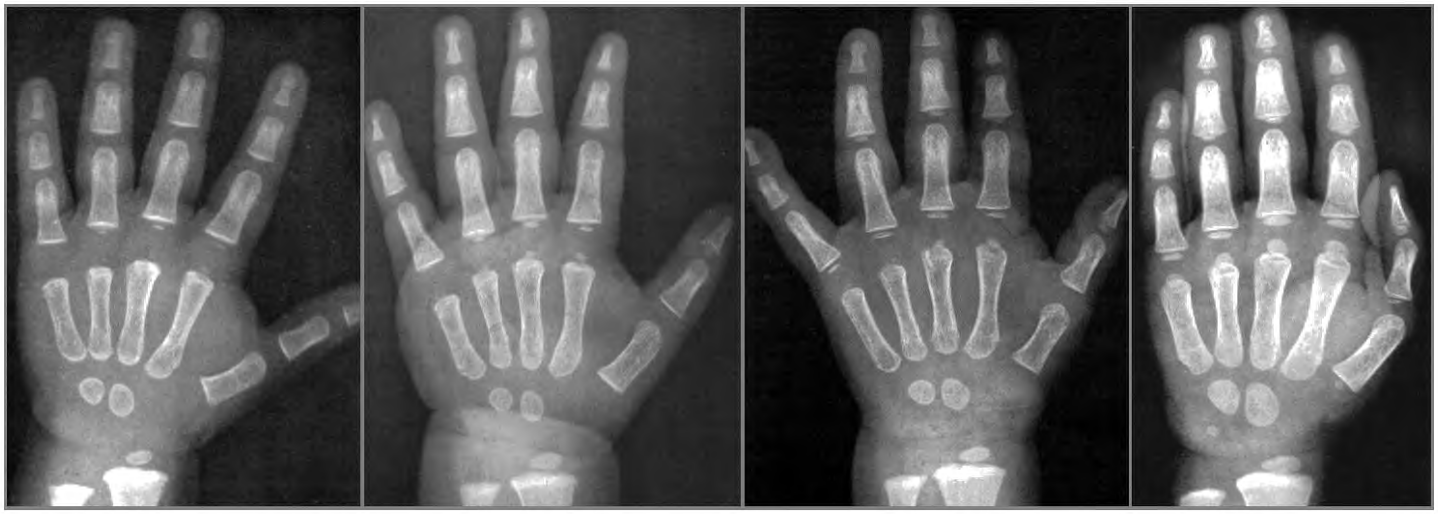

1 Year | 1 Year 3 Months | 1 Year 6 Months | 2 Years

2 Years 6 Months | 3 Years | 3 Years 6 Months | 4 Years 2 Months

APPENDIX B:

GP Atlas Standards for Females (5 Years – 13 Years)

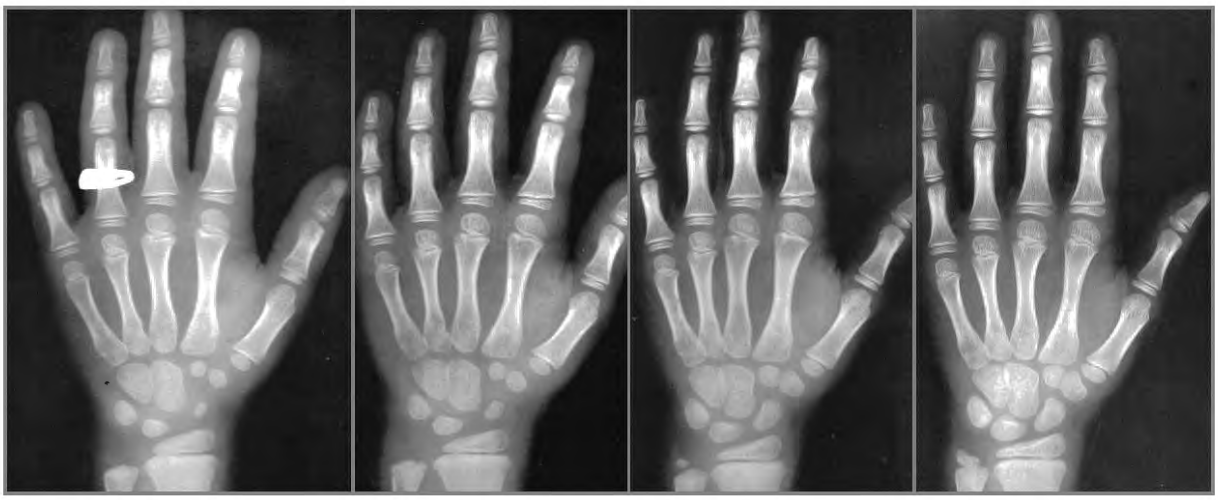

5 Years | 5 Years 9 Months | 6 Years 10 Months | 7 Years 10 Months

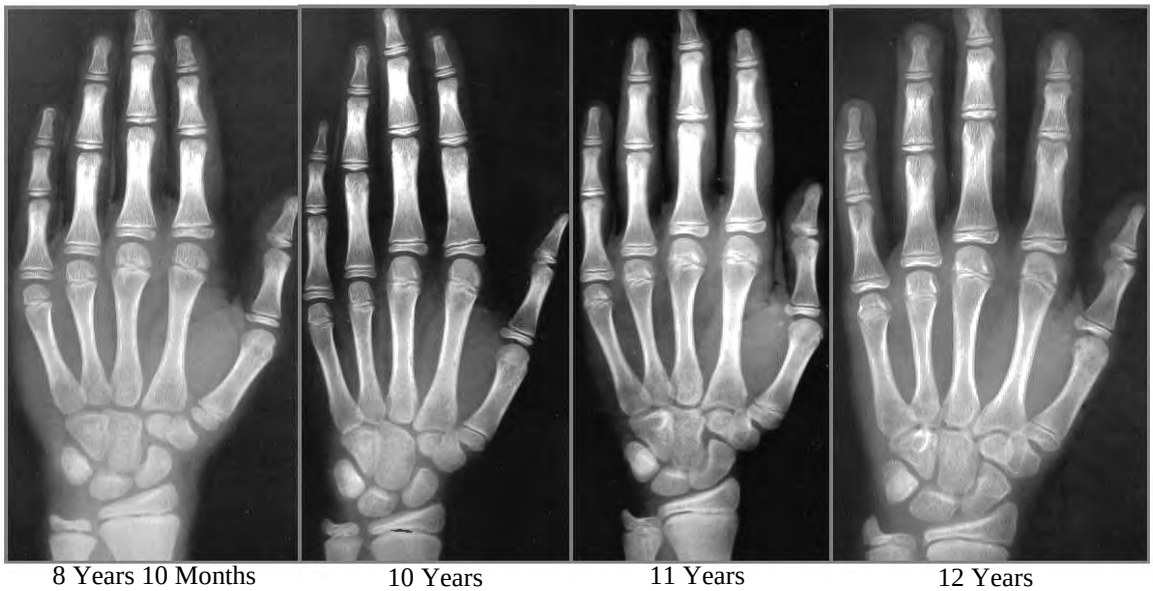

8 Years 10 Months | 10 Years | 11 Years | 12 Years

13 Years

APPENDIX C:

Examples of (a) inclusion and (b) exclusion criteria when selecting radiographs

(a) Inclusion:

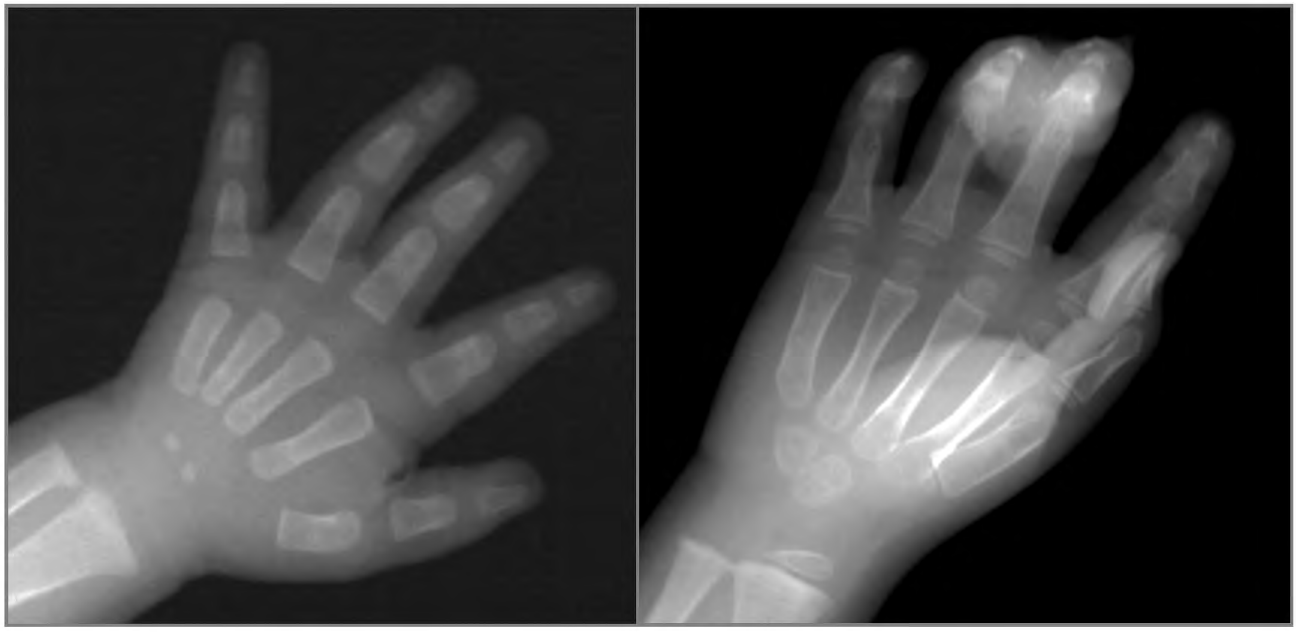

(i) Ideal hand position

(ii) Accepted position as the Carpal, Metacarpal and Proximal Phalangeal regions are visible

(b) Exclusion:

(i) Hospital equipment covering the hand

(ii) Hand in incorrect position

(iii) Movement whilst the image was captured

APPENDIX D:

Exemplar Data Sheet (Full Data Sheet can be found on the CD attached)

Ref #	Data #	Sex	Race	Hand (L/R)	Date of Birth/ Age	Date of Radiograph/ Date of Death	Chronologial Age	Skeletal Age[1]	Error[1] (SA - CA)	Under (1)/ Over (2) Estimate	Notes
SRMF67	19082	Female	C	R	2M	21-Jan-09	0.17	0.13	-0.04	1	
SRMF68	19488	Female	C	L	1M	13-May-09	0.17	0.00	-0.17	1	
SRMF69	19536	Female	B	L	2M	22-May-09	0.17	0.50	0.33	2	
SRMF70	19601	Female	B	L	2M	1-Jun-09	0.17	0.25	0.08	2	
SRMF71	19852	Female	C	L	2M	19-Jul-09	0.17	0.13	-0.04	1	OC'S ONLY JUST VISIBLE
SRMF72	19861	Female	B	L	2M	21-Jul-09	0.17	0.50	0.33	2	
SRMF73	20184	Female	B	L	2M	7-Sep-09	0.17	0.63	0.46	2	CARPALS SLIGHTLY LARGER THAN @6M
SRMF74	20778	Female	C	L	2M	27-Dec-09	0.17	0.25	0.08	2	
SRMF85	17649	Female	B	L	1-Feb-08	21-Apr-08	0.22	0.38	0.16	2	M'S NOT ROUNDED YET
SRMF75	17266	Female	C	L	3M	28-Jan-08	0.25	0.50	0.25	2	
SRMF76	17446	Female	C	L	3M	12-Mar-08	0.25	0.50	0.25	2	
SRMF77	17705	Female	B	L	3M	28-Apr-08	0.25	0.13	-0.13	1	
SRMF78	17948	Female	C	R	3M	25-Jun-08	0.25	0.00	-0.25	1	
SRMF79	17985	Female	B	L	3M	1-Jul-08	0.25	0.25	0.00	EQUAL	
SRMF80	18210	Female	B	L	3M	5-Aug-08	0.25	0.63	0.38	2	
SRMF81	18974	Female	B	R	3M	17-Dec-08	0.25	0.75	0.50	2	TRIQUETRAL O/S PRESENT
SRMF82	19353	Female	B	L	3M	9-Apr-09	0.25	0.00	-0.25	1	
SRMF83	20510	Female	C	L	3M	9-Nov-09	0.25	0.00	-0.25	1	
SRMF84	20686	Female	B	L	3M	8-Dec-09	0.25	0.63	0.38	2	
SRMF86	16875	Female	C	L	4M	19-Nov-07	0.33	0.75	0.42	2	
SRMF87	17569	Female	C	L	4M	6-Apr-08	0.33	0.63	0.30	2	BASE OF M2 NOT AS ROUNDED AS 9M
SRMF88	17926	Female	B	L	4M	21-Jun-08	0.33	0.50	0.17	2	
SRMF89	19652	Female	B	L	4M	13-Jun-09	0.33	0.25	-0.08	1	
TYMF14	10327	Female	B	L	4M	7-Jun-08	0.33	0.50	0.17	2	
TYMF15	11133	Female	B	R	4M	2-Aug-09	0.33	0.50	0.17	2	
TYMF16	11134	Female	B	R	4M	31-Jul-09	0.33	0.88	0.55	2	RADIAL EPI PRESENT BUT NO PHALANGEAL EPIS
RXHF1	12919	Female		L	13-May-06	27-Sep-06	0.38	0.38	0.00	EQUAL	
RXHF2	12807	Female		L	8-Apr-06	25-Aug-06	0.38	0.00	-0.38	1	
RXHF3	10377	Female		L	22-Oct-04	15-Mar-05	0.39	0.75	0.36	2	
SRMF90	16957	Female	C	R	5M	1-Dec-07	0.42	0.50	0.08	2	
SRMF91	18239	Female	B	L	5M	8-Aug-08	0.42	0.38	-0.04	1	
SRMF92	20194	Female	B	L	5M	9-Sep-09	0.42	0.75	0.33	2	
TYMF17	11122	Female	C	R	5M	27-Jul-09	0.42	0.13	-0.29	1	ONLY CAPITATE O/C PRESENT
SRMF93	18308	Female	B	L	5M	23-Aug-08	0.42	0.63	0.21	2	
RXHF4	10468	Female		L	19-Oct-04	30-Mar-05	0.44	0.50	0.06	2	
SRMF94	17952	Female	B	R	0.5	22-Jun-08	0.50	0.75	0.25	2	
SRMF95	19216	Female	B	R	0.5	26-Feb-09	0.50	0.88	0.38	2	
SRMF96	19490	Female	B	L	0.5	10-May-09	0.50	0.75	0.25	2	
SRMF97	19528	Female	B	L	0.5	20-May-09	0.50	0.75	0.25	2	
SRMF98	19917	Female	B	L	0.5	31-Jul-09	0.50	0.88	0.38	2	
TYMF18	11201	Female	B	L	6M	24-Aug-09	0.50	0.63	0.13	2	
TYMF19	11214	Female	B	L	6M	1-Sep-09	0.50	0.25	-0.25	1	
SRMF99	17417	Female	B	R	7M	3-Mar-08	0.58	0.50	-0.08	1	
SRMF100	17286	Female	B	R	7M	3-Feb-08	0.58	0.88	0.30	2	TRIQUETRAL PRESENT
SRMF101	19930	Female	B	L	7M	1-Aug-09	0.58	0.75	0.17	2	DISTAL P1 PRESENT
SRMF102	20004	Female	B	L	7M	10-Aug-09	0.58	0.20	-0.38	1	

APPENDIX E:

Explanation of skeletal age assessments – taken from pages 35 – 37 of the GP Atlas

HOW TO PROCEED IN ASSESSING A HAND-FILM

It is believed that a satisfactory assessment of the hand-films of most normal children can be made by comparing them carefully with the standards illustrated in this *Atlas*. The following suggested method of procedure may prove helpful to the reader, at least until he has replaced it by a method of his own devising that he finds better adapted to his individual needs or preferences.

Begin by comparing the film to be assessed with the standard of the same sex and nearest chronological age in the *Atlas*. Next, compare the film with adjacent standards, both older and younger than the one which is of the nearest chronological age. Select for a more detailed comparison the standard which superficially appears to resemble it most closely.

The features to be used in making the preliminary selection will, of course, vary with the age of the child. During infancy and early childhood the presence or absence of certain carpal or epiphysial ossification centers will often provide the most useful clue. Beginning at about the time of puberty and ending in late adolescence, the degree of fusion of epiphyses with their shafts furnishes additional information that will be helpful in making the preliminary selection. During the intermediate period, the selection will depend more upon those changes in the shape of the bones and on other skeletal features visible in the hand-film which are described in the list of maturity indicators. The maturity indicators provide also the basis for the detailed assessment of the hand-film throughout the entire period from birth to early adulthood.

After finding the standard which superficially resembles most closely the film to be assessed, one should proceed to make a more detailed comparison of the individual bones and epiphyses visible in them. It is well to form the habit of considering the bones in a regular order, for, once formed, this habit will help to prevent one from overlooking features which may be important in making the assessment. A good way is to begin at the distal ends of the radius and ulna, proceeding next to the carpals, then to the metacarpals, and then to the phalanges. As added insurance against missing some of their significant developmental features, it is suggested that the carpals too be studied in a regular sequence—preferably in the order in which they usually appear: Capitate, Hamate, Triquetral, Lunate, Scaphoid, Trapezium, Trapezoid, Pisiform. The adductor and flexor sesamoids of the thumb appear in that order, usually several years after the Pisiform has begun to ossify.

If an individual bone in the film to be assessed is in the same stage of development as the corresponding bone in the standard selected for the detailed comparison, it should be given the skeletal age that has been assigned

APPENDIX E:

Explanation of skeletal age assessments – taken from pages 35 – 37 of the GP Atlas

to that bone in that standard. If it appears to be either less advanced or more advanced than its counterpart in that standard, it should be compared with the same bone in adjacent standards. The proper skeletal age to be assigned to it is that which is given in the standard to the corresponding bone that shows the same degree of development. If none is found that corresponds exactly in developmental status with the bone to be assessed, its skeletal age should be estimated from that of those which it most closely resembles.

The developmental status of all bones of the hand to be assessed will occasionally correspond exactly to that of some one hand standard in this Atlas. When such is the case, the skeletal age of that standard is the skeletal age to he assigned to the child's hand. If, however, its developmental status does not correspond exactly to that of any one standard but is, rather, intermediate between those of two adjacent standards, the age assigned to the film should be correspondingly intermediate between the ages of the two standards which it most closely resembles. After one becomes familiar with the rate at which skeletal development proceeds during various phases of infancy and childhood, one can make quite reliable judgments as to the proper intermediate skeletal ages to be assigned in such cases.

THE ASSESSMENT OF HAND-FILMS WHICH SHOW MARKED IMBALANCE IN SKELETAL DEVELOPMENT

As previously mentioned, the bones of the hand and wrist, like those of other areas, tend to maintain a regular sequence in the beginning and in the various subsequent stages of their ossification. In most normal children there is a sufficiently good balance in osseous development to permit one to assign to the hand a single skeletal age which describes adequately the status of the bones which compose it. It should be remembered, however, that the bones of the hand and wrist are an aggregation of partially independent elements, despite the fact that they tend to behave more or less as a unit in their development. In many children who have had severe illnesses or prolonged nutritional inadequacies, this anatomical individuality of the bones is reflected in a marked departure from the normal developmental equilibrium. Hand-films of such children show certain hones to he significantly retarded in their development as compared with others.

Since the object of the assessment is to determine and to describe as accurately as possible the developmental status of the bones of the hand and wrist, it is not sufficient, in such cases, merely to assign to the hand-film the single skeletal age which corresponds most closely to that of the majority of the bony

APPENDIX E:

Explanation of skeletal age assessments – taken from pages 35 – 37 of the GP Atlas

centers visible in it. One should also list the centers that are either significantly retarded or advanced as compared with the others, and record their skeletal age as determined by the maturity indicators present in them. This procedure provides a really adequate description of skeletal status, because it calls attention to, rather than obscures, any significant imbalance in skeletal development that might be detectable in the hand-film. Moreover, it prompts one to seek in the health history of the child for the illnesses or other incidents to which that imbalance might reasonably be attributed. Thus, the recognition of such imbalance is often of more immediate value to the physician than is any other part of the skeletal assessment.

APPENDIX F:

GP Atlas Standard Deviation (SD) Values for Males – taken from page 51 of the GP Atlas

TABLE III

THE VARIABILITY OF SKELETAL AGE OF BOYS IN THE BRUSH FOUNDATION STUDY

CHRONOLOGICAL AGE	NUMBER OF HAND-FILMS	SKELETAL AGE (IN MONTHS) MEAN	STANDARD DEVIATION
3 mo.	121	3.01	0.69
6 mo.	129	6.09	1.13
9 mo.	137	9.56	1.43
12 mo.	130	12.74	1.97
18 mo.	106	19.36	3.52
2 yr.	105	25.97	3.92
2½ yr.	107	32.40	4.52
3 yr.	127	38.21	5.08
3½ yr.	138	43.89	5.40
4 yr.	170	49.04	6.66
4½ yr.	176	56.00	8.36
5 yr.	191	62.43	8.79
6 yr.	186	75.46	9.17
7 yr.	182	88.20	8.91
8 yr.	168	101.38	9.10
9 yr.	160	113.90	9.00
10 yr.	177	125.68	9.79
11 yr.	154	137.32	10.09
12 yr.	165	148.82	10.38
13 yr.	175	158.39	10.44
14 yr.	163	170.02	10.72
15 yr.	124	182.72	11.32
16 yr.	99	195.32	12.86
17 yr.	68	206.21	13.05

APPENDIX F:

GP Atlas Standard Deviation (SD) Values for Females – taken from page 53 of the GP Atlas

TABLE IV

THE VARIABILITY OF SKELETAL AGE OF GIRLS IN THE BRUSH FOUNDATION STUDY

CHRONOLOGICAL AGE	NUMBER OF HAND-FILMS	SKELETAL AGE (IN MONTHS)	
		MEAN	STANDARD DEVIATION
3 mo.	108	3.02	0.72
6 mo.	121	6.04	1.16
9 mo.	122	9.05	1.36
12 mo.	117	12.04	1.77
18 mo.	93	18.22	3.49
2 yr.	101	24.16	4.64
2½ yr.	98	30.96	5.37
3 yr.	133	36.63	5.97
3½ yr.	131	43.50	7.48
4 yr.	154	50.14	8.98
4½ yr.	152	60.06	10.73
5 yr.	167	66.21	11.65
6 yr.	191	78.50	10.23
7 yr.	200	89.30	9.64
8 yr.	201	100.66	10.23
9 yr.	195	113.86	10.74
10 yr.	206	125.66	11.73
11 yr.	203	137.87	11.94
12 yr.	198	149.62	10.24
13 yr.	179	162.28	10.67
14 yr.	170	174.25	11.30
15 yr.	117	183.62	9.23
16 yr.	64	189.44	7.31